UC Berkeley
UC Berkeley Electronic Theses and Dissertations

Title
Synthesis and Biological Evaluation of Acid-Degradable Polymeric Materials for Protein-Based Vaccines

Permalink
https://escholarship.org/uc/item/5xg9b4ct

Author
Beaudette, Tristan Thomas

Publication Date
2010

Peer reviewed|Thesis/dissertation

eScholarship.org Powered by the California Digital Library
University of California

Synthesis and Biological Evaluation of Acid-Degradable Polymeric Materials for Protein-Based Vaccines

by

Tristan Thomas Beaudette

A dissertation submitted in partial satisfaction of the

requirements for the degree of

Doctor of Philosophy

in

Chemistry

in the

Graduate Division

of the

University of California, Berkeley

Committee in charge:

Professor Jean M. J. Fréchet, Chair
Professor Matthew Francis
Professor Kevin Healy

Spring 2010

Synthesis and Biological Evaluation of Acid-Degradable Polymeric Materials for Protein-Based Vaccines

Copyright 2010

by

Tristan Thomas Beaudette

Abstract

Synthesis and Biological Evaluation of Acid-Degradable Polymeric Materials for Protein-Based Vaccines

by

Tristan Thomas Beaudette

Doctor of Philosophy in Chemistry

University of California, Berkeley

Professor Jean M. J. Fréchet, Chair

Vaccination represents one of the most cost-effective methods for the treatment and prevention of disease. Due to safety concerns surrounding the use of live attenuated and killed/inactivated pathogens, there has been significant interest in the development of subunit vaccines, which are composed of discrete antigenic proteins or polysaccharides. Unfortunately, protein-based vaccines are poorly immunogenic and typically require the use of adjuvants for the induction of protective immunity. Because of their tunability and synthetic addressability, polymeric particulate carriers represent a promising approach for enhancing the efficacy of protein-based vaccines, and are the subject of this dissertation. In particular, we report on the development of acid-degradable materials, which are capable of releasing encapsulated protein antigens and immunostimulatory molecules following uptake by cells of the immune system and subsequent trafficking to acidic endosomal vesicles. Specific emphasis is placed on the development, functionalization and immunological evaluation of biodegradable acid-sensitive particle systems.

Chapter 1 introduces various delivery strategies for enhancing the potency of subunit vaccines and discusses the basics of vaccine immunology. Additionally, the field of polymeric particulate antigen carriers is reviewed, with a focus on relevant design criteria for materials intended to interact with the immune system.

In Chapter 2, the synthesis of acid-sensitive acrylamide-based microparticles containing an immunomodulatory agent is discussed. The optimal conjugation strategy for an immunostimulatory DNA sequence is investigated and particles containing a model protein antigen are studied in several models, including a cancer immunotherapy study, to ascertain *in vivo* the importance of co-delivering antigen and maturation signals to cells of the adaptive immune system.

Chapter 3 discusses the synthesis of a second generation acid-sensitive polyurethane particle system which is designed to degrade entirely into biocompatible small molecule byproducts. The ability of these particles to elicit an immune response to a model antigen is studied and a method to monitor the production of polymer degradation byproducts in cells is presented.

Chapters 4 and 5 investigate the synthesis, characterization, and a method for the functionalization of a third generation acid-sensitive particle system. The preparation of these particles from acetal-modified dextran and their pH-dependent degradation behavior is

described. Additionally, a facile method for the surface functionalization of these particles using alkoxyamine reagents is presented.

Acknowledgments

This doctoral work would not have been possible without the help of many people. I would like to start by thanking my advisor, Professor Fréchet, for his guidance over the years and for giving me the independence and freedom to grow as a scientist. I would also like to acknowledge all of my coworkers that were involved in my projects over the past five years. In particular, Joel Cohen, Eric Bachelder, and Kyle Broaders have been wonderful collaborators and teammates, each bringing a unique perspective and set of skills to our joint projects. I would like to thank my friends, family, and fellow Fréchet group members (past and present) for their support and for making my time in graduate school so enjoyable. Lastly, I would like to thank my wife Erica for her love, support, and for helping me stay sane – I'm looking forward to starting the next chapter in our lives!

Chapter 1 — Advanced Polymeric Materials for Particulate Antigen Delivery Systems

Abstract

This chapter introduces the concept of subunit vaccines and gives an overview of the adaptive and innate immune systems. A brief discussion of various strategies currently under investigation for enhancing the immunogenicity of protein-based vaccines is presented, and the field of polymeric particulate antigen carriers is reviewed in detail. In particular, this chapter focuses on the development of novel antigen delivery vehicles from a polymer chemistry and materials science perspective, highlighting how physicochemical properties, responsive polymers, and carrier design can be used to manipulate the immune system for vaccine and cancer immunotherapy applications.

Introduction

As illustrated by the worldwide eradication of smallpox,[1] vaccination represents an enormously powerful and cost-effective means for the prevention and control of infectious disease. Despite their potential, vaccines for only a limited number of illnesses have been developed,[2] which is not surprising considering the hefty demands placed on a treatment administered primarily to children or otherwise healthy individuals.[3] A successful vaccine must accomplish the difficult task of inducing long lasting protective immunity in nearly all recipients without actually causing illness or any undesirable side effects. Vaccines that fulfill these requirements and have been approved for use in humans can be categorized as either live attenuated, killed/inactivated, or subunit/protein-based.[4] Live vaccines are typically produced through the serial passage of an organism in non-human animals or cell lines, a largely empirical process, which ultimately attenuates the virulence of the pathogen.[5,6] Although they often generate the most complete and long lasting immune responses, live vaccines replicate in the host and therefore possess inherent safety risks including the potential for reversion to virulence and persistent infections, especially in immunocompromised patients.[3,5] Inactivated vaccines are prepared by killing a pathogen with heat or chemicals, and represent a somewhat safer approach to immunization, although the potential for inoculation site side effects or incomplete inactivation of the pathogen does exist (e.g., the Cutter incident[7]). As opposed to attenuated or killed vaccines which are based on whole organisms, subunit vaccines are based on pathogenic proteins, polysaccharides, or other antigenic molecules. Because they lack inflammatory microbial components or the ability to replicate, subunit vaccines are generally considered to be the safest, but also the least immunogenic of the three approaches. Unfortunately, aluminum compounds (alum), the only adjuvants approved for use in the U.S., do not sufficiently enhance the potency of protein-based vaccines.[8] Nonetheless, subunit vaccines represent a promising immunization strategy; given a known antigen, it should be theoretically possible to produce vaccines against a large number of diseases using established recombinant technologies. For example, a number of cancer-specific protein antigens have been identified and are being studied for their ability to generate an immune response against tumors, an approach known as cancer immunotherapy.[9-11]

To increase the immunogenicity of subunit vaccines, a number of strategies have been investigated (see below). In this chapter, we focus on polymeric particulate vehicles used for the delivery of protein antigens to cells of the adaptive immune system for the development of safe

and effective vaccines. We concentrate on new polymers and materials that have been specifically engineered to interact with and modulate elements of the immune system. In particular, we discuss the immunological implications of several design considerations for particulate delivery vehicles including rate/mechanism of antigen release, surface chemistry, size, and the incorporation of targeting groups. However, before analyzing these parameters, we first review the basics of vaccine immunology and give a brief overview of other subunit vaccine delivery strategies under investigation.

Overview of the Adaptive and Innate Immune Systems

The generation of protective immunity requires input from both the adaptive and innate arms of the immune system.[12] Central to the adaptive immune system are professional antigen presenting cells (APCs), most notably B cells, macrophages, and dendritic cells (DCs). Whereas B cells are responsible for antibody-mediated immune responses, also known as humoral immunity, DCs and macrophages are responsible for activating T cell-mediated immune responses, or cellular immunity. Although all three APC types are capable of capturing pathogens, DCs are generally considered to be the most important class of cells for the induction and orchestration of adaptive immune responses.[13,14] Various subsets of DCs exist in the blood and tissue in an immature state where they sample their environment for the presence of pathogens. Following uptake of pathogens and the receipt of various signals from the innate immune system, DCs undergo a maturation process and migrate to the lymph nodes where they present antigen to naïve T cells.

APCs distinguish between intracellular and extracellular pathogens using distinct pathways of antigen presentation.[15,16] Protein antigens from extracellular pathogens, which are typically captured by APCs by phagocytosis or receptor-mediated endocytosis, are degraded into peptide fragments in endosomal compartments and presented *via* major histocompatibility complex (MHC) class II molecules to $CD4^+$ T cells. Depending on the cytokine signals they receive, $CD4^+$ T cells can differentiate into a number of effector cells with either regulatory[17] (T_{reg}) or helper[18,19] (T_h1, T_h2, or T_h17) functions. Of critical importance to vaccine immunologists are T_h1 and T_h2-type immune responses, which are generally considered important for the clearance of intracellular pathogens, or the induction of antibody responses, respectively. On the other hand, cytosolic antigens derived from intracellular pathogens, such as viruses, are degraded by APCs into peptide fragments and presented on their surface *via* MHC class I molecules to $CD8^+$ T cells. When properly primed, $CD8^+$ T cells can differentiate into cytotoxic T lymphocytes (CTLs), a class of effector cells capable of recognizing and directly killing infected cells or tumor tissue in an antigen-specific manner. It should also be noted that a third, and less well understood presentation pathway, termed "cross-presentation" and discussed below in more detail, provides a route for the presentation of exogenous antigens on MHC class I molecules.[20-22]

The innate immune system is the first line of defense against infection and provides crucial imunnostimulatory "danger" signals to the adaptive immune system.[23,24] In contrast to the high degree of specificity of an adaptive immune response, the innate immune system identifies a broad range of organisms using pattern-recognition receptors for conserved microbial motifs, known as "pathogen associated molecular patterns" (PAMPs). For example, Toll-like receptors (TLRs), which are found in DCs as well as other cell types, recognize a diverse array of PAMPs including lipopolysaccharide (LPS), unmethylated CpG DNA motifs, double stranded RNA, and flagellin.[24-26] Immunostimulatory signals provided by TLR ligand binding cause DCs to undergo maturation, secrete cytokines, and increase expression of MHC and co-stimulatory molecules.[27]

This last point is especially significant for vaccine development, as antigen presentation without sufficient co-stimulation can cause T cell anergy and tolerance as opposed to the desired immune response.[28,29]

Delivery Strategies for Subunit Vaccines

As protein-based vaccines often demonstrate suboptimal immunogenicity, many delivery methods have been explored to increase their efficacy.[30,31] Although a full discussion of these various strategies is beyond the scope of this review, the following examples should serve to demonstrate the breadth of delivery vehicles under investigation. One major approach being studied, known as "DNA vaccination," involves the transfection of human cells such that pathogen-associated protein antigens are expressed *in vivo*.[32-34] An adaptive immune response can therefore be generated if these antigens are taken up by APCs in the context of appropriate immunostimulatory signals. Viral vectors have been extensively studied for this application,[34] but safety concerns over the immune response[35] to the viral vector and their potential to cause cancer[36-38] have led others to investigate alternative methods. The use of polymeric materials and polymer-based microparticles for DNA vaccination may be a promising non-viral strategy, and is the subject of several recent reviews.[39,40]

Another major approach for enhancing the efficacy of subunit vaccines involves the use of carrier vehicles or assemblies to facilitate delivery of protein antigens to APCs. Examples of this approach include biological methods such as the use of bacterial vectors[41] or virus-like particles,[42,43] which are typically composed of self-assembled recombinant viral proteins. Other relevant examples include the use of lipid-based carriers such as liposomes and immunostimulatory complexes (ISCOMS).[44-47] Additionally, protein antigens have been conjugated to inorganic or other non-degradable particulate carriers.[43] In order to avoid long-term toxicity issues associated with non-degradable systems, there has been significant interest in the development of biodegradable and biocompatible nano- and microparticles for use as delivery vehicles in subunit vaccines.

Polymeric Particles as Antigen Delivery Vehicles

Polymer-based particles are promising vaccine adjuvants due to their synthetic addressability, tunability and their ability to perform the multiple functions necessary for the successful induction of an adaptive immune response. On the most basic level, particulate matter is efficiently and selectively taken up by phagocytic cells, which provides a basis for targeting APCs in the body. Beyond this, polymer-based antigen delivery systems can be engineered to interact with APCs in defined ways to produce specific immune responses. For example, carriers can be generated which present certain targeting or functional groups at the surface, release antigen at specific rates or under certain physiological conditions, localize to specific parts of the body, or mimic pathogens by delivering antigens simultaneously with activators of the innate immune system. This chapter focuses on the development of particulate antigen delivery vehicles from a polymer chemistry and materials science perspective, with an emphasis on how physicochemical properties, responsive polymers, and carrier design can be used to manipulate the immune system. There are obviously a large number of challenges and parameters to consider when developing polymeric subunit vaccines, but as a set of guiding principles, these new formulations should ideally (1) induce an appropriate immune response(s) for the disease of interest, (2) protect antigen from premature degradation before delivery to appropriate APCs, (3) generate immunity after a minimal number of doses, (4) be cost effective to produce and

transport, (5) not cause unwanted side effects or illness, and (6) be composed of biocompatible/biodegradable materials that can be readily cleared from the body.

PLGA-based Particles

By far, the most studied material for use in polymeric nano- and microparticulate antigen delivery vehicles is poly(lactic-co-glycolic acid) (PLGA), and the progress in this field has been reviewed extensively.[8,48-52] PLGA is an FDA approved material with an impressive safety record associated with its use in resorbable sutures and implantable devices. Its biocompatibility is due to the fact that PLGA slowly hydrolyzes to yield lactic and glycolic acid, two non-toxic metabolic intermediates. PLGA is readily available from a number of suppliers, including "good manufacturing practice" (GMP) grade material, and this accessibility has led to an enormous amount of research by investigators in the fields of engineering, materials science, and immunology. However, several significant challenges exist with the use of PLGA in antigen delivery vehicles, an application it was not originally designed for, and addressing these obstacles has been the focus of a large body of work. One major problem involves the generation of acidic byproducts, which can cause an extremely acidic microenvironment inside PLGA particles and subsequently lead to antigen stability issues.[48,53] To circumvent this problem, O'Hagan and co-workers have studied the use of charged PLGA-based particles with surface adsorbed protein antigens.[50,51] Additionally, it is well known that PLGA particles suffer from an initial "burst release" phase in which a large portion of encapsulated antigen is released in an uncontrolled fashion.[54,55] Following this phase, PLGA-based materials slowly release the remainder of their encapsulated cargo, typically over the course of several weeks, and a large amount of research has been carried out to obtain better control over this process.[52,56] Despite these issues, a wealth of knowledge has been generated using PLGA-based materials and this knowledge will unquestionably be valuable in the design of new polymers and materials for use in particulate antigen delivery vehicles.

Stimuli Responsive Particle Systems

In contrast to PLGA, which was originally designed to degrade slowly in the body, there exist a number of polymeric delivery systems which have been engineered to rapidly release their cargo under specific biological conditions.[57,58] For the purpose of delivering protein or peptide antigens to APCs, the most relevant stimuli for antigen release include acidic and oxidizing environments, both of which are found in phagolysosomal compartments where particulate delivery vehicles are processed.[16,59] These systems therefore have the potential to deliver a concentrated bolus of antigen and immunomodulatory agents directly to APCs, a process which mimics the uptake and destruction of actual pathogens by phagocytic cells of the immune system. The rate of payload release under the conditions of interest is an important parameter to consider and could be useful in optimizing the timing of APC maturation and antigen presentation such that predictable and robust adaptive immune responses are generated.[60,61] The slow and sustained release of antigen from PLGA has been proposed as a method to reduce or eliminate the need for vaccine booster doses. However, release of antigen over the course of weeks to months may not be ideally suited to the timescale of biological/immunological processes. For example, following uptake of fluorescently labeled particulate probes, mouse bone marrow-derived macrophages acidify their phagosomes within minutes[62] and mouse DCs migrate to draining lymph nodes for antigen presentation to T cells within 18 hours.[63] In some cases, the use of stimuli-responsive materials may alter the strength

or type of immune response generated and in some applications, may lead to more desirable results compared to slow-release systems, though different types of carriers should be tested side-by-side for accurate comparisons to be made.

Oxidation-Sensitive Delivery Vehicles

Pathogens taken up by APCs are initially subjected to an antimicrobial "superoxide burst" in the phagosome.[59,64] Superoxide is produced by the NADPH oxidase complex and can be converted into other reactive oxygen species (ROS) such as hydrogen peroxide.[64] Using an oxidation-sensitive fluorescent probe, Russel et al. have demonstrated in bone marrow-derived macrophages, that IgG-coated silica beads are subjected to intense oxidative activity for only about 20-25 mins following phagocytosis, suggesting that the NADPH oxidase complex is only active for a relatively short period of time.[65] In contrast to the relatively short superoxide burst in macrophages, it has been observed that bone marrow-derived DCs (BMDCs) produce sustained levels of ROS for approximately three hours following phagocytosis of a latex bead.[66] This process actually causes the alkalinization of phagosomes for the first several hours, which is hypothesized to lead to decreased proteolytic activity and thus better control over the generation of peptide epitopes for subsequent presentation to T cells.[66-68] Given its implications for antigen processing and presentation, novel materials that respond to the oxidative conditions found in APCs may be useful in the initiation of well-defined immune responses.

One such oxidation-sensitive polymeric particle system has been developed by Rehor et al., and is based on crosslinked poly(propylene sulfide) (PPS).[69,70] These particles are synthesized using an emulsion-based anionic polymerization of propylene sulfide using a four-armed thiolate initiator. During the course of the polymerization, a Pluronic surfactant is incorporated into the particle matrix at the surface to yield a hydrophilic poly(ethylene glycol) (PEG) corona. In order to increase stability and prevent agglomeration, the particles must be further crosslinked by exposure to air, which creates disulfide bonds between the PPS thiol chain ends. Under oxidative conditions, the hydrophobic poly(sulfide) core is converted to hydrophilic poly(sulfoxides) and poly(sulfones), thus creating an oxidation-sensitive solubility switching mechanism. Indeed, when exposed to 5% H_2O_2, these particles were found to first swell and then become completely water-soluble over the course of several days. Although the immunological relevance of various physicochemical properties (e.g., the size and surface chemistry) of this PPS-based particle system has been extensively investigated,[70-72] the importance of its oxidation-sensitive degradation mechanism and its possible effects on immunological activity have yet to be determined.

Acid-Sensitive Delivery Vehicles

In addition to an oxidative burst, pathogens or other matter phagocytosed by APCs are exposed to acidic conditions, which are critical for the activity of proteolytic enzymes.[59] During their maturation process phagosomes fuse with lysosomes, forming phagolysosomes, which contain ATP-driven proton pumps that lower the pH of the vesicle.[73] Macrophages tend to acidify their phagosomes relatively quickly, reaching pH 5 in as short as 12-15 minutes, when probed with dye-labeled silica beads.[62] Acidification in DCs has been found to occur more slowly, on the order of several hours,[66] although the extent and rate of acidifcation appears to be influenced by factors such as the size of the internalized particulate matter[74] and the maturation state[75] or the subpopulation[68] of DCs under study.

Polymeric particles that respond to the near 250-fold difference in proton concentration between physiological (pH 7.4) and phagolysosomal (pH ~5.0) conditions have been investigated as materials for the controlled delivery of antigens and immunomodulatory agents. In general, these vehicles are prepared from (1) polymers that contain amine groups that become protonated at pH values near 5.0 or (2) neutral polymers that contain hydrolyzable linkages which degrade significantly faster under acidic conditions compared to physiological conditions. Interestingly, delivery vehicles made from both types of polymers affect immune responses in a similar way, though presumably through different mechanisms. Specifically, delivery of antigen to APCs using pH-sensitive particulate vehicles leads to enhanced MHC class I presentation of the associated antigen. Based on the pioneering work of Rock et al., it is well known that directing antigen into the phagocytic uptake pathway using *any* type of particulate carrier causes increased class I presentation relative to the soluble version of that antigen.[76-78] However, it has been shown by our laboratory and others, using several different polymeric systems, that the use of an acid-sensitive carrier significantly increases the level of class I antigen presentation compared to non-responsive, non-degradable, or slowly-degrading vehicles. This finding is significant because antigen presentation *via* MHC I molecules is necessary for the induction of CTL responses, which are typically not generated using alum, the only adjuvant currently approved for use in the US.[8] Examples of the two types of pH-sensitive antigen delivery vehicles, their immunological activity and possible mechanisms by which they enhance MHC class I antigen presentation are discussed below in more detail.

Acid-sensitive carriers based on amine-containing polymers

The first class of acid-sensitive antigen delivery vehicles relies on the protonation of amine moieties that are pendant to, or incorporated into the backbone of the polymeric carrier. To obtain a pH-sensitive material that specifically targets phagolysosomal conditions, the pK_a of the protonated amine moieties should be approximately 5-7 such that the polymer is not significantly protonated under physiological conditions (pH 7.4), but becomes readily ionized in a mature phagosome (~ pH 5). Beyond an increase in charge, protonation may also cause the polymeric vehicle to swell or become water-soluble due to an increase in hydrophilicity compared to the uncharged material. Delivery vehicles of this type have been extensively studied for gene delivery and DNA vaccine applications due to their ability to disrupt endosomes/phagosomes and deliver their associated cargo to the cytoplasm of a cell.[40,79] The proposed mechanism for cytoplasmic delivery is often referred to as the "proton sponge effect," in which the buffering capacity of amine-containing materials is thought to increase chloride counter ion concentrations, and thus the osmotic pressure in vesicles undergoing acidification, which ultimately leads to membrane destabilization and leakage of its contents into the cytoplasm.[80,81] In terms of the immune system, using pH-sensitive vehicles to deliver a peptide or protein antigen into the cytoplasm of an APC thus provides a direct route for accessing the classical MHC class I antigen presentation pathway[16] (i.e., degradation of cytosolic proteins by the proteosome followed by transport of the peptide fragments to the endoplasmic reticulum for loading onto MHC class I molecules), and largely explains their observed immunological activity.

Despite their ability to direct antigen presentation, it is well known from the gene delivery literature that proton sponge-like materials often exhibit unacceptable levels of cytotoxicity. To mitigate their inherent toxicity, pH-sensitive polymers may be blended with other, more biocompatible materials.[40,82,83] For example, Kohane and co-workers have prepared

microparticles for antigen delivery by blending 20% (w/w) of the pH-sensitive polymer Eudragit E100 (a copolymer prepared from a 1:2:1 ratio of the monomers butyl methacrylate, 2-(*N*,*N*-dimethylamino)ethyl methacrylate, and methyl methacrylate) with 80% (w/w) of the relatively inert phospholipid, dipalmitoyl-phosphatidylcholine.[84,85] Using a spray drying technique, these researchers were able to formulate particles (~ 4-6 μm in diameter) from these two components that were capable of encapsulating a model MHC class I-restricted peptide antigen derived from the influenza A matrix protein.[85] Despite the relatively large weight percent of the phospholipid component, these particles were found to be non-toxic only below concentrations of 10 μg/mL when cultured with human DCs. However, the microparticles were found to possess desirable immunological activity at concentrations well below this threshold. Importantly, when tested *in vitro*, particles containing the pH-sensitive polymer were found to elicit significantly higher levels of stimulation of antigen-specific $CD8^+$ T cells when compared to soluble peptide or otherwise identical particles in which the Eudragit E100 polymer was replaced with the pH-insensitive material, poly(2-hydroxyethyl methacrylate).

In another approach to reduce the toxicity of antigen delivery vehicles containing proton sponge-like materials, Hu and co-workers have developed pH-sensitive particles with a core-shell architecture.[86,87] Using a two-stage emulsion polymerization technique, these researchers synthesized particles containing a crosslinked pH-sensitive core, composed of poly(2-(*N*,*N*-diethylamino)ethyl methacrylate), surrounded by a pH-insensitive shell, composed of poly(2-aminoethyl methacrylate). Compared to the tertiary amines in the core (pK_a ~ 7), the primary amines in the shell (pK_a ~ 11) are more basic and should therefore remain protonated over the entire range of physiologically relevant pH values. The authors propose that the cationic shell could serve not only as a means to adsorb antigen or other therapeutic payloads to the particle, but also as hydrophilic shield capable of physically sequestering the membrane-disruptive, and potentially toxic hydrophobic particle core. Indeed, when tested at a concentration of 25 μg/mL in a DC-like cell line (DC2.4), these pH-sensitive core-shell particles were found to exhibit minimal toxicity whereas similar particles lacking a hydrophilic shell were significantly cytotoxic.[86] Additionally, the core-shell particles were convincingly shown to facilitate endosomal escape of a membrane-impermeable fluorophore in DC2.4 cells; this activity was found to be dependent on the presence of a pH-sensitive core (as verified using otherwise identical particles made with a pH-insensitive core of poly(methyl methacrylate) and the ability of cells to acidify their endosomal compartments, but not dependent on the presence of the cationic shell layer, suggesting the critical importance of the responsive core material. Consistent with other proton sponge materials, these particles were found to significantly enhance MHC class I antigen presentation. When tested in BMDCs, pH-responsive core-shell particles with the model antigen ovalbumin (OVA) adsorbed to their cationic surface led to stimulation of OVA-specific $CD8^+$ T cells at 100-fold lower concentrations compared to soluble antigen or particles containing a pH-insensitive core.[87] Despite these promising results, *in vivo* use of these core-shell particles for vaccine delivery applications may be limited by biocompatibility issues surrounding the non-degradable vinyl polymer backbone and the fact that cells other than APCs were found to readily internalize these highly cationic particles.

Acid-sensitive vehicles based on the degradation of neutral polymers

Perhaps due to the biocompatibility issues mentioned above, the majority of polymers classically studied for drug delivery applications are neutral (i.e., poly(esters), poly(ethers), poly(anhydrides), poly(acrylamides) and poly(acrylates)). A minority of these polymers,

including poly(acetals) and poly(ortho esters), contain hydrolyzable linkages that degrade faster under phagolysosomal conditions (pH ~ 5) compared to physiological conditions (pH 7.4). Four generations of poly(ortho esters) have been developed over their nearly 40 year history,[88,89] with recent vaccine-related work involving the latest generation of these polymers focused mainly on gene delivery approaches.[61,83] On the other hand, our laboratory has had significant experience in the study of poly(acetals) and other acetal-containing materials, mainly in the area of particulate protein antigen delivery vehicles. Similar to the carriers based on amine-containing polymers discussed above, use of acetal-based, acid-sensitive delivery vehicles leads to enhanced MHC class I antigen presentation compared to slowly-degrading or non-degradable systems. The first possible explanation for this observed activity, known as the "colloid osmotic mechanism," is predicated on the hypothesis that the generation of a large concentration of small molecule or polymeric byproducts from the degradation of a particulate vehicle can lead to an increase in osmotic pressure and the subsequent destabilization of endosomal vesicles.[90,91] Conceptually similar to the proton sponge effect, this proposed mechanism thus provides a direct route into the classical MHC I processing pathway through disruption of phagolysosomal vesicles and cytosolic antigen delivery. An alternate mechanism for the observed immunological activity of acid-degradable antigen carriers is based on the phenomenon known as cross-presentation, or the inherent ability of APCs to present exogenous antigens to $CD8^+$ T cells.[20-22] Although less well understood than the classical antigen presentation pathways, cross-presentation of phagocytosed antigens may occur through (1) the "phagosome-to-cytosol pathway," in which antigens are transported from phagosomal compartments to the cytosol for processing by the traditional class I machinery, (2) the "phagosome-to-cytosol-to-phagosome" pathway, which is similar to the previous pathway except antigenic peptides produced by the proteasome are transported from the cytosol back into phagosomes where they bind MHC I molecules and are transported to the cell surface, or (3) by the "vacuolar pathway," in which production of antigenic peptides and subsequent loading onto MHC I molecules occurs entirely within endocytic vacuoles.[21] In any case, cross-presentation is generally considered an inefficient process, and is typically observed experimentally only using high antigen concentrations. Delivery vehicles which degrade quickly under acidic conditions and release a bolus of antigen in phagolysosomal compartments may therefore enhance class I presentation simply by providing a high local concentration of protein for the cross-presentation machinery to process.[92] It should be noted that this mechanism may partially be responsible for some of the effects seen with Eudragit/phospholipid particles described above, as these particles demonstrated a pronounced antigen release profile when exposed to acidic conditions.

Our laboratory began investigating the use of acid-sensitive particles for protein-based vaccines in 2002 when we reported the synthesis of acetal-crosslinked poly(acrylamide) hydrogel microparticles.[93] These vehicles, which served largely as a proof-of-concept platform to test a number of hypotheses, were prepared using an inverse emulsion free radical polymerization technique that allowed for the facile encapsulation of protein antigens and the incorporation of a number of functional monomers, including immunostimulatory agents.[63,93-103] Upon exposure to acidic conditions, these microparticles were designed to rapidly degrade *via* hydrolysis of the acetal crosslinks, releasing the encapsulated protein cargo, linear poly(acrylamide) chains and small molecules derived from the crosslinker. Particle degradation and protein release were found to be pH-dependent, influenced slightly by the degree of crosslinking, and to occur on the order of hours or minutes when using a *para*-alkoxy benzylidene[94] or dimethyl[98] acetal crosslinker, respectively. When tested *in vitro* using OVA as a

model antigen, these particles were found to significantly enhance presentation of the OVA-derived immunodominant MHC class I-restricted peptide SIINFEKL ($OVA_{258-265}$) relative to soluble OVA[94] and otherwise identical particles prepared with the non-degradable crosslinker *N*,*N*'-methylene bisacrylamide.[96] Additionally, these particles demonstrated the ability to generate an OVA-specific CTL response and enhance survival in a cancer immunotherapy experiment performed in mice.[96] Despite these promising results, the microparticles discussed above were only intended for use as a proof-of-concept platform due to concerns over the potential for toxicity caused by residual acrylamide monomers and the lack of biodegradability of the high molecular weight poly(acrylamide) degradation byproducts.

In an effort to generate a more biocompatible acid-degradable particle system capable of degrading entirely into innocuous small molecules, our laboratory and others have investigated linear poly(acetals) for use in antigen delivery vehicles. Various strategies have been used to produce polymers with acetals in the backbone including metathesis chemistry,[104] reaction of diols with divinyl ethers,[105] acetal exchange reactions,[106-108] or reaction of an acetal-containing diamine with bis(active carbonate/carbamate) or diisocyanate monomers.[109,110] For successful particle formation and encapsulation of protein antigens using traditional emulsion-evaporation methods[111] (i.e., those designed for PLGA-based particles), these polymers must be hydrophobic, soluble in organic solvents, and solids. In analogy with trends observed in the poly(ortho ester) literature,[88,89] poly(acetals) with the extremely sensitive dimethyl acetal linkage in the backbone tend to degrade very slowly under acidic conditions, with kinetics that are dependent largely on the hydrophobicity of the polymer. Even minor changes to the structure of the polymer repeat unit, such as the addition of a few carbon atoms, have been found to significantly affect the degradation rate of poly(acetal) microparticles.[110] The need to strike the often difficult balance between polymer hydrophobicity (for particle formulation considerations), hydrophilicity (for reasonable degradation kinetics), and crystalinity has led researchers to explore synthetic approaches based on the generation of polymer libraries,[110] or alternatively, copolymers made from a mixture of hydrophobic and hydrophilic monomers.[108] Despite the demanding materials requirements described above, our laboratory was able to prepare poly(acetal)-based antigen-loaded microparticles that were found to degrade in a pH-dependent manner with a half-life at pH 5.0 of approximately three hours.[110] These particles were found to be non-toxic in a murine macrophage cell line up to the highest concentration tested of 1 mg/mL. Additionally, the small molecule byproduct derived from these particles was independently synthesized and found to be non-toxic at concentrations up to 6 mg/mL; using a liquid chromatography-mass spectrometry method, we also detected the intracellular production and subsequent exocytosis of this small molecule byproduct in macrophages.[109] Importantly, when compared to free antigen or otherwise identical particles made from a slower-degrading poly(acetal) analog ($t_{1/2}$ ~ 80 hours at pH 5), these fast-degrading OVA-loaded particles were found to generate significantly enhanced class I antigen presentation in BMDCs as well as induce significantly higher CTL activity in mice.[109]

In an effort to combine the positive attributes of the two acetal-based particle systems described above, namely the tunability of the former and the biocompatibility of the latter, our laboratory has recently developed a third generation of acid-degradable antigen delivery vehicles. For this system we chose to employ acetals as acid-sensitive protecting groups, a role they are perhaps best known for in synthetic organic chemistry, and not as degradable linkages embedded in the backbone of a polymeric material. In a one step reaction, acetals were used to mask the hydroxyl groups of dextran, rendering this biopolymer insoluble in water, but freely soluble in a number of organic solvents used in common techniques for the fabrication of

antigen-loaded polymeric particles.[112,113] Upon exposure to acidic conditions, acetalated-dextran (Ac-DEX) particles are designed to degrade *via* hydrolysis of the acetal protecting groups, releasing the encapsulated cargo and generating native dextran[114] (a thoroughly vetted, clinically approved biopolymer) and minimal amounts of small molecule byproducts. When tested in two different cell lines, Ac-DEX was very well tolerated, with a toxicity profile exactly mirroring that of the ubiquitous polyester PLGA.[112] Perhaps the most fascinating feature of Ac-DEX is that the degradation rate is easily tuned by modulating a single reaction parameter, time, which dictates the degree and type of acetal modification of the dextran backbone.[113] By varying the ratio of faster-degrading acyclic acetals to slower-degrading cyclic acetals, a range of materials were prepared with particle degradation rates spanning two orders of magnitude (from 16 minutes to 27 hours at pH 5.0). When tested in BMDCs using OVA-loaded particles, degradation rate was found to significantly affect not only the level of MHC class I antigen presentation, but also the involvement of TAP, and thus potentially the biological mechanism by which cross-presentation was occurring. Moreover, fast-degrading Ac-DEX particles were found to induce 10-fold higher levels of class I antigen presentation in an *in vitro* assay when compared side-by-side with particles made from PLGA, iron oxide, or slow-degrading Ac-DEX. The *in vivo* relevance of particle degradation rate has yet to be shown with this polymer system, but it may prove significant given the report by Wang et al. suggesting the importance of synchronizing the timing of APC maturation and migration with plasmid release kinetics from poly(ortho ester) particles used for DNA vaccines.[60,61]

Methods for Targeting Polymeric Particles to APCs

For many drug delivery applications, carrier systems are intentionally designed to avoid interactions with the immune system and minimize clearance by phagocytes.[115-117] However, for vaccines, there is significant interest in precisely controlling the details of delivery vehicle recognition and enhancing uptake by phagocytic cells, especially APCs. Because they are considered critical for the induction of adaptive immunity, various strategies have also been investigated for targeting polymeric particles specifically to DCs. In addition, it should be noted that several groups have explored the complimentary strategy of using chemoattractants to direct the migration of APCs to the site of polymeric materials.[118,119] In general, new strategies for targeting APCs should be evaluated *in vivo*, as complex physiological environments and particle trafficking phenomena are difficult to replicate *in vitro*. Below, we focus on recent methods for targeting particles to APCs based on conjugating ligands to their surface or modulating their size. Other physicochemical properties such as shape and charge are also important factors affecting particle uptake, however these two parameters appear to be less promising for promoting APC-specific targeting. For example, cationic particles are known to enhance phagocytosis, presumably through interactions with the negatively charged cell membrane.[120,121] However, cationic materials are often toxic and they can be internalized by non-phagocytic cells,[87,122] thus attenuating any potential advantages. Additionally, macrophages have been found to phagocytose particles of many different shapes,[123] with the only exception being materials having high aspect ratios, such as the "worm-like" particles described by Champion et al.[124] Therefore spherical particles, which are by far the most commonly employed carrier geometry, represent a reasonable choice for antigen delivery vehicles.

Effect of Particle Size

Despite a large number of studies, there remains considerable disagreement in the literature over the optimal size for polymeric particulate antigen carriers. For example, O'Hagan et al. advocate the use of microparticles with sizes in the range of 1-3 μm,[50] whereas Plebanski and co-workers propose that smaller particles with diameters of 40-100 nm are the optimal size.[125-127] Indeed, particles with sizes spanning the range of viruses to bacteria (~ 20 nm – 5 μm) are internalized effectively by APCs,[120,128,129] and it seems plausible that size-related effects may be dependent on a number of variables including the specific polymeric carrier material under investigation, particle surface chemistry, method of antigen attachment (entrapped vs. adsorbed antigen), route of administration, and use of immunomodulatory agents. Therefore, like many other parameters, identifying the optimal size(s) for novel particulate antigen delivery vehicles may require experimental verification, especially in the context of a desired immune response or a particular disease.[102,125]

While difficult to assign an ideal size for all polymeric antigen carriers, several groups have recently demonstrated that particle size can be used to target distinct populations of APCs *in vivo*. Following intradermal administration, polymeric particles typically remain at the injection site where they are taken up and transported to draining lymph nodes by peripheral APCs.[63,130] However, particles with diameters below approximately 100 nm have been found to traffic efficiently to draining lymph nodes *via* convective transport through lymphatic capillaries.[71,72,131] These particles thus have the potential to interact with lymph-node resident APCs, including a number of DC subtypes which were recently found to exist predominantly in an immature state.[132] Using the PEG-stabilized, oxidation-sensitive particle system described above, Reddy and co-workers have demonstrated in mice that nanoparticles with diameters of 20-45 nm traffic to draining lymph nodes where they are efficiently retained and internalized by APCs.[71] For example, 24 hours after intradermal administration, 25 nm particles were found in approximately 50% of DCs ($CD11c^+$ cells) present in the draining lymph node, whereas 100 nm particles were found in only 6% of these cells.[72] In a similar report, Manolova et al. used fluorescently-labeled polystyrene particles and analysis of cell surface markers to determine which APC populations were targeted by different particle sizes.[131] After administration into the footpads of mice, 1000 nm particles were transported to popliteal lymph nodes largely by DCs, which were primarily derived from skin-resident phagocytic monocytes ($CD11c^+$, $CD8\alpha^-$, $CD40^{low}$, $CD205^{low/-}$). A smaller number of these particles were also found in $CD205^+$ DCs, which may correspond to Langerhans cells, an epidermal DC subtype. On the other hand, 20 nm particles were found to freely traffic to the draining lymph node where they were internalized primarily by macrophages ($CD11c^-$, $CD11b^+$, ~70% of the particle positive cells), and to a lesser extent by DCs ($CD11c^+$). A small portion of these DCs were identified with dermal ($CD11c^{high}$, $CD40^{hi}$, $CD205^{low/-}$) or plasmacytoid ($PDCA\text{-}1^+$) phenotypes, with the remainder characterized as lymph node-resident myeloid DCs ($CD11c^{high}$, $CD40^{int}$), including a large number of $CD8\alpha^+$ cells. Significantly, $CD8\alpha^+$ DCs are thought to preferentially induce CTL-mediated[133] and T_h1-type immune responses.[134] Given the therapeutic potential of targeting discrete classes of APCs based on particle size, it will prove interesting whether the findings discussed above are widely applicable to other polymeric antigen delivery systems.

To date, the majority of studies addressing the role of particle size have been performed with polystyrene beads,[120,125,127-129,131] which can be synthesized with narrowly defined sizes using emulsion-based polymerizations. As current methods such as emulsion-evaporation[111] and spray-drying[84] procedures often generate particles with broad size distributions, novel particle

fabrication techniques may be required to accurately determine size-dependent effects in newly designed biocompatible materials. In one such approach, Oh et al. have developed a procedure for the synthesis of crosslinked acrylate-based hydrogel particles using atom transfer radical polymerization (ATRP) in inverse miniemulsions.[135-137] In addition to the precise control over particle size typically afforded by emulsion-based polymerizations, use of ATRP produces materials that degrade to yield well-defined polymeric byproducts ($M_W/M_n < 1.5$) with molecular weights small enough to be eliminated from the body. Besides synthetic approaches, several "top-down" engineering-based strategies have been developed, which are capable of producing homogeneous particles with precise control over size and shape.[138-140] One especially promising strategy pioneered by DeSimone and co-workers, and referred to as "particle replication in non-wetting templates" (PRINT), is predicated on the fabrication of particle molds from perfluoropolyether-based materials.[141,142] Using the PRINT technology, monodisperse particles have been prepared from a number of polymeric materials with a wide range of physicochemical properties including size, shape and deformability.[143] Beyond serving as a platform for pursuing a number of fundamental scientific questions, PRINT may eventually provide a means for manufacturing precisely controlled, GMP-grade polymeric antigen delivery vehicles.

Use of Targeting Groups

The second approach for the *in vivo* targeting of polymeric antigen carriers to APCs involves the use of molecules specific for a number of cell surface receptors. Of particular interest are a number of endocytosis/phagocytosis receptors such as scavenger receptors, Fc receptors, and the C-type lectin family, which includes the mannose receptor, DC-SIGN, Dectin-1, Dectin-2, and CD205 (also known as DEC-205).[144,145] Based on their expression profiles, DC-SIGN and CD205 are thought to be promising candidates for promoting DC-specific targeting. A large number of studies in the immunology literature have investigated targeting antigen to these APC receptors using water-soluble constructs such as fusion proteins or antigens conjugated to receptor ligands or antibodies.[144,145] From these studies, it is becoming clear that directing antigen to specific receptors is useful not only as a targeting strategy, but also as a means to control antigen presentation and the generation of specific immune responses. For example, several reports have suggested that targeting antigen to the mannose receptor significantly enhances cross-presentation[146] and the generation of CTL responses.[147]

Interestingly, there have been relatively few reports on the use of APC-targeting agents in conjunction with polymeric particulate protein carriers.[148,149] In contrast to the soluble systems described above, the internalization of polymeric particles by APCs may be influenced by a number of factors, including their charge, size and surface chemistry.[120] Further, proteins in biological fluids (opsonins) are known to adsorb very rapidly to the surface of polymeric particles, especially those made from hydrophobic materials, thus significantly altering their original surface chemistry and potentially masking any surface-bound targeting groups.[116,120,150] To circumvent this problem, several groups have investigated the functionalization of particles with mannose receptor ligands conjugated to the exterior of a hydrophilic PEG layer.[151,152] In one report, Wattendorf et al. synthesized a poly(L-lysine)-*graft*-PEG copolymer with mono- and trimannose ligands attached as terminal substitutions on the PEG chains.[151] After adsorbing this polymer onto anionic polystyrene microparticles, these researchers verified that the PEG shielded the particles from protein adsorption, and also that the mannose moieties were accessible to receptors using a fluorescently-labeled lectin. However, when tested in human monocyte-derived macrophages and DCs, the mannose-modified particles were actually taken up

less efficiently than unmodified polystyrene particles, perhaps reflecting the well-known capacity of PEG coatings to inhibit phagocytosis.

In another example of using an APC-targeting group attached to a hydrophilic carrier, Kwon et al. have described the conjugation of monoclonal anti-CD205 antibodies to the acid-degradable acrylamide-based hydrogel particles discussed above.[63] In this report, a primary amine-containing monomer was included in an inverse emulsion polymerization to produce antigen-loaded particles bearing reactive amine groups. Anti-CD205 antibodies were subsequently conjugated to these particles using a bis(sulfosuccinimidyl ester) reagent. Following injection in mice, these particles were found in a higher number of $CD205^+$ DCs in the draining lymph node, and to slightly enhance the generation of an OVA-specific CTL response when compared to otherwise identical particles conjugated to an isotype antibody. Although this study demonstrates the potential for targeting polymeric particulate antigen carriers to APCs, it remains to be determined how effective this strategy will be in other, more biocompatible particle systems, including those made from hydrophobic polymers. Future work in this area will require the development of mild and selective particle functionalization strategies[153] as well as extensive *in vivo* characterization of targeted antigen carriers.

References

(1) Behbehani, A. M. *Microbiol. Rev.* **1983**, *47*, 455-509.
(2) CDC. List of Vaccine-Preventable Diseases. http://www.cdc.gov/vaccines/vpd-vac/vpd-list.htm (2/11/2010).
(3) Wilson, C. B.; Marcuse, E. K. *Nat. Rev. Immunol.* **2001**, *1*, 160-165.
(4) FDA. Complete List of Vaccines Licensed for Immunization and Distribution in the US. http://www.fda.gov/BiologicsBloodVaccines/Vaccines/ApprovedProducts/ucm093833.htm (2/11/2010).
(5) Horaud, F. *Biologicals* **1993**, *21*, 311-316.
(6) Pulendran, B. *Nat. Rev. Immunol.* **2009**, *9*, 741-747.
(7) Offit, P. A. *N. Engl. J. Med.* **2005**, *352*, 1411-1412.
(8) Wilson-Welder, J. H.; Torres, M. P.; Kipper, M. J.; Mallapragada, S. K.; Wannemuehler, M. J.; Narasimhan, B. *J. Pharm. Sci.* **2009**, *98*, 1278-1316.
(9) Sheng, K. C.; Pietersz, G. A.; Wright, M. D.; Apostolopoulos, V. *Curr. Med. Chem.* **2005**, *12*, 1783-1800.
(10) Apostolopoulos, V.; Weiner, D. B.; Gong, J. L. *Expert Review of Vaccines* **2008**, *7*, 861-862.
(11) Goldman, B.; DeFrancesco, L. *Nat. Biotechnol.* **2009**, *27*, 129-139.
(12) Janeway, C.; Travers, P.; Walport, M.; Shlomchik, M. *Immunobiology : The Immune System in Health and Disease* 6th ed.; Garland Science Publishing: New York, 2005.
(13) Banchereau, J.; Steinman, R. M. *Nature* **1998**, *392*, 245-252.
(14) Steinman, R. M.; Banchereau, J. *Nature* **2007**, *449*, 419-426.
(15) Jensen, P. E. *Nat. Immunol.* **2007**, *8*, 1041-1048.
(16) Savina, A.; Amigorena, S. *Immunological Reviews* **2007**, *219*, 143-156.
(17) Wing, K.; Sakaguchi, S. *Nat. Immunol.* **2010**, *11*, 7-13.
(18) Coffman, R. L. *Nat. Immunol.* **2006**, *7*, 539-541.
(19) Dong, C. *Nat. Rev. Immunol.* **2008**, *8*, 337-348.
(20) Heath, W. R.; Carbone, F. R. *Nat. Rev. Immunol.* **2001**, *1*, 126-134.
(21) Rock, K. L.; Shen, L. *Immunological Reviews* **2005**, *207*, 166-183.
(22) Vyas, J. M.; Van der Veen, A. G.; Ploegh, H. L. *Nat. Rev. Immunol.* **2008**, *8*, 607-618.
(23) Janeway, C. A.; Medzhitov, R. *Annu. Rev. Immunol.* **2002**, *20*, 197-216.
(24) Akira, S.; Uematsu, S.; Takeuchi, O. *Cell* **2006**, *124*, 783-801.
(25) Takeda, K.; Kaisho, T.; Akira, S. *Annu. Rev. Immunol.* **2003**, *21*, 335-376.
(26) Barton, G. M.; Kagan, J. C. *Nat. Rev. Immunol.* **2009**, *9*, 535-542.
(27) Iwasaki, A.; Medzhitov, R. *Nat. Immunol.* **2004**, *5*, 987-995.
(28) Schwartz, R. H. *Annu. Rev. Immunol.* **2003**, *21*, 305-334.
(29) Mueller, D. L. *Nat. Immunol.* **2010**, *11*, 21-27.
(30) Friede, M.; Aguado, M. T. *Adv. Drug Delivery Rev.* **2005**, *57*, 325-331.
(31) Apostolopoulos, V. *Mol. Pharmaceutics* **2007**, *4*, 1-3.
(32) Ulmer, J. B.; Donnelly, J. J.; Parker, S. E.; Rhodes, G. H.; Felgner, P. L.; Dwarki, V. J.; Gromkowski, S. H.; Deck, R. R.; Dewitt, C. M.; Friedman, A.; Hawe, L. A.; Leander, K. R.; Martinez, D.; Perry, H. C.; Shiver, J. W.; Montgomery, D. L.; Liu, M. A. *Science* **1993**, *259*, 1745-1749.
(33) Gurunathan, S.; Klinman, D. M.; Seder, R. A. *Annu. Rev. Immunol.* **2000**, *18*, 927-974.
(34) Brave, A.; Ljungberg, K.; Wahren, B.; Liu, M. A. *Mol. Pharmaceutics* **2007**, *4*, 18-32.

(35) Muruve, D. A. *Hum. Gene Ther.* **2004**, *15*, 1157-1166.
(36) Check, E. *Nature* **2002**, *420*, 116-118.
(37) Check, E. *Nature* **2003**, *421*, 305.
(38) Check, E. *Nature* **2005**, *433*, 561.
(39) Luten, J.; van Nostrum, C. F.; De Smedt, S. C.; Hennink, W. E. *J. Control. Release* **2008**, *126*, 97-110.
(40) Nguyen, D. N.; Green, J. J.; Chan, J. M.; Longer, R.; Anderson, D. G. *Advanced Materials* **2009**, *21*, 847-867.
(41) Parsa, S.; Pfeifer, B. *Mol. Pharmaceutics* **2007**, *4*, 4-17.
(42) Grgacic, E. V. L.; Anderson, D. A. *Methods* **2006**, *40*, 60-65.
(43) Scheerlinck, J. P.; Greenwood, D. L. *Drug Discovery Today* **2008**, *13*, 882-887.
(44) Morein, B.; Sundquist, B.; Hoglund, S.; Dalsgaard, K.; Osterhaus, a. *Nature* **1984**, *308*, 457-460.
(45) Copland, M. J.; Rades, T.; Davies, N. M.; Baird, M. A. *Immunology and Cell Biology* **2005**, *83*, 97-105.
(46) Pearse, M. J.; Drane, D. *Adv. Drug Delivery Rev.* **2005**, *57*, 465-474.
(47) Peek, L. J.; Middaugh, C. R.; Berkland, C. *Adv. Drug Delivery Rev.* **2008**, *60*, 915-928.
(48) Jiang, W.; Gupta, R. K.; Deshpande, M. C.; Schwendeman, S. P. *Adv. Drug Delivery Rev.* **2005**, *57*, 391-410.
(49) Waeckerle-Men, Y.; Groettrup, M. *Adv. Drug Delivery Rev.* **2005**, *57*, 475-482.
(50) O'Hagan, D. T.; Singh, M.; Ulmer, J. B. *Methods* **2006**, *40*, 10-19.
(51) Singh, M.; Kazzaz, J.; Ugozzoli, M.; Malyala, P.; Chesko, J.; O'Hagan, D. T. *Curr. Drug Delivery* **2006**, *3*, 115-120.
(52) Mundargi, R. C.; Babu, V. R.; Rangaswamy, V.; Patel, P.; Aminabhavi, T. M. *J. Control. Release* **2008**, *125*, 193-209.
(53) Fu, K.; Pack, D. W.; Klibanov, A. M.; Langer, R. *Pharm. Res.* **2000**, *17*, 100-106.
(54) Yeo, Y.; Park, K. N. *Arch. Pharmacal Res.* **2004**, *27*, 1-12.
(55) Allison, S. D. *Expert Opinion on Drug Delivery* **2008**, *5*, 615-628.
(56) Anderson, J. M.; Shive, M. S. *Adv. Drug Delivery Rev.* **1997**, *28*, 5-24.
(57) Alexander, C.; Shakesheff, K. M. *Advanced Materials* **2006**, *18*, 3321-3328.
(58) Tirelli, N. *Curr. Opin. Colloid Interface Sci.* **2006**, *11*, 210.
(59) Russell, D. G.; Vanderven, B. C.; Glennie, S.; Mwandumba, H.; Heyderman, R. S. *Nat. Rev. Immunol.* **2009**, *9*, 594-600.
(60) Pack, D. W. *Nat. Mater.* **2004**, *3*, 133.
(61) Wang, C.; Ge, Q.; Ting, D.; Nguyen, D.; Shen, H. R.; Chen, J. Z.; Eisen, H. N.; Heller, J.; Langer, R.; Putnam, D. *Nat. Mater.* **2004**, *3*, 190-196.
(62) Yates, R. M.; Hermetter, A.; Russell, D. G. *Traffic* **2005**, *6*, 413-420.
(63) Kwon, Y. J.; James, E.; Shastri, N.; Frechet, J. M. J. *Proc. Natl. Acad. Sci. U. S. A.* **2005**, *102*, 18264-18268.
(64) Winterbourn, C. C. *Nat. Chem. Biol.* **2008**, *4*, 278-286.
(65) VanderVen, B. C.; Yates, R. M.; Russell, D. G. *Traffic* **2009**, *10*, 372-378.
(66) Savina, A.; Jancic, C.; Hugues, S.; Guermonprez, P.; Vargas, P.; Moura, I. C.; Lennon-Dumenil, A. M.; Seabra, M. C.; Raposo, G.; Amigorena, S. *Cell* **2006**, *126*, 205-218.
(67) Jancic, C.; Savina, A.; Wasmeier, C.; Tolmachova, T.; El-Benna, J.; Dang, P. M.; Pascolo, S.; Gougerot-Pocidalo, M. A.; Raposo, G.; Seabra, M. C.; Amigorena, S. *Nat. Cell Biol.* **2007**, *9*, 367-378.

(68) Savina, A.; Peres, A.; Cebrian, I.; Carmo, N.; Moita, C.; Hacohen, N.; Moita, L. F.; Amigorena, S. *Immunity* **2009**, *30*, 544-555.
(69) Rehor, A.; Hubbell, J. A.; Tirelli, N. *Langmuir* **2005**, *21*, 411-417.
(70) Rehor, A.; Schmoekel, H.; Tirelli, N.; Hubbell, J. A. *Biomaterials* **2008**, *29*, 1958-1966.
(71) Reddy, S. T.; Rehor, A.; Schmoekel, H. G.; Hubbell, J. A.; Swartz, M. A. *J. Control. Release* **2006**, *112*, 26-34.
(72) Reddy, S. T.; van der Vlies, A. J.; Simeoni, E.; Angeli, V.; Randolph, G. J.; O'Neill, C. P.; Lee, L. K.; Swartz, M. A.; Hubbell, J. A. *Nat. Biotechnol.* **2007**, *25*, 1159-1164.
(73) Sun-Wada, G. H.; Wada, Y.; Futai, M. *Cell Structure and Function* **2003**, *28*, 455-463.
(74) Tran, K. K.; Shen, H. *Biomaterials* **2009**, *30*, 1356-1362.
(75) Trombetta, E. S.; Ebersold, M.; Garrett, W.; Pypaert, M.; Mellman, I. *Science* **2003**, *299*, 1400-1403.
(76) Kovacsovics-Bankowski, M.; Clark, K.; Benacerraf, B.; Rock, K. L. *Proc. Natl. Acad. Sci. U. S. A.* **1993**, *90*, 4942-4946.
(77) Falo, L. D.; Kovacsovics-Bankowski, M.; Thompson, K.; Rock, K. L. *Nature Medicine* **1995**, *1*, 649-653.
(78) Kovacsovics-Bankowski, M.; Rock, K. L. *Science* **1995**, *267*, 243-246.
(79) Park, T. G.; Jeong, J. H.; Kim, S. W. *Adv. Drug Delivery Rev.* **2006**, *58*, 467-486.
(80) Sonawane, N. D.; Szoka, F. C.; Verkman, A. S. *J. Biol. Chem.* **2003**, *278*, 44826-44831.
(81) Akinc, A.; Thomas, M.; Klibanov, A. M.; Langer, R. *Journal of Gene Medicine* **2005**, *7*, 657-663.
(82) Little, S. R.; Lynn, D. M.; Puram, S. V.; Langer, R. *J. Control. Release* **2005**, *107*, 449-462.
(83) Nguyen, D. N.; Raghavan, S. S.; Tashima, L. M.; Lin, E. C.; Fredette, S. J.; Langer, R. S.; Wang, C. *Biomaterials* **2008**, *29*, 2783-2793.
(84) Kohane, D. S.; Anderson, D. G.; Yu, C.; Langer, R. *Pharm. Res.* **2003**, *20*, 1533-1538.
(85) Haining, W. N.; Anderson, D. G.; Little, S. R.; von Berwelt-Baildon, M. S.; Cardoso, A. A.; Alves, P.; Kosmatopoulos, K.; Nadler, L. M.; Langer, R.; Kohane, D. S. *J. Immunol.* **2004**, *173*, 2578-2585.
(86) Hu, Y.; Litwin, T.; Nagaraja, A. R.; Kwong, B.; Katz, J.; Watson, N.; Irvine, D. J. *Nano Lett.* **2007**, *7*, 3056-3064.
(87) Hu, Y. H.; Atukorale, P. U.; Lu, J. J.; Moon, J. J.; Um, S. H.; Cho, E. C.; Wang, Y.; Chen, J. Z.; Irvine, D. J. *Biomacromolecules* **2009**, *10*, 756-765.
(88) Heller, J.; Barr, J.; Ng, S. Y.; Abdellauoi, K. S.; Gurny, R. *Adv. Drug Delivery Rev.* **2002**, *54*, 1015-1039.
(89) Heller, J.; Barr, J. *Biomacromolecules* **2004**, *5*, 1625-1632.
(90) Okada, C. Y.; Rechsteiner, M. *Cell* **1982**, *29*, 33-41.
(91) Moore, M. W.; Carbone, F. R.; Bevan, M. J. *Cell* **1988**, *54*, 777-785.
(92) Howland, S. W.; Wittrup, K. D. *J. Immunol.* **2008**, *180*, 1576-1583.
(93) Murthy, N.; Thng, Y. X.; Schuck, S.; Xu, M. C.; Frechet, J. M. J. *J. Am. Chem. Soc.* **2002**, *124*, 12398-12399.
(94) Murthy, N.; Xu, M.; Schuck, S.; Kunisawa, J.; Shastri, N.; Frechet, J. M. *Proc. Natl. Acad. Sci. U. S. A.* **2003**, *100*, 4995-5000.
(95) Goh, S. L.; Murthy, N.; Xu, M. C.; Frechet, J. M. J. *Bioconjugate Chem.* **2004**, *15*, 467-474.

(96) Standley, S. M.; Kwon, Y. J.; Murthy, N.; Kunisawa, J.; Shastri, N.; Guillaudeu, S. J.; Lau, L.; Frechet, J. M. J. *Bioconjugate Chem.* **2004**, *15*, 1281-1288.
(97) Kwon, Y. J.; Standley, S. M.; Goh, S. L.; Frechet, J. M. J. *J. Control. Release* **2005**, *105*, 199-212.
(98) Kwon, Y. J.; Standley, S. M.; Goodwin, A. P.; Gillies, E. R.; Frechet, J. M. J. *Mol. Pharmaceutics* **2005**, *2*, 83-91.
(99) Standley, S. M.; Mende, I.; Goh, S. L.; Kwon, Y. J.; Beaudette, T. T.; Engleman, E. G.; Frechet, J. M. J. *Bioconjugate Chem.* **2007**, *18*, 77-83.
(100) Cohen, J. L.; Almutairi, A.; Cohen, J. A.; Bernstein, M.; Brody, S. L.; Schuster, D. P.; Frechet, J. M. J. *Bioconjugate Chem.* **2008**, *19*, 876-881.
(101) Beaudette, T. T.; Bachelder, E. M.; Cohen, J. A.; Obermeyer, A. C.; Broaders, K. E.; Frechet, J. M. J.; Kang, E. S.; Mende, I.; Tseng, W. W.; Davidson, M. G.; Engleman, E. G. *Mol. Pharmaceutics* **2009**, *6*, 1160-1169.
(102) Cohen, J. A.; Beaudette, T. T.; Tseng, W. W.; Bachelder, E. M.; Mende, I.; Engleman, E. G.; Frechet, J. M. J. *Bioconjugate Chem.* **2009**, *20*, 111-119.
(103) Liu, Y. J.; Ibricevic, A.; Cohen, J. A.; Cohen, J. L.; Gunsten, S. P.; Frechet, J. M. J.; Walter, M. J.; Welch, M. J.; Brody, S. L. *Mol. Pharmaceutics* **2009**, *6*, 1891-1902.
(104) Khaja, S. D.; Lee, S.; Murthy, N. *Biomacromolecules* **2007**, *8*, 1391-1395.
(105) Tomlinson, R.; Klee, M.; Garrett, S.; Heller, J.; Duncan, R.; Brocchini, S. *Macromolecules* **2002**, *35*, 473-480.
(106) Heffernan, M. J.; Murthy, N. *Bioconjugate Chem.* **2005**, *16*, 1340-1342.
(107) Lee, S.; Yang, S. C.; Heffernan, M. J.; Taylor, W. R.; Murthy, N. *Bioconjugate Chem.* **2007**, *18*, 4-7.
(108) Yang, S. C.; Bhide, M.; Crispe, I. N.; Pierce, R. H.; Murthy, N. *Bioconjugate Chem.* **2008**, *19*, 1164-1169.
(109) Bachelder, E. M.; Beaudette, T. T.; Broaders, K. E.; Paramonov, S. E.; Dashe, J.; Frechet, J. M. J. *Mol. Pharmaceutics* **2008**, *5*, 876-884.
(110) Paramonov, S. E.; Bachelder, E. M.; Beaudette, T. T.; Standley, S. M.; Lee, C. C.; Dashe, J.; Frechet, J. M. J. *Bioconjugate Chem.* **2008**, *19*, 911-919.
(111) Bilati, U.; Allemann, E.; Doelker, E. *Pharm. Dev. Technol.* **2003**, *8*, 1-9.
(112) Bachelder, E. M.; Beaudette, T. T.; Broaders, K. E.; Dashe, J.; Frechet, J. M. J. *J. Am. Chem. Soc.* **2008**, *130*, 10494-10495.
(113) Broaders, K. E.; Cohen, J. A.; Beaudette, T. T.; Bachelder, E. M.; Frechet, J. M. J. *Proc. Natl. Acad. Sci. U. S. A.* **2009**, *106*, 5497-5502.
(114) Naessens, M.; Cerdobbel, A.; Soetaert, W.; Vandamme, E. J. *J. Chem. Technol. Biotechnol.* **2005**, *80*, 845-860.
(115) Alexis, F.; Pridgen, E.; Molnar, L. K.; Farokhzad, O. C. *Mol. Pharmaceutics* **2008**, *5*, 505-515.
(116) Dobrovolskaia, M. A.; Aggarwal, P.; Hall, J. B.; McNeil, S. E. *Mol. Pharmaceutics* **2008**, *5*, 487-495.
(117) Li, S. D.; Huang, L. *Mol. Pharmaceutics* **2008**, *5*, 496-504.
(118) Zhao, X. J.; Jain, S.; Larman, H. B.; Gonzalez, S.; Irvine, D. J. *Biomaterials* **2005**, *26*, 5048-5063.
(119) Ali, O. A.; Huebsch, N.; Cao, L.; Dranoff, G.; Mooney, D. J. *Nat. Mater.* **2009**, *8*, 151-158.
(120) Tabata, Y.; Ikada, Y. *Adv. Polym. Sci.* **1990**, *94*, 107-141.

(121)Thiele, L.; Merkle, H. P.; Walter, E. *Pharm. Res.* **2003**, *20*, 221-228.
(122)Gratton, S. E. A.; Ropp, P. A.; Pohlhaus, P. D.; Luft, J. C.; Madden, V. J.; Napier, M. E.; DeSimone, J. M. *Proc. Natl. Acad. Sci. U. S. A.* **2008**, *105*, 11613-11618.
(123)Champion, J. A.; Mitragotri, S. *Proc. Natl. Acad. Sci. U. S. A.* **2006**, *103*, 4930-4934.
(124)Champion, J. A.; Mitragotri, S. *Pharm. Res.* **2009**, *26*, 244-249.
(125)Fifis, T.; Gamvrellis, A.; Crimeen-Irwin, B.; Pietersz, G. A.; Li, J.; Mottram, P. L.; McKenzie, I. F.; Plebanski, M. *J. Immunol.* **2004**, *173*, 3148-3154.
(126)Xiang, S. D.; Scholzen, A.; Minigo, G.; David, C.; Apostolopoulos, V.; Mottram, P. L.; Plebanski, M. *Methods* **2006**, *40*, 1-9.
(127)Mottram, P. L.; Leong, D.; Crimeen-Irwin, B.; Gloster, S.; Xiang, S. D.; Meanger, J.; Ghildyal, R.; Vardaxis, N.; Plebanski, M. *Mol. Pharmaceutics* **2007**, *4*, 73-84.
(128)Reece, J. C.; Vardaxis, N. J.; Marshall, J. A.; Crowe, S. M.; Cameron, P. U. *Immunology and Cell Biology* **2001**, *79*, 255-263.
(129)Champion, J. A.; Walker, A.; Mitragotri, S. *Pharm. Res.* **2008**, *25*, 1815-1821.
(130)Randolph, G. J.; Inaba, K.; Robbiani, D. F.; Steinman, R. M.; Muller, W. A. *Immunity* **1999**, *11*, 753-761.
(131)Manolova, V.; Flace, A.; Bauer, M.; Schwarz, K.; Saudan, P.; Bachmann, M. F. *Eur. J. Immunol.* **2008**, *38*, 1404-1413.
(132)Wilson, N. S.; El-Sukkari, D.; Belz, G. T.; Smith, C. M.; Steptoe, R. J.; Heath, W. R.; Shortman, K.; Villadangos, J. A. *Blood* **2003**, *102*, 2187-2194.
(133)Dudziak, D.; Kamphorst, A. O.; Heidkamp, G. F.; Buchholz, V. R.; Trumpfheller, C.; Yamazaki, S.; Cheong, C.; Liu, K.; Lee, H.-W.; Park, C. G.; Steinman, R. M.; Nussenzweig, M. C. *Science* **2007**, *315*, 107-111.
(134)Maldonado-Lopez, R.; De Smedt, T.; Michel, P.; Godfroid, J.; Pajak, B.; Heirman, C.; Thielemans, K.; Leo, O.; Urbain, J.; Moser, M. *The Journal of Experimental Medicine* **1999**, *189*, 587-592.
(135)Oh, J. K.; Tang, C.; Gao, H.; Tsarevsky, N. V.; Matyjaszewski, K. *J. Am. Chem. Soc.* **2006**, *128*, 5578-5584.
(136)Oh, J. K.; Siegwart, D. J.; Lee, H. I.; Sherwood, G.; Peteanu, L.; Hollinger, J. O.; Kataoka, K.; Matyjaszewski, K. *J. Am. Chem. Soc.* **2007**, *129*, 5939-5945.
(137)Oh, J. K.; Siegwart, D. J.; Matyjaszewski, K. *Biomacromolecules* **2007**, *8*, 3326-3331.
(138)Euliss, L. E.; DuPont, J. A.; Gratton, S.; DeSimone, J. *Chem. Soc. Rev.* **2006**, *35*, 1095-1104.
(139)Champion, J. A.; Katare, Y. K.; Mitragotri, S. *J. Control. Release* **2007**, *121*, 3-9.
(140)Acharya, G.; Shin, C. S.; McDermott, M.; Mishra, H.; Park, H.; Kwon, I. C.; Park, K. *J. Control. Release* **2010**, *141*, 314-319.
(141)Rolland, J. P.; Hagberg, E. C.; Denison, G. M.; Carter, K. R.; DeSimone, J. M. *Angew. Chem., Int. Ed.* **2004**, *43*, 5796-5799.
(142)Rolland, J. P.; Maynor, B. W.; Euliss, L. E.; Exner, A. E.; Denison, G. M.; DeSimone, J. M. *J. Am. Chem. Soc.* **2005**, *127*, 10096-10100.
(143)Gratton, S. E. A.; Williams, S. S.; Napier, M. E.; Pohlhaus, P. D.; Zhou, Z. L.; Wiles, K. B.; Maynor, B. W.; Shen, C.; Olafsen, T.; Samulski, E. T.; Desimone, J. M. *Acc. Chem. Res.* **2008**, *41*, 1685-1695.
(144)Proudfoot, O.; Apostolopoulos, V.; Pietersz, G. A. *Mol. Pharmaceutics* **2007**, *4*, 58-72.
(145)Tacken, P. J.; de Vries, I. J.; Torensma, R.; Figdor, C. G. *Nat. Rev. Immunol.* **2007**, *7*, 790-802.

(146) Burgdorf, S.; Kautz, A.; Bohnert, V.; Knolle, P. A.; Kurts, C. *Science* **2007**, *316*, 612-616.
(147) Apostolopoulos, V.; Barnes, N.; Pietersz, G. A.; McKenzie, I. F. C. *Vaccine* **2000**, *18*, 3174-3184.
(148) Reddy, S. T.; Swartz, M. A.; Hubbell, J. A. *Trends Immunol.* **2006**, *27*, 573-579.
(149) Irache, J. M.; Salman, H. H.; Gamazo, C.; Espuelas, S. *Expert Opinion on Drug Delivery* **2008**, *5*, 703-724.
(150) Thiele, L.; Diederichs, J. E.; Reszka, R.; Merkle, H. P.; Walter, E. *Biomaterials* **2003**, *24*, 1409-1418.
(151) Wattendorf, U.; Coullerez, G.; Voros, J.; Textor, M.; Merkle, H. P. *Langmuir* **2008**, *24*, 11790-11802.
(152) Rieger, J.; Freichels, H.; Imberty, A.; Putaux, J.-L.; Delair, T.; Jerome, C.; Auzely-Velty, R. *Biomacromolecules* **2009**, *10*, 651-657.
(153) Beaudette, T. T.; Cohen, J. A.; Bachelder, E. M.; Broaders, K. E.; Cohen, J. L.; Engleman, E. G.; Frechet, J. M. J. *J. Am. Chem. Soc.* **2009**, *131*, 10360-10361.

Chapter 2 – Synthesis and *In Vivo* Evaluation of Acid-Degradable Microparticle Vaccines Co-Encapsulating Antigen and Immunostimulatory CpG DNA

Abstract

Protein-based vaccines have been explored as a safer alternative to traditional weakened or killed whole-organism-based vaccination strategies and have been investigated for their ability to activate the immune system against certain cancers. For optimal stimulation of T cells, protein-based vaccines should deliver protein antigens to antigen presenting cells in the context of appropriate immunostimulatory signals, thus mimicking actual pathogens. In this chapter, we describe the synthesis, characterization, and biological evaluation of immunostimulatory acid-degradable microparticles, which are suitable delivery vehicles for use in protein-based vaccines and cancer immunotherapy. Using a 3' conjugation strategy, we optimized the attachment of immunostimulatory CpG DNA to our vaccine carriers and demonstrated that under acidic conditions similar to that found in endosomal compartments, these new particles were capable of simultaneously releasing a model protein antigen and a CpG DNA adjuvant. We found in an *in vivo* cytotoxicity assay that the co-encapsulation of ovalbumin, a model antigen, and immunostimulatory agent in the same particle led to superior cytotoxic T lymphocyte activity compared to particles co-administered with adjuvant in an unbound form. In addition, we investigated the ability of these acid-degradable particles to induce protective immunity in the MO5 murine melanoma model and found that they were effective until tumor escape, which appeared to result from a loss of antigen expression by the cancer cells due to *in vivo* selection pressure.

Introduction

Traditional vaccination strategies utilizing live attenuated viruses or inactivated (killed) pathogens have been employed widely for the treatment and prevention of disease. Although these approaches have generated successful results for a large number of diseases, safety concerns have led to the development of vaccines based on pathogen-derived protein antigens (subunit vaccines).[1] As protein antigens have been discovered for certain tumors, there has also been significant interest in the activation of the immune system against cancer cells expressing these antigens.[2,3] To date, the most promising cancer immunotherapy approaches have relied on the collection and *ex vivo* manipulation of dendritic cells (DCs),[4] which are crucial for the initiation and orchestration of adaptive immune responses, or the drastic *in vivo* expansion of DCs using the systemic administration of Flt3 ligand, a bone marrow growth factor.[5] Despite promising early clinical results, these strategies may ultimately be too laborious and expensive for widespread application. An ideal protein-based vaccine should target and activate DCs *in vivo* and effectively generate protective immunity while limiting the use of potentially hazardous immunostimulatory agents.

To meet these challenging demands, antigen delivery vehicles have been explored for use in subunit vaccines and cancer immunotherapy.[6] For optimal performance, antigen delivery vehicles should closely mimic the composition and immunological processing of actual pathogens; they should actively or passively target antigen presenting cells (APCs) such as DCs, protect the antigenic protein from degradation until reaching these cells, direct the nature of the resulting immune response (i.e., cellular vs. humoral responses), and lastly, induce APC

maturation by interacting with elements of the innate immune system such as Toll-like receptors (TLRs). To address some of these issues, several strategies have been reported in the literature such as directly conjugating TLR ligands to protein antigens[7] or co-encapsulating immunostimulatory agents and proteins in liposomes[8] or hydrophobic polymeric particles.[9]

We have explored an antigen delivery system capable of performing all of the above-mentioned functions, which is based on acid-degradable, acetal-crosslinked, hydrogel particles designed for uptake by APCs.[10,11] Compared to non-degradable systems, these microparticles greatly enhance the efficacy of major histocompatibility complex class I (MHC I) antigen presentation and the subsequent activation of $CD8^+$ cytotoxic T lymphocytes (CTLs),[12,13] which are crucial in cancer immunotherapy and other applications demanding strong cellular immune responses. To effect APC maturation, we have recently reported a method for the incorporation of an immunostimulatory CpG oligonucleotide into the polymer backbone of the particles.[14] Following phagocytosis by APCs, these particles were designed to degrade in the acidic environment of endosomal vesicles (Figure 2.1a-b) and release their protein payload as well as a CpG-polymer conjugate capable of binding TLR9, an intracellular receptor for unmethylated viral and bacterial DNA.[15,16] TLR9 ligation results in APC activation and maturation and leads to the subsequent migration of APCs to draining lymph nodes.[17-19] Although these microparticles were effective in generating antigen specific immunity, they required a relatively high CpG content, which, we hypothesized, was due to a loss in activity of the CpG caused by its covalent linkage to the polymer scaffold.

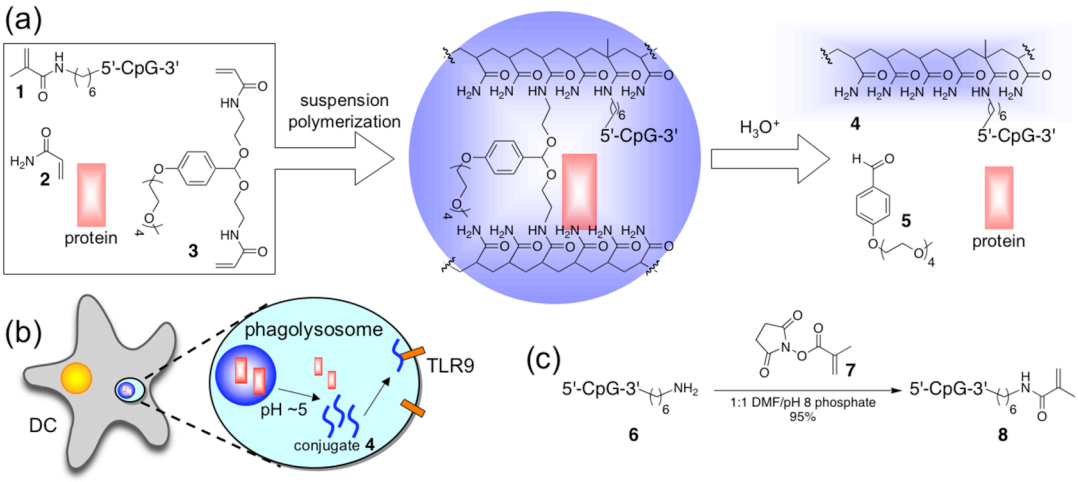

Figure 2.1. (a) General scheme for the preparation and acid-catalyzed degradation of microparticles loaded with protein and immunostimulatory DNA (CpG = 5'-TCCATGACGTTCCTGACGTT-3'). (b) Following internalization by APCs, acid-labile particles degrade to release their protein payload and a polymer-CpG conjugate, which can interact with TLR9. (c) Synthesis of macromonomer **8** from 3' amine-functionalized oligonucleotide **6**.

Building on our previous work, we describe an optimized attachment strategy of CpG DNA to acid-degradable protein-loaded microparticles, which shows no loss in immunostimulatory activity as a consequence of the covalent linkage. Ovalbumin (OVA) was encapsulated in these microparticles as a model antigen as there exist a number of immunological assays and disease models specific to this protein. We then studied the ability of this optimized system to induce a CTL response *in vivo*. In addition, we investigated the ability

of these particles to generate protective immunity to a lethal tumor challenge in the MO5 murine melanoma model. In these studies, our aim was to analyze the synergistic effects arising from the delivery of a protein antigen and adjuvant to the same APC. We were specifically interested in determining if our particles would perform better than treatments relying on the potentially hazardous systemic administration of free immunostimulatory agents. Herein, we demonstrate that by incorporating both protein antigen and a TLR agonist, our delivery vehicles, in a single formulation, provide all the necessary components for the induction of robust cellular immune responses.

Results and Discussion

Synthesis of CpG-loaded acid-degradable particles

We recently described the incorporation of a CpG oligonucleotide into acid-degradable polyacrylamide particles to facilitate co-delivery of a model protein antigen, OVA, and an immunostimulatory agent to the same APC (Figure 2.1a-b).[14] CpG DNA was chosen as an adjuvant because its receptor, TLR9, is located in endosomal compartments, the same location in which our particles are designed to degrade.[17,19] Incorporation of the immunostimulatory DNA was achieved by copolymerizing a methacrylamide-modified CpG oligonucleotide, macromonomer **1**, with acrylamide (**2**) and an acid-degradable crosslinker (**3**). In initial work, the CpG was covalently linked to the particle's polymer scaffold through its 5' terminus.[20] Although these particles were found to generate antigen specific immunity in a number of assays, we hypothesized that the covalent attachment of the CpG oligonucleotide to the high molecular weight polymer in conjugate **4** may diminish its activity and lead to suboptimal DC activation. This hypothesis was supported by *in vitro*

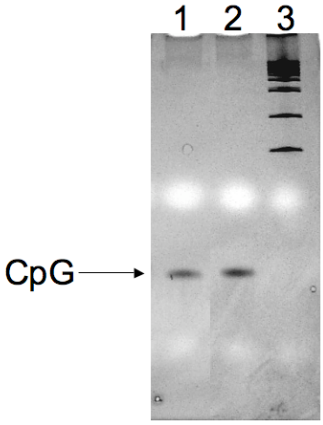

Figure 2.2. Analysis of macromonomer **8** by PAGE. Lane 1: unmodified CpG DNA; lane 2: macromonomer **8**; lane 3: 50-2000 bp ladder.

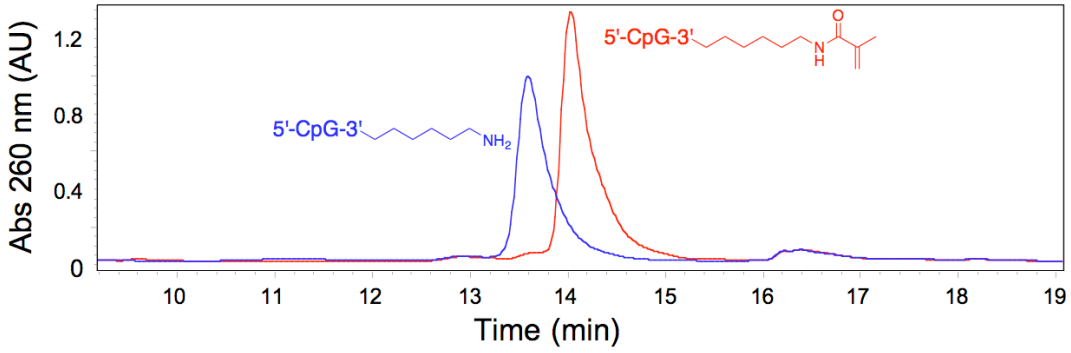

Figure 2.3. Analysis of macromonomer **8** by HPLC showed a single signal with a slightly longer retention time than the amine-modified oligonucleotide **6**.

experiments in which bone marrow derived dendritic cells (BMDCs) were activated by free CpG oligonucleotides to a greater extent than with particles containing an equivalent amount of covalently bound oligonucleotide (see below).

In contrast to the 5' end, modifications involving the 3' terminus of CpG oligonucleotides are generally better tolerated and cause significantly less, if any, reduction in immunostimulatory activity.[21,22] Therefore, particles were prepared using a 20-mer of single-stranded CpG DNA that was modified on its 3' terminus with a methacrylamide group (monomer **8**). Polymerizable CpG monomer **8** was prepared in one step from *N*-hydroxysuccinimidyl ester **7** and amine functionalized oligonucleotide **6** with a good recovery of the product (Figure 2.1c). Following purification by size exclusion chromatography, macromonomer **8** was characterized using MALDI-TOF mass spectrometry and found to have a molecular weight within 0.04% of the predicted value. High-performance liquid chromatography and polyacrylamide gel electrophoresis were used to analyze the purity of CpG conjugate **8** (Figures 2.2 and 2.3). Both methods revealed the presence a single species, indicating that no significant degradation or polymerization reactions occurred during the synthesis and purification of **8**.

Macromonomer **8** was used to prepare acid-degradable particles containing 3'-linked CpG DNA. Characterization of the particles by SEM (Figure 2.4) showed that they were similar in size, shape, and morphology to previously prepared particles with 5'-linked CpG.[14] Based on SEM data, the particles were approximately 100-800 nm in diameter in the dry state, which we have previously found to be a suitable size for use in protein-based vaccines.[23] To quantify the amount of CpG DNA incorporated, the particles were degraded in acidic buffer and the resulting solutions analyzed via a fluorescence-based assay utilizing the commercially available OliGreen reagent. Both CpG macromonomers were incorporated equally well into the particles with efficiencies of 60-70% based on the masses of starting monomers. Particles with loadings between 1 and 9 μg CpG/mg particles (see below) were easily obtained by varying the initial feed of monomers **1** or **8**. Analysis of hydrolyzed particles by gel permeation chromatography was used to confirm the successful copolymerization of both CpG macromonomers into the polyacrylamide backbone of the carriers (see Figure 2.5).

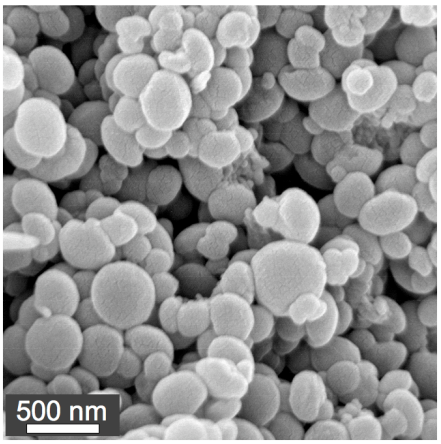

Figure 2.4. Representative SEM image of acid-degradable particles containing 3'-linked CpG.

3'-linked CpG particles are more immunostimulatory than 5'-linked CpG particles

To assess the relative immunostimulatory activity of acid-degradable particles containing **1** and **8**, sets of particles were prepared containing no protein antigen and a low, medium or high loading of either 3' or 5'-linked CpG (approximately 1, 3, and 9 μg CpG oligonucleotide per mg particles, respectively). These particles were then evaluated for their capacity to induce activation of immature BMDCs *in vitro*. The percentage of DCs producing interleukin-12 (IL-12),[24] a pro-inflammatory cytokine, after overnight culture with CpG-containing particles was used to compare the stimulatory capacity of 3'- and 5'-linked CpG. For this experiment, particle concentrations were normalized such that all DCs were pulsed with the equivalent of 300 ng of

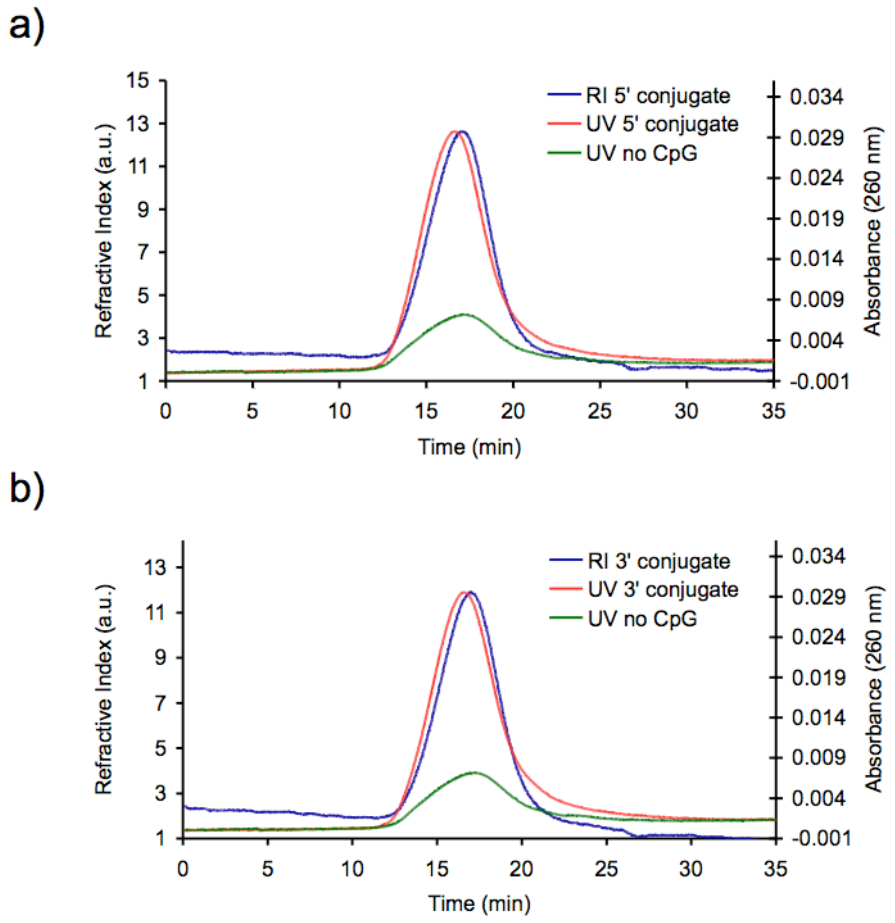

Figure 2.5. Analysis of CpG-polymer conjugates using gel permeation chromatography. Polymers containing (a) 5'-linked and (b) 3'-linked CpG gave overlapping refractive index and UV traces, thus suggesting successful copolymerization of the CpG macromonomers into the polyacrylamide backbone with an even distribution of the CpG throughout the polymer sample. The UV trace of particles made without a CpG macromonomer is included as a negative control for DNA absorption at 260 nm.

CpG. As the particle formulations were almost entirely polyacrylamide by mass, CpG-free particles were used as a negative control to ensure that the carriers were not inherently immunostimulatory. As demonstrated in Figure 2.6, the 3'-linked CpG particles induced a consistently higher percentage of BMDCs to produce IL-12 compared to 5'-linked particles. In contrast to the 5'-linked CpG particles, DC activation levels correlated well with the total amount of CpG used in the 3'-linked particles, except for the particles with the lowest loading, suggesting that there might be a minimum CpG/particle ratio in order to achieve optimal DC activation. For all concentrations tested, the medium and high loaded 3' CpG particles were as stimulatory, if not more so, than an equivalent amount of soluble CpG, indicating no loss in activity of the particle-associated CpG (data not shown). These findings are therefore in agreement with the structure-activity studies discussed above.

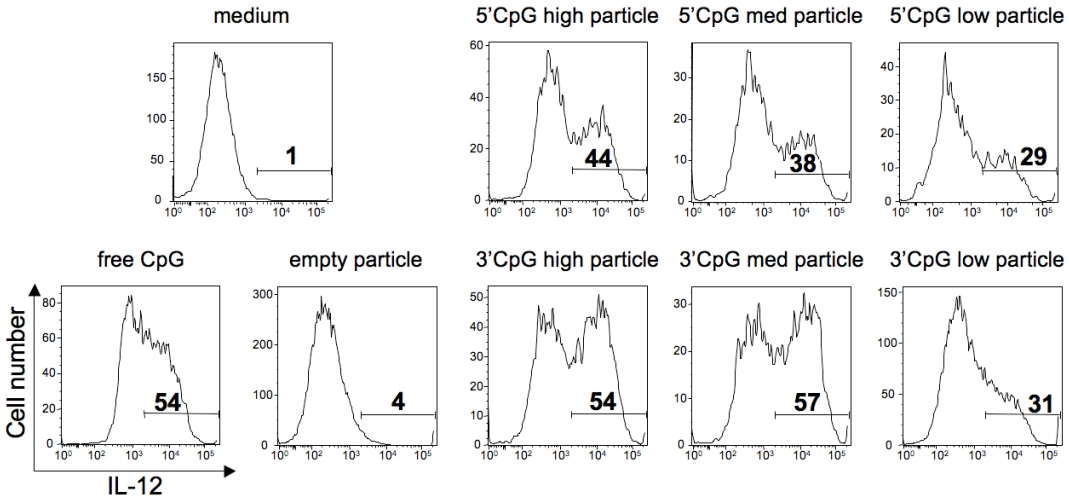

Figure 2.6. IL-12 production by CD11c$^+$ BMDCs pulsed with 3'- or 5'-linked CpG particles. Numbers in histograms represent percentages of intracellular IL-12 positive DCs after overnight culture with particles. The CpG concentration in each sample was normalized to 300 ng/mL. Data are representative of three experiments with similar results.

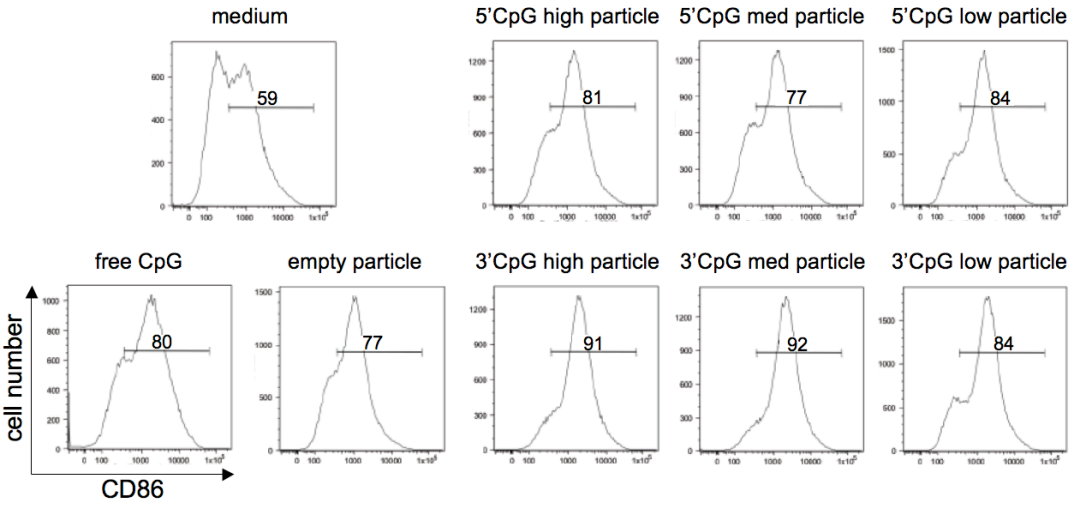

Figure 2.7. Expression of CD86 by BMDCs pulsed with 3'- or 5'-linked CpG particles or control samples. Numbers in histograms represent percent of CD86 postive DCs after overnight culture with samples normalized to 300 ng CpG. Data are representative of three experiments with similar results.

In addition, the expression levels of CD86 on BMDCs treated with the CpG-loaded particles described above were determined. CD86 provides a necessary co-stimulatory signal to naïve T cells during priming *via* CD86-CD28 interaction.[25] As was the case for the IL-12 assay, the 3'-linked CpG particles were superior at inducing high levels of CD86 expression in BMDCs compared to 5'-linked particles (see Figure 2.7 for representative flow cytometry histograms). These data demonstrate that by carefully controlling the direction of conjugation, CpG DNA can be covalently linked to particulate vaccine carriers without compromising the overall

immunostimulatory activity of the oligonucleotide. Based on these results, all subsequently used CpG-loaded particles involved attachment exclusively via a 3'-linkage.

Co-encapsulation of CpG and protein antigen leads to superior *in vivo* CTL responses

For the generation of optimal immune responses, APCs need to receive antigens in the context of appropriate maturation signals. In the natural processing of microbes by APCs, these signals are provided by elements of the innate immune system which are capable of recognizing a diverse array of pathogen-associated molecular patterns (PAMPs) such as unmethylated CpG dinucleotide motifs, lipopolysaccharides, heat shock proteins, flagellin, and double-stranded RNA.[26,27] Recognition of one or more PAMPs induces APC maturation, which typically includes the secretion of cytokines, upregulation of co-stimulatory molecule expression and increased antigen presentation. In comparison, APC processing of protein antigens without concomitant immunostimulation may lead to T cell anergy and immunological tolerance rather than the desired immune response.[28]

Having determined the optimal CpG attachment chemistry, OVA was next encapsulated in the acid-degradable, CpG-loaded particles to provide a vehicle capable of delivering both a model antigen and an immunostimulatory agent to the same APC. As was done for CpG quantification, protein-loaded particles were degraded in acidic buffer and the resulting solutions were analyzed for OVA content using a bicinchoninic acid-based assay. The protein loading was found to be approximately 40 μg OVA/mg particles, an incorporation efficiency of about 70% based the mass of starting materials, and this loading was used in all particles tested in this report.

To investigate the ability of the particles to simultaneously deliver an antigen and an immunostimulatory agent, a release experiment was performed to model the behavior of particles prior to and after uptake by APCs (Figure 2.8). Particles containing both 3'-linked CpG and

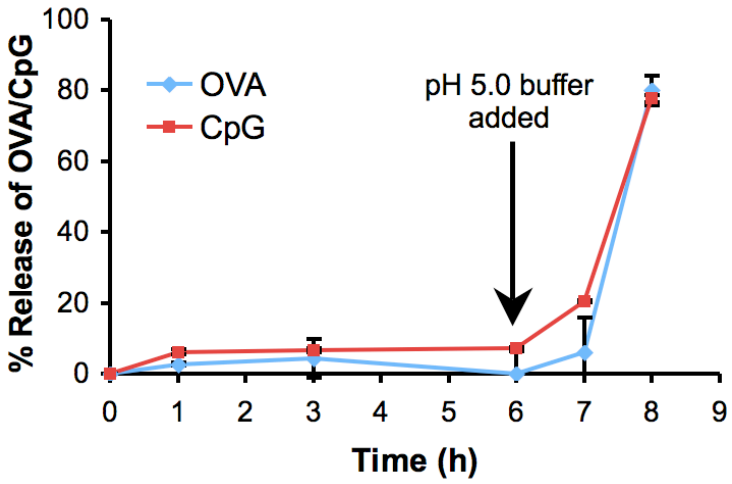

Figure 2.8. Release of OVA and 3'-linked CpG from acid-degradable particles in a bulk model phagocytosis experiment. 3'-CpG/OVA particles were first incubated at 37 ºC at physiological pH (7.4). After 6 hours, the buffer was replaced with acidic buffer (pH 5). The release of OVA and CpG from the particles was quantified at various time points before and after acidification. Total release was determined after overnight incubation at pH 5 and 37 ºC.

OVA (3'CpG/OVA particles) were incubated at 37 ºC in PBS (pH 7.4), modeling the neutral environment prior to uptake by APCs. After 6 hours, the PBS was replaced with an acidic buffer to simulate phagocytosis and particle degradation by APCs. At various time points throughout the experiment, the particle solutions were analyzed for the release of OVA and CpG using the assays described above. After 6 hours under neutral conditions the particles had released no more than 10% of their encapsulated OVA or CpG. In contrast, nearly all of the OVA and CpG was released within 2 hours after introduction of the acidic buffer. These bulk release data suggest that our particles are indeed capable of simultaneously delivering antigen and immunostimulatory CpG DNA, which should be beneficial in the generation of robust immune responses.

To investigate the synergistic effects arising from the co-delivery of antigen and immunostimulatory agent to the same APC *in vivo*, three types of 3'CpG/OVA particles were prepared, each with a constant protein loading (approximately 40 μg OVA/mg particles) and a low, medium or high loading of CpG (approximately 1, 3 or 9 μg CpG per mg particles, respectively). These particles were then tested for their capacity to induce OVA-specific CTL activity compared to OVA-loaded particles co-administered with a corresponding amount of free CpG (Figure 2.9). In this experiment, mice were vaccinated subcutaneously (s.c.) with the particle samples described above normalized to a constant dose of OVA (50 μg). Seven days later, an equal mixture of two populations of CFSE labeled splenocytes was injected intravenously. A target cell population was pulsed with SIINFEKL ($OVA_{258-265}$), the immunodominant OVA-derived $CD8^+$ T cell epitope in C57BL/6 mice. As a control, a second population was not pulsed with SIINFEKL and was stained with a lower CFSE concentration.

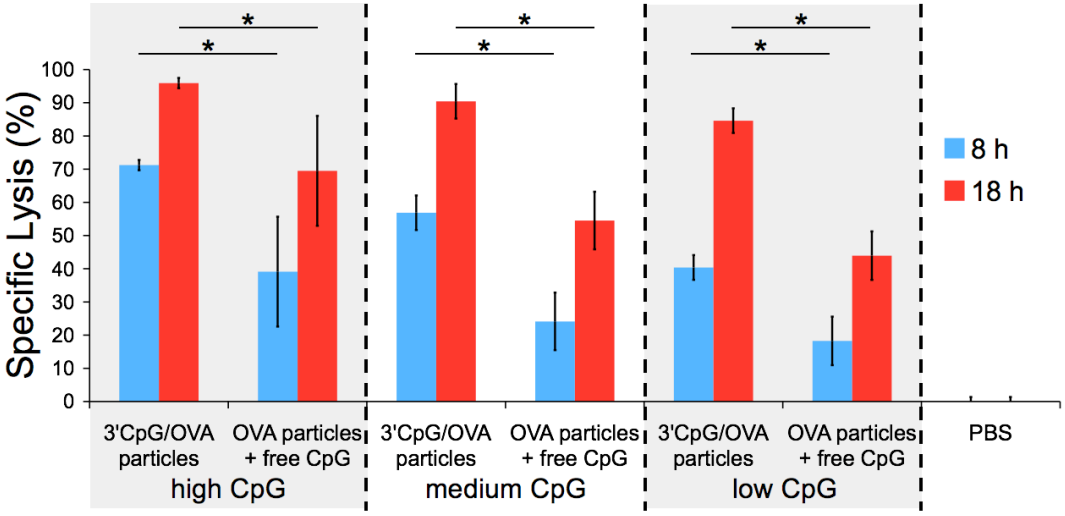

Figure 2.9. Specific lysis of SIINFEKL-pulsed target cells in mice immunized with PBS, 3'CpG/OVA particles, or OVA particles plus free CpG after 8 and 18 hours using 3 different CpG doses. High, medium and low CpG doses correspond to 9, 3, and 1 μg CpG per mg particles (or an equivalent amount of free CpG) respectively. Specific lysis was determined using flow cytometry by comparing the remaining population of stained target cells to a population of unpulsed control cells (see Figure 2.10). In all cases, vaccination with 3'CpG/OVA combination particles produced a superior immune response compared to the co-injection of OVA particles plus free CpG (* $p < 0.01$, $n = 10$, mean ± 95% confidence intervals).

To determine the extent of antigen-specific cytotoxicity, the relative amount of each population remaining after 8 and 18 hours was quantified by flow cytometric analysis (see Figure 2.10 for representative histograms). The percentage of target cell-specific lysis was found to be highly dependent on the absolute quantity of CpG administered at both time points tested. In addition, for all CpG particle loadings and for both time points studied, the 3'CpG/OVA combination particles induced a significantly higher level of specific lysis ($p < 0.01$) of target cells compared to the co-injected mixture of OVA particles plus an equivalent amount of free CpG. The largest differences (approximately 2-fold) in induced cytotoxicity between these two samples were observed at the lower CpG doses, and after 18 hours these differences tended to decrease as the amount of CpG increased. Beyond suggesting co-delivery related synergistic effects, our data indicate that, at least in the case of our optimized particles, the magnitude of these effects increases as stimulant doses are lowered. This is a significant finding because, for vaccine purposes, it may be desirable to avoid the use of free adjuvants or at least use the lowest possible dose in order to minimize the likelihood of developing autoimmune disorders or provoking other side effects.[29]

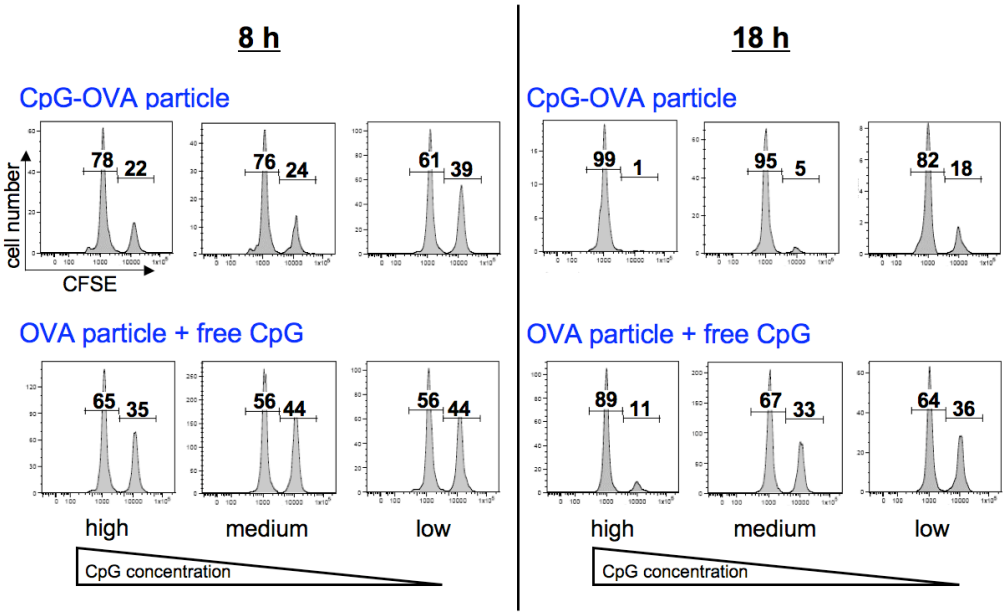

Figure 2.10. Specific lysis of SIINFEKL-pulsed cells in mice immunized with 3'-CpG-OVA particles or OVA particles plus free CpG after 8 (left side) and 18 hours (right side). Histograms show percentage of remaining CFSE stained target cells (SIINFEKL-pulsed, population on right) or unpulsed control cells (population on left) and are representative of five experiments with similar results. High, medium and low CpG loadings correspond to 9, 3, and 1 μg CpG per mg particles respectively.

3'CpG/OVA particles enhance survival in a tumor protection experiment

Having demonstrated their promising *in vivo* activity, the ability of the 3'CpG/OVA particles to induce protective immunity and prevent the growth of an OVA expressing tumor using a murine melanoma model system was investigated. For this study, different groups of C57BL/6 mice (n = 10) were vaccinated (on day -7) s.c in their left flank with PBS, OVA-containing particles plus free CpG, 3'CpG/OVA particles, or free CpG plus free OVA. In the case of the treatment groups, each mouse received the equivalent of 50 μg of OVA and 10 μg of

CpG. Seven days later (day 0), the mice were challenged with a s.c. injection in the contralateral flank of $6x10^5$ MO5 cells, a derivative of the B16 melanoma cell line transfected with the OVA gene,[30] and the subsequent tumor growth was monitored for the next 64 days. The survival of each treatment group as a function of time is shown in Figure 2.11 (see Figure 2.12 for plots of tumor volume vs. time). The mice in the PBS group developed tumors first (9 of 10 mice had visible tumors by day 9) and all mice from this group were removed from the study due to large tumor burdens within 28 days. In contrast, tumors were not visible in those mice receiving the 3'CpG/OVA particles until much later, with only two mice developing visible tumors by day 23. Throughout the study, mice in this group maintained the highest probability of survival compared to all other groups. The probability of survival for the OVA-particle plus free CpG group remained higher than the free OVA plus free CpG group until approximately day 33 at which point they became nearly identical. Importantly, the 3'CpG/OVA combination particles performed at least as well, if not better, than two other treatments employing the potentially hazardous administration of unbound immunostimulatory agents. Based on the results obtained in the *in vivo* cytotoxicity experiment described above, it is possible that more pronounced differences between the treatment groups may have been observed if the CpG dose were lowered.

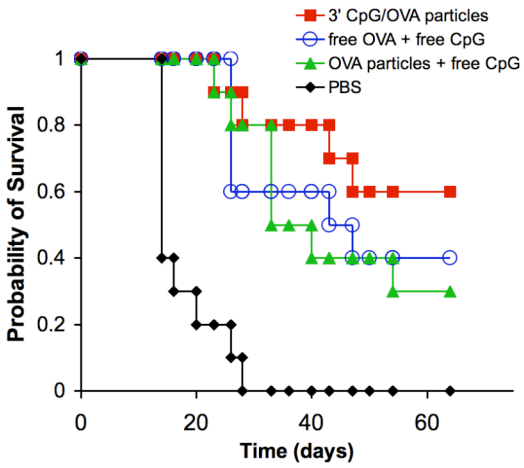

Figure 2.11. Kaplan-Meier survival plot from *in vivo* tumor protection experiment. The different groups of C57BL/6 mice (n = 10) were immunized on day -7 s.c in their left flank with PBS, OVA-containing particles plus free CpG, 3'CpG/OVA particles, or free CpG plus free OVA. In the case of the treatment groups, each mouse received the equivalent of 50 μg of OVA and 10 μg of CpG. Seven days later (day 0), the mice were challenged with a s.c. injection in the right flank of $6x10^5$ MO5 cells, a derivative of the B16 melanoma cell line transfected with the OVA gene, and the subsequent tumor growth was monitored for the next 64 days. The survival of each treatment group as a function of time is plotted.

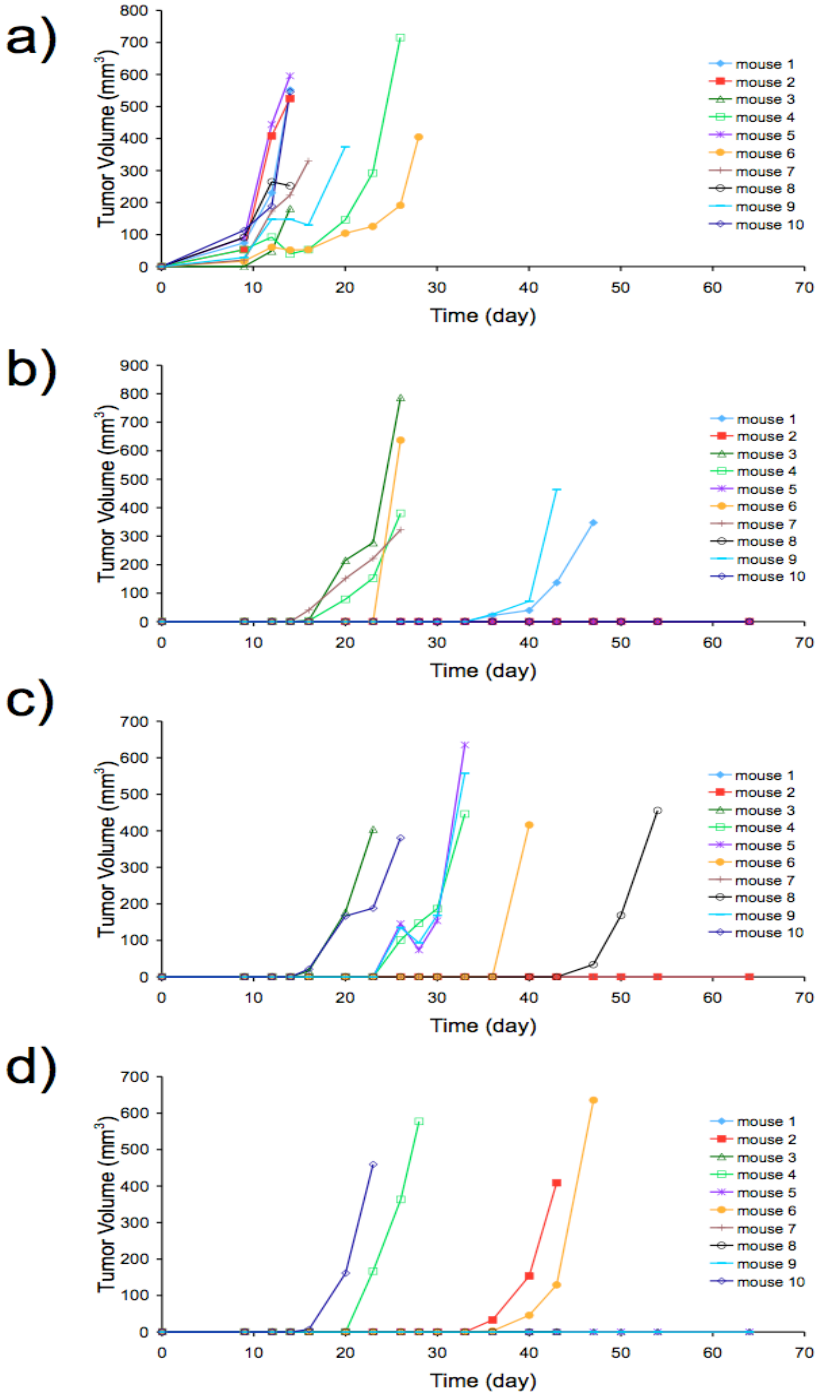

Figure 2.12. Plots of tumor volume vs. time for mice treated with (a) PBS, (b) free OVA plus free CpG, (c) OVA particles plus free CpG, or (d) 3'-CpG/OVA particles.

Tumor escape is caused by a loss of OVA expression *in vivo*

The co-encapsulation of antigen and immunostimulatory agent in the same acid-degradable vehicle appears to have produced a robust immune response, however complete tumor rejection was not achieved even in this experimental group. We hypothesized that the late onset of tumors in the treatment groups may have been related to the loss of OVA expression by the MO5 cells *in vivo*. In addition to the absence of antibiotics, which are used to select for OVA-expressing cells in culture, the selection pressure of a strong *in vivo* CTL response may have led to the appearance of tumors with low or even no OVA expression, a phenomenon referred to as immunoediting.[31] To explore this hypothesis, we excised and saved tumor tissue from each mouse as it was removed from the experiment. After the final mouse was removed from the study on day 54, the tumor tissue samples were analyzed using an ELISA to look for the presence of OVA (Figure 2.13a). Consistent with our hypothesis, we only observed OVA

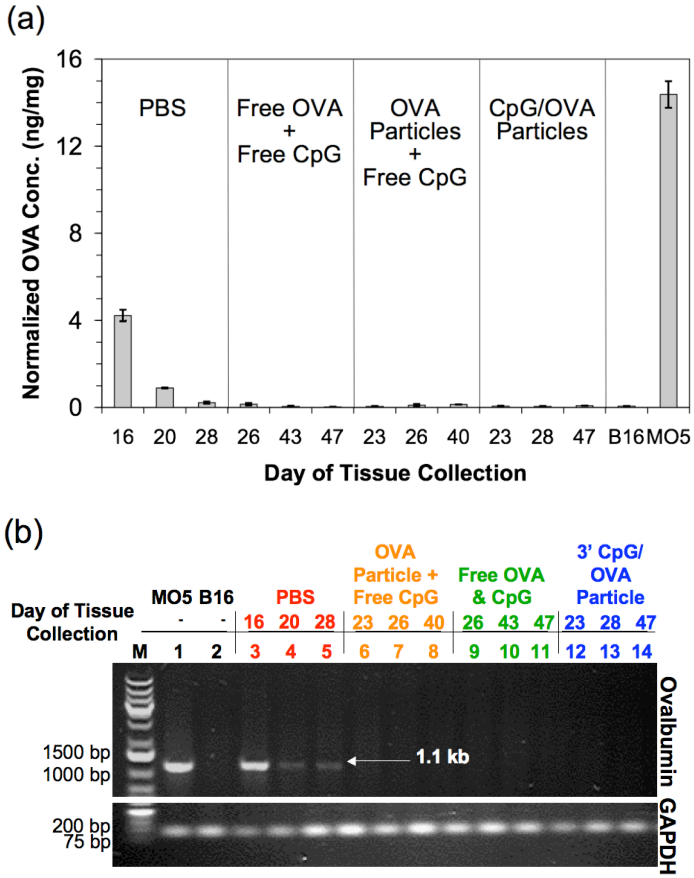

Figure 2.13. Time dependent loss of OVA expression in tumors. (a) Loss of OVA expression in tumors from treatment groups, but not PBS group, as analyzed by ELISA. The concentration of OVA in tumor tissue from the first, middle and last mouse from each group to be removed from the study was analyzed and compared to MO5 and B16 cells prepared from cultures (positive and negative controls, respectively). (b) Loss of OVA gene in tumors from treatment groups, but not PBS group as analyzed by PCR. The presence of the OVA gene (1.1 kb) in the first, middle and last mouse from each group to be removed from the study was analyzed.

protein above background levels in tumor tissue removed from mice in the PBS group. Additionally, the OVA content from tumors in this group decreased the longer the mice remained in the study. To further explore our hypothesis, the tumor tissue was analyzed for the presence of OVA-encoding DNA using PCR. As shown in Figure 2.13b, only mice in the PBS group were positive for this gene, and, consistent with our ELISA data, the intensity of the corresponding band decreased the longer the mice remained in the study. In contrast, the tumors from mice in all of the treatment groups were negative for the OVA-encoding gene. Based on these data, the MO5 cells used in our study likely lost their expression of OVA after approximately 25 days *in vivo*. This result agrees well with a study by Goldberger *et al.* in which mice with greater than 90% OVA-specific CTLs developed tumors after approximately the same time following a challenge of MO5 cancer cells.[32] Although it is clear that the treatment groups generated a significantly better immune response compared to PBS ($p < 0.0001$), we found no significant differences between the 3'CpG/OVA particles and treatment with free antigen and CpG ($p = 0.38$) or treatment with OVA particles plus free CpG ($p = 0.21$). It must be noted however, that the loss of OVA expression by the tumor cells complicates the interpretation of these data.

Despite the tumor escape, these tumor rejection and other results are encouraging and provide validation for our proof-of-concept acrylamide-based system. In future immunotherapy experiments using more biocompatible particle platforms,[33] we plan to explore the incorporation of multiple natural cancer antigens in the same carrier, which may make immune system evasion by the tumor cells more difficult.

Conclusions

This study demonstrates the validity of the design of a model delivery vehicle for protein-based vaccines that is capable of simultaneously delivering protein antigens and immunostimulatory CpG DNA. This design is based on an understanding of the uptake and processing of pathogenic species, which consist of discrete units composed of antigens and immunostimulatory moieties. A clear advantage of the CpG conjugation strategy used is that it avoids the potentially hazardous use of unbound immunostimulatory agents. In an *in vivo* CTL activity assay, we found that for all time points and stimulant concentrations tested, packaging CpG DNA and protein antigen in a single particle formulation induced significantly stronger immune responses compared to controls in which these components were administered separately. In a preliminary cancer immunotherapy experiment, we found that our microparticles were capable of inducing protective immunity in a mouse model until the tumors lost antigen expression, presumably due to selection pressure by the immune system. In general, this study validates the concept of covalently attaching immunostimulatory CpG DNA to delivery vehicles for use in antigen-based vaccine formulations.

Experimental

General Procedures and Materials. All reagents were purchased from commercial sources and used without further purification unless specified otherwise. Water for buffers was purified to a resistance of 18 MΩ using a NANOpure Diamond (Barnstead) purification system. Organic solvents were dried by passing through two columns of neutral alumina within a commercial solvent purification apparatus. Functionalized oligonucleotides (**1** and **6**) with phosphorothioate backbones were purchased from Integrated DNA Technologies (CpG-1826 sequence: 5'-

TCCATGACGTTCCTGACGTT-3'). Particle samples were characterized by scanning electron microscopy (SEM) using an S-5000 microscope (Hitachi) after being sputter coated with a 2 nm layer of a palladium/gold alloy. Fluorescence measurements were obtained on a Spectra Max Gemini XS (Molecular Devices), absorbance measurements were obtained using a Lambda 35 spectrophotometer (Perkin Elmer) or, for microplate-based assays using a Spectra Max 190 (Molecular Devices). Matrix-assisted laser desorption ionization time-of-flight mass spectrometry (MALDI-TOF) data was collected on a PerSeptive Biosystems Voyager-DE PRO instrument (Applied Biosystems) in positive ion mode; accelerating voltage: 25,000 V, grid: 95%, guide wire: 0.2%, delay time: 550 ns. MALDI samples were prepared in a matrix of a saturated solution of 3-hydroxypicolinic acid in a 1:1 mixture of acetonitrile/water. A 17-mer oligonucleotide with a known mass was used as an internal standard.

Acid-degradable Crosslinker 3 was synthesized as previously described.[12]

NHS Ester 7 was synthesized as previously reported[34] and recrystallized from ethyl acetate/hexanes (1:3) prior to use.

3'-Methacrylamide-modified CpG Macromonomer 8 was prepared according to a procedure adapted from Hermanson.[35] Briefly, a solution of NHS ester **7** (4.33 mg, 23.6 μmol) in DMF (250 μL) was added to a solution of 3'-amine-modified oligonucleotide **6** (1.29 mg, 0.197 μmol) dissolved in a 50 mM phosphate buffer (pH 8.0, 250 μL). The resulting mixture was vortexed gently then incubated at 37 ºC for 4 h in the dark. The reaction mixture was diluted with distilled water (2 mL) and washed with CH_2Cl_2 (500 μL). The modified oligonucleotide was purified using size exclusion gel filtration (PD-10 column, GE Healthcare) and lyophilized. The purified DNA conjugate was quantified prior to use (1.22 mg, 95% yield) by an absorbance measurement at 260 nm. $[M+H]^+$ m/z = 6612.4. Found MALDI-TOF: $[M+H]^+$ m/z = 6609.8.

Analysis of 3'-CpG Macromonomer by HPLC. The 3'-methacrylamide-modified oligonucleotide **8** was analyzed for purity by reversed phase high-performance liquid chromatography (HPLC) using a 0.1 M triethylammonium acetate buffer (pH 7.0) and a gradient of 0 to 40% acetonitrile over 15 min followed by a gradient to 100% acetonitrile over the next 5 min. All HPLC runs were performed at a flow rate of 0.2 mL/min using a Symmetry C-18 column (3.5 μm, 2.1 x 150 mm, Waters) and an inline 996 photodiode array detector (Waters).

PAGE Analysis of Macromonomer 8. The 3'-CpG macromonomer **8** was further analyzed for purity using polyacrylamide gel electrophoresis (PAGE). Oligonucleotides (150 ng/well) were run on a 15% TBE-urea gel (BioRad) for 1 h at 150 V in TBE buffer (pH 8.3, 1 mM EDTA, 45 mM boric acid, 45 mM Tris). The gel was stained with ethidium bromide and imaged under UV irradiation.

General Acid-degradable Particle Preparation. Acid-degradable particles containing both ovalbumin (OVA, grade VI, Sigma Aldrich) and a CpG macromonomer were prepared using an inverse-suspension free-radical polymerization as described previously.[14] Briefly, OVA (7.0 mg) was dissolved in a 300 mM phosphate buffer (pH 8.0, 200 μL) followed by acrylamide (62.3 mg, 0.88 mmol), crosslinker **3** (62.9 mg, 0.12 mmol), and ammonium persulfate (6.6 mg, 0.029 mmol). The CpG macromonomer (either **1** or **8**, amounts noted below) was added to the

monomer solution in the same buffer (50 μL) and the combined solution was quickly added to an organic phase (2.5 mL) composed of 2.25% Span 80 (w/v) and 0.75% Tween 80 (w/v) in hexanes. This mixture was then sonicated for 30 s using a Branson Sonifier 450 with an output setting of 2, a duty cycle of 40%, and with a ½" flat tip probe. Polymerization was initiated by the addition of *N*,*N*,*N*',*N*'-tetramethylethylenediamine (25 μL), and the resulting mixture was stirred at rt for 10 min. The particles were isolated by centrifugation (1400 x *g*), washed with hexanes (3 x 2 mL) and acetone (4 x 2 mL), and finally dried overnight under vacuum to yield a fine white powder (typical yields: 50-60 mg).

Particles with low, medium or high CpG content: To obtain particles with different CpG loadings, the amount of CpG macromonomer (**1** or **8)** used in the particle preparation was varied. Specifically, 0.19 mg, 0.58 mg, or 1.71 mg of the appropriate macromonomer was used to prepare particles containing a low, medium, or high quantity of CpG, respectively.

CpG-free particles: Particles containing only OVA were prepared in the same fashion except that the monomers and protein were dissolved in 250 μL buffer and the CpG macromonomer was omitted.

OVA-free particles: Particles containing only CpG were prepared as described above except that the OVA was omitted from the aqueous phase.

Empty particles: Particles containing neither OVA nor CpG were prepared as described above omitting both the OVA and CpG macromonomer from the aqueous phase.

Oligonucleotide and Protein Quantification. Particle samples were weighed out in triplicate and washed twice with a 300 mM phosphate buffer (pH 8.0). The washing procedure involved first suspending the particles in buffer by vortexing and sonication, collecting the particles by centrifugation (2500 x *g*), and removing the supernatant. The particles were then suspended in a 300 mM acetate buffer (pH 5.0) at a final concentration of 5 mg/mL to hydrolyze the acetal crosslinks. The resulting solutions were allowed to stand overnight at rt and were subsequently analyzed for protein content using the MicroBCA assay (Pierce) or, for oligonucleotide content, using the fluorescent probe OliGreen (Invitrogen) according to the manufacturers' protocol. OVA-free particles and CpG-free particles were degraded in the same manner as described above and used to determine background values for the MicroBCA and OliGreen assays, respectively.

Analysis of CpG-polymer Conjugates using Gel Permeation Chromatography. Particles containing either 3'- or 5'-linked CpG were hydrolyzed overnight in acidic buffer (300 mM acetate, pH 5). The resulting solutions were dialyzed against deionized water at 4 ºC for 2 d using dialysis tubing with a 10,000 molecular weight cutoff. The purified polymers were then lyophilized and analyzed using gel permeation chromatography with 0.1 M $NaNO_3$ as a mobile phase, injected polymer concentrations of 5 mg/mL, two Suprema columns (1000 then 3000) connected in series (both 10 μm, 8 x 300 mm, Polymer Standards Service), a flow rate of 1 mL/min, and a 2414 differential refractometer (Waters) and a 996 photodiode array detector (Waters). Particles containing no CpG were also degraded and analyzed in the same fashion to serve as a negative control. As illustrated in Figure 2.5, the 3'- and 5'-linked CpG-polymer conjugates gave similar chromatograms with the refractive index (arising from the polymer backbone) and UV (arising from absorption of DNA at 260 nm) traces overlapping almost exactly. These data provide evidence for the successful copolymerization of both CpG

macromonomers into the polyacrylamide backbone with an even distribution of the CpG throughout the polymer samples.

Animals. C57BL/6 mice 6 to 8 weeks of age were purchased from the Jackson Laboratory. All mice were housed in the Stanford and UC Berkeley Animal Facilities in accordance with NIH guidelines. All procedures were approved by the Stanford and UC Berkeley Animal Care and Use Committees.

Cell Lines and Culture. MO5 is a B16 melanoma cell line transfected with OVA cDNA,[30] and was a kind gift from Dr. K. Rock (University of Massachusetts Medical Center, Worcester, MA). MO5 cells were maintained in RPMI-1640 supplemented with 10% fetal bovine serum, 4.5 g/L glucose, 2 mM L-glutamine (GlutaMAX-I), 0.1 mM non-essential amino acids, 1 mM sodium pyruvate, 0.055 mM 2-mercaptoethanol, 10 mM HEPES, and 2 mg/ml G418 (for antibiotic selection). B16-F10 cells were obtained from ATCC, and were maintained in Dulbecco's Modified Eagle Medium supplemented with 10% fetal bovine serum, 4.5 g/L glucose, and 2 mM L-glutamine. All culture media components were from Invitrogen-Gibco with the exception of the serum, which was from Hyclone. Cells were incubated in a water-jacketed 37 ºC/5% CO_2 incubator. Bone marrow derived dendritic cells (BMDCs) were isolated from C57BL/6 mice and cultured as previously described.[36]

Detection of Intracellular Interleukin-12 Expression. BMDCs were plated in a 96-well plate at a density of $2x10^5$ cells/well and incubated at 37 °C for 20 h with particle or control samples normalized to 300 ng CpG/well, then treated with Brefeldin A (1 mM final concentration) and incubated for another 4 h. Cells were washed, surface-stained with CD11c-PE (a DC specific surface marker) and CD86-Pacific Blue. The cells were then washed, fixed, and permeabilized with Cytofix/Cytoperm (Pharmingen), and stained with IL-12p40-APC. Relative expression of surface markers and intracellular IL-12 was then determined by flow cytometry.

Simultaneous Release of Protein and CpG. Particles containing both OVA and 3'-linked CpG were weighed out in triplicate and washed as described above. The particles were suspended in phosphate buffered saline (PBS, pH 7.4) at a concentration of 5 mg/mL and incubated at 37 ºC under gentle agitation (300 rpm) using a Thermomixer R heating block (Eppendorf). After various time points, the samples were centrifuged (2500 x *g*), the supernatant collected and an equivalent volume of fresh PBS added. After time points beyond 6 h, the particles were suspended in 300 mM acetate buffer (pH 5.0) instead of PBS. The collected supernatants were analyzed for protein and single-stranded DNA content using the assays described above. Values for complete protein and DNA release were determined by incubating the samples overnight in pH 5.0 buffer at 37 ºC. OVA-free particles and CpG-free particles were degraded in parallel and used to determine an appropriate background for the MicroBCA and OliGreen assays, respectively. Results represent the mean ± standard deviation of triplicate measurements.

***In Vivo* Cytotoxicity Assay.** C57BL/6 mice (n=10) were vaccinated subcutaneously (s.c.) with PBS or each particle type normalized to 50 μg ovalbumin in 200 μL PBS. For mice receiving CpG-free particles, a corresponding low, medium or high amount of free CpG-1826 DNA (phosphorothioate backbone, Oligos Etc.), was co-injected in a final volume of 200 μL PBS. At day 7 after vaccination, mice were injected intravenously with 1 x 10^7 CFSE-labeled target cells

consisting of 50% SIINFEKL($OVA_{258-265}$)-pulsed splenocytes labeled with 5 μM 5-(and 6)-carboxyfluorescein diacetate, succinimidyl ester (CFSE, Invitrogen) and 50% unpulsed splenocytes labeled with 0.5 μM CFSE. Mice were tail vein bled 8 or 18 h after adoptive transfer and the CFSE profile of transferred cells was determined by flow cytometry for analysis of OVA-specific cytotoxicity. Results are presented as means ± 95% confidence intervals. Statistical significance was analyzed using a two-tailed Student's t-Test.

***In Vivo* Tumor Protection Experiment.** The protection experiment was performed with age-matched female C57BL/6 mice. All immunizations were administered s.c. using 27.5 gauge needles. On day -7, mice were immunized in the left flank with PBS or with 3' CpG/OVA particles, OVA particles plus free CpG, or free OVA plus free CpG in 100 μL PBS. All treatments doses were normalized to 50 μg OVA and 10 μg CpG per mouse. On day 0, tumors were established by administering a s.c. injection of 6×10^5 MO5 cells in 100 μL PBS into the contralateral flank of each mouse. Tumor growth was measured using calipers and mice with tumors 1.5 cm in diameter were removed from the experiment and euthanized. Mice were also removed if they showed other signs of pain or distress such as immobility, a hunched posture or a lack of eating. Tumors from euthanized mice were removed and stored at -20 ºC in Allprotect Tissue Reagent (Qiagen) prior to analysis. Survival data was analyzed using MedCalc software (version 8.2.0.2) and statistical significance was determined using a logrank test. Tumor volume was calculated using the equation: volume = 0.5 x (longest diameter) x (shortest diameter)^2.

Analysis of Tumor Tissue for OVA Content by ELISA. Tumor samples from each mouse (10-55 mg) were blotted dry and placed in 2 mL microcentrifuge tubes to which 400 uL of T-PER extraction reagent containing Halt Protease Inhibitor Cocktail and 5 mM EDTA (Pierce) was added. Samples were disrupted/homogenized at rt for 30 s at full speed (33,000 rpm) using a TissueRuptor with disposable probes (Qiagen), then centrifuged three times (10,000 x *g*, rt, 5 min each) to remove residual solids. Samples were stored at -20 ºC before analysis. B16 and MO5 cells from *in vitro* culture (approximately $8x10^6$ cells each) were prepared in the same manner.

The wells of a 96-well microtiter plate (Falcon Pro-Bind, BD Labware) were coated with 100 uL of a 1:1000 dilution of goat anti-OVA antibody (IgG fraction, MP Biomedicals) overnight at 4 ºC. After washing the wells once with PBS containing 0.2% Tween-20 (PBS-T), 200 μL of blocking buffer (2% fetal bovine serum in PBS) was added to each well and incubated at 37 ºC for 1 h. After washing once with PBS-T, 100 μL of samples diluted in blocking buffer were added to the wells and incubated for 1 h at rt. The wells were washed three times with PBS-T, and 100 μL of a 1:4000 dilution of rabbit anti-OVA antibody (IgG fraction, MP Biomedicals) in blocking buffer was added to each well. After incubation at rt for 1 h, the wells were washed four times with PBS-T, and 100 μL of a 1:5000 dilution of AffiniPure HRP-conjugated donkey anti-rabbit IgG antibody (Jackson Immunoresearch) in blocking buffer was added to each well. After incubation at rt for 1 h, the wells were washed six times with PBS-T, and the plate was developed with 100 μL of 1-Step Ultra TMB-ELISA per well for 20 min at rt. The development was stopped by adding 100 μL of 2 M H_2SO_4, and absorbances were recorded at 450 nm. Dilutions of free OVA were used as a standard, and OVA content was normalized to total protein in each sample as determined by the Bradford method[37] using the Coomassie Assay Protein Reagent (Pierce) according to the manufacturer's instructions. Results represent the mean ± standard deviation of triplicate measurements.

Analysis of Tumor Tissue for OVA-encoding DNA. Tumor samples from each mouse (5-20 mg) were blotted dry and placed in 2 mL microcentrifuge tubes. Samples were disrupted/homogenized at rt for 30 s at full speed (33,000 rpm) using a TissueRuptor with disposable probes (Qiagen). Genomic DNA was purified with the AllPrep DNA/RNA/Protein Mini Kit (Qiagen) according to the manufacturer's instructions. Genomic DNA was similarly purified from B16 and MO5 cells from *in vitro* culture (approximately $6x10^5$ cells each).

Genomic DNA was amplified using the HotStarTaq Master Mix Kit (Qiagen), according to the manufacturer's instructions. OVA transcripts were amplified using the forward primer 5'-(GGCTCCATCGGCGCAGCAAG)-3' and reverse primer 5'-(GGGGAAACACATCTGCCAAA)-3'.[32] GAPDH was amplified using QuantiTect Primer Assay validated primers (Qiagen). Each PCR reaction mixture (50 μl) contained 0.25 μg of template DNA and 25 pmol of each primer. PCR products were analyzed by electrophoresis on a 1% agarose gel (120 V) using TAE buffer (pH 8.0, 40 mM Tris, 20 mM acetic acid, 1 mM EDTA). The gel was stained with ethidium bromide and imaged under UV irradiation.

References and Footnotes

(1) Byrd, W.; de Lorimier, A.; Zheng, Z. R.; Cassels, F. J. *Adv. Drug Delivery Rev.* **2005**, *57*, 1362-1380.
(2) van der Bruggen, P.; Zhang, Y.; Chaux, P.; Stroobant, V.; Panichelli, C.; Schultz, E. S.; Chapiro, J.; Van den Eynde, B. T. J.; Brasseur, F.; Boon, T. *Immunol. Rev.* **2002**, *188*, 51-64.
(3) Sheng, K. C.; Pietersz, G. A.; Wright, M. D.; Apostolopoulos, V. *Curr. Med. Chem.* **2005**, *12*, 1783-1800.
(4) Tacken, P. J.; de Vries, I. J. M.; Torensma, R.; Figdor, C. G. *Nat. Rev. Immunol.* **2007**, *7*, 790-802.
(5) Merad, M.; Sugie, T.; Engleman, E. G.; Fong, L. *Blood* **2002**, *99*, 1676-1682.
(6) Reddy, S. T.; Swartz, M. A.; Hubbell, J. A. *Trends Immunol.* **2006**, *27*, 573-579.
(7) Datta, S. K.; Cho, H. J.; Takabayashi, K.; Horner, A. A.; Raz, E. *Immunol. Rev.* **2004**, *199*, 217-226.
(8) Jerome, V.; Graser, A.; Muller, R.; Kontermann, R. E.; Konur, A. *J. Immunother.* **2006**, *29*, 294-305.
(9) Kaiser-Schulz, G.; Heit, A.; Quintanilla-Martinez, L.; Hammerschmidt, F.; Hess, S.; Jennen, L.; Rezaei, H.; Wagner, H.; Schatzl, H. M. *J. Immunol.* **2007**, *179*, 2797-2807.
(10) Murthy, N.; Thng, Y. X.; Schuck, S.; Xu, M. C.; Frechet, J. M. J. *J. Am. Chem. Soc.* **2002**, *124*, 12398-12399.
(11) Murthy, N.; Xu, M. C.; Schuck, S.; Kunisawa, J.; Shastri, N.; Frechet, J. M. J. *Proc. Natl. Acad. Sci. U. S. A.* **2003**, *100*, 4995-5000.
(12) Standley, S. M.; Kwon, Y. J.; Murthy, N.; Kunisawa, J.; Shastri, N.; Guillaudeu, S. J.; Lau, L.; Frechet, J. M. J. *Bioconjugate Chem.* **2004**, *15*, 1281-1288.
(13) Broaders, K. E.; Cohen, J. A.; Beaudette, T. T.; Bachelder, E. M.; Frechet, J. M. J. *Proc. Natl. Acad. Sci. U. S. A.* **2009**, *106*, 5497-5502.
(14) Standley, S. M.; Mende, I.; Goh, S. L.; Kwon, Y. J.; Beaudette, T. T.; Engleman, E. G.; Frechet, J. M. J. *Bioconjugate Chem.* **2007**, *18*, 77-83.
(15) Krieg, A. M.; Yi, A. K.; Matson, S.; Waldschmidt, T. J.; Bishop, G. A.; Teasdale, R.; Koretzky, G. A.; Klinman, D. M. *Nature* **1995**, *374*, 546-549.
(16) Klinman, D. M. *Nat. Rev. Immunol.* **2004**, *4*, 248-257.
(17) Barton, G. M.; Kagan, J. C.; Medzhitov, R. *Nat. Immunol.* **2006**, *7*, 49-56.
(18) Krieg, A. M. *Nat. Rev. Drug Discovery* **2006**, *5*, 471-484.
(19) Kumagai, Y.; Takeuchi, O.; Akira, S. *Adv. Drug Delivery Rev.* **2008**, *60*, 795-804.
(20) Macromonomer 1 was used in initial work due to synthetic convenience. As opposed to macromonomer 8, this molecule can be prepared entirely using solid phase DNA synthesis.
(21) Kandimalla, E. R.; Bhagat, L.; Yu, D.; Cong, Y. P.; Tang, J.; Agrawal, S. *Bioconjugate Chem.* **2002**, *13*, 966-974.
(22) Lenert, P.; Goeken, A. J.; Ashman, R. F. *Immunology* **2006**, *117*, 474-481.
(23) Cohen, J. A.; Beaudette, T. T.; Tseng, W. W.; Bachelder, E. M.; Mende, I.; Engleman, E. G.; Frechet, J. M. J. *Bioconjugate Chem.* **2009**, *20*, 111-119.
(24) Trinchieri, G. *Nat. Rev. Immunol.* **2003**, *3*, 133-146.
(25) Sharpe, A. H.; Freeman, G. J. *Nat. Rev. Immunol.* **2002**, *2*, 116-126.
(26) Medzhitov, R.; Janeway, C. *Trends Microbiol.* **2000**, *8*, 452-456.
(27) Janeway, C. a.; Medzhitov, R. *Annu. Rev. Immunol.* **2002**, *20*, 197-216.
(28) Schwartz, R. H. *Annu. Rev. Immunol.* **2003**, *21*, 305-334.

(29) Marshak-Rothstein, A. *Nat. Rev. Immunol.* **2006**, *6*, 823-835.
(30) Falo, L. D.; Kovacsovics-Bankowski, M.; Thompson, K.; Rock, K. L. *Nat. Med.* **1995**, *1*, 649-653.
(31) Dunn, G. P.; Bruce, A. T.; Ikeda, H.; Old, L. J.; Schreiber, R. D. *Nat. Immunol.* **2002**, *3*, 991-998.
(32) Goldberger, O.; Volovitz, B.; Machlenkin, A.; Vadai, E.; Tzehoval, E.; Eisenbach, L. *Cancer Res.* **2008**, *68*, 3450-3457.
(33) Bachelder, E. M.; Beaudette, T. T.; Broaders, K. E.; Dashe, J.; Frechet, J. M. J. *J. Am. Chem. Soc.* **2008**, *130*, 10494-10495.
(34) Mammen, M.; Dahmann, G.; Whitesides, G. M. *J. Med. Chem.* **1995**, *38*, 4179-4190.
(35) Hermanson, G. T. *Bioconjugate Techniques*; Academic Press: San Diego, 1996.
(36) Bachelder, E. M.; Beaudette, T. T.; Broaders, K. E.; Paramonov, S. E.; Dashe, J.; Frechet, J. M. J. *Mol. Pharmaceutics* **2008**, *5*, 876-884.
(37) Bradford, M. M. *Anal. Biochem.* **1976**, *72*, 248-254.

Chapter 3 – Immunological Activity and *In Vitro* Analysis of Particle Hydrolysis Products from Acid-Degradable Polyurethane Delivery Vehicles for Protein-Based Vaccines

Abstract

Although the acid-labile polyacrylamide particle system described in Chapter 1 was successful as a proof-of-concept system, biocompatibility issues with the high molecular weight polyacrylamide by-products may necessitate the use of more biofriendly materials. Therefore, in this chapter we investigate the synthesis and immunological activity of fully acid-degradable polymeric particles. Specifically, acid-labile particles containing a model protein antigen, ovalbumin, were prepared from a polyurethane with acetal moieties embedded throughout the polymer, and characterized by dynamic light scattering and transmission electron microscopy. The small molecule degradation by-product of the particles was synthesized and tested *in vitro* for toxicity indicating an LC_{50} of 12,500 μg/ml. A new liquid chromatography-mass spectrometry technique was developed to monitor the *in vitro* degradation of these particles. The degradation by-product inside RAW macrophages was at its highest level after 24 hours of culture and was efficiently exocytosed until it was no longer detectable after four days. When tested *in vitro*, these particles induced a substantial increase in the presentation of the immunodominant ovalbumin-derived peptide SIINFEKL in both macrophages and dendritic cells. In addition, vaccination with these particles generated a cytotoxic T-lymphocyte response that was superior to both free ovalbumin and particles made from an analogous but slower-degrading acid-degradable polyurethane polymer. Overall, we present a fully degradable polymer system with non-toxic by-products, which may find use in various biomedical applications including protein-based vaccines.

Introduction

Prophylactic treatment of viral infections with attenuated viruses has been successfully employed for many diseases including polio,[1] smallpox,[2] and measles.[3] Attenuated viruses infect the host in a limited manner, resulting in the presentation of viral peptide fragments on major histocompatibility complex class I (MHC I) molecules. Presentation of antigens via the MHC I pathway leads to an effective $CD8^+$ cytotoxic T lymphocyte (CTL) response, resulting in protective immunity against certain viruses.[4] However, using attenuated or inactivated viruses as vaccine formulations is unacceptable for many diseases such as HIV or hepatitis C due to the safety risks inherent to the treatment. Recombinant viral proteins are an attractive alternative to attenuated viruses and have been used successfully to generate high antibody titers in the treatment of diseases such as hepatitis B.[5] The efficacy of recombinant protein-based vaccines is frequently limited due to their inability to deliver antigens directly to the MHC I presentation pathway, resulting in a limited CTL response.

Several methods have been developed to increase recombinant protein presentation via the MHC I pathway including genetically modifying bacterial toxins to possess CTL epitopes,[6] fusion of antigens with heat shock proteins,[7] and adsorbing proteins on the surface of iron oxide or polystyrene beads.[8,9] Delivery of proteins in particles capable of being phagocytosed by antigen presenting cells represents a robust method of generating CTL responses against any recombinant protein. Expanding on earlier work done on conjugating proteins to insoluble

carriers, we have developed acid-labile particles that encapsulate proteins in a crosslinked polyacrylamide-based hydrogel network.[10-13] Upon phagocytosis, these particles quickly degrade under the acidic conditions found in endo- and lysosomal compartments, resulting in the release of the encapsulated protein. We have found that MHC I presentation is dramatically increased with such acid-degradable particle systems when compared to free protein and non-degradable microgels.[14]

Although our acid-labile polyacrylamide particles have been successful as a proof of concept system, biocompatibility issues with the high molecular weight polyacrylamide by-products may necessitate the use of fully acid-degradable materials. Polymers that can break down completely into low molecular weight by-products have a distinct advantage over our prior system since they should be easily cleared from the body once fully degraded. Several polymers of this type have previously been reported including poly(β-amino) esters,[15-17] poly(ketal)s,[18] and poly(acetal)s,[19] all of which degrade faster at the acidic pH of 5.0-6.0 than at physiological pH

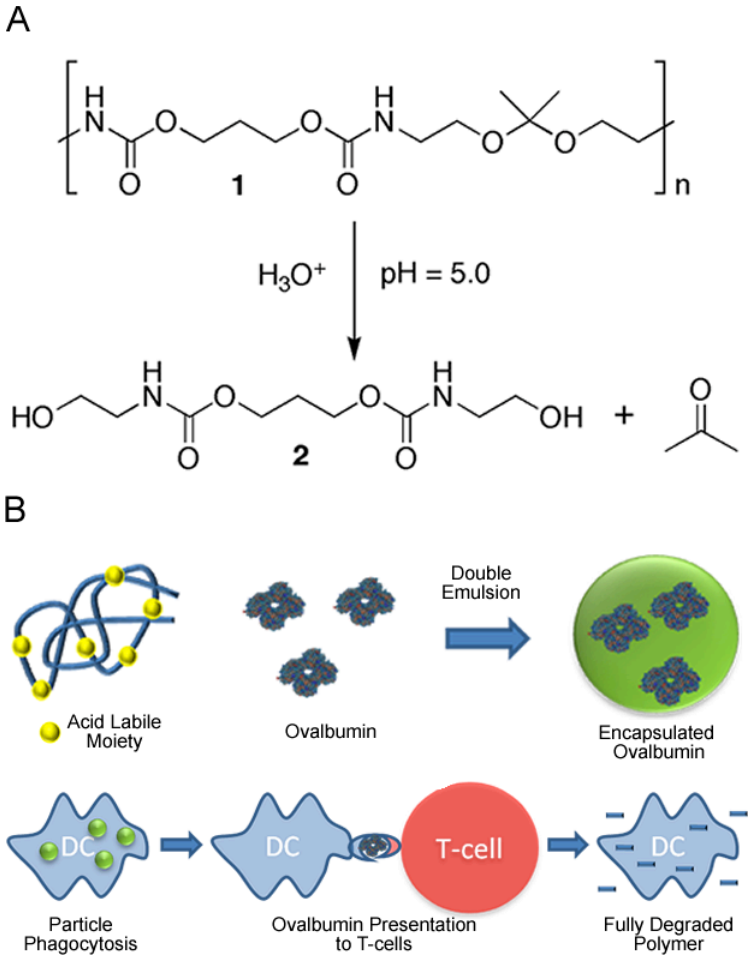

Figure 3.1. (A) Under acidic conditions (pH 5.0) polymer **1** degrades into acetone and compound **2**. (B) OVA is encapsulated in acid-degradable microparticles made from polymer **1** via a double emulsion method. OVA-containing particles are phagocytosed by dendritic cells resulting in antigen presentation to $CD8^+$ T-cells. Following phagocytosis, polymer **1** is fully degraded into small molecules.

(7.4). However, the complete degradation of these polymers into small molecule products typically occurs on the order of several days to a few weeks, which may increase their toxicity. We recently generated a library of polyurethanes that possess dimethyl acetal moieties in the polymer backbone, which hydrolyze fully under acidic conditions to yield small molecule diols and acetone (Figure 3.1A).[20] Further exploring the utility of these acid-degradable materials, we made microparticles out of polymer **1** and evaluated their potential as carriers for protein-based vaccines. Herein we demonstrate that particles made from polymer **1** are more effective in generating an immune response compared to free protein and analogous particles prepared from a slower degrading polymer. Finally, to analyze the fate of intracellular degradation products (Figure 3.1B), a chromatographic technique was developed to study the localization of diol **2**. Together, these studies demonstrate that particles made from polymer **1** are promising materials for vaccine applications due to their acid-sensitivity, ability to induce an antigen-specific CTL response *in vivo*, and innocuous degradation products.

Results and Discussion

Particle Formation and Characterization

We have previously reported the synthesis of a library of polyurethane polymers with tunable acid-sensitivity.[20] These step-growth polymers were prepared by reactions involving an acetal-containing diamine monomer and a library of bis(*p*-nitrophenyl carbamate/carbonate) or diisocyanate monomers. The degradation half-life at pH 5.0 of microparticles prepared from this family of polyacetals was highly dependent on the hydrophobicity of the constituent polymer from which the particles were prepared. In general, we found that the hydrophilic polymers degraded significantly faster than their more hydrophobic counterparts. However, polymers that were too hydrophilic were incapable of generating particles via standard emulsion techniques.[21] In balancing degradability versus processability, we chose polymer **1** as a suitable material for protein-based vaccine applications due to its ability to form stable microparticles via a double emulsion procedure and a reasonably short protein release half-life (approximately 15 hours at pH 5.0 and 37 ºC) from these particles.

Microparticles encapsulating a model antigen, OVA, were made by a standard double emulsion protocol.[21] After the final emulsification step and evaporation of the organic solvent, the particles were isolated using tangential flow filtration (TFF).[22] Prior to lyophilization of an aqueous suspension of the particles, a 10 wt% solution of sucrose was added as a cryprotectant to prevent particle aggregation. The OVA loading efficiency was found to be 25% and the particle recovery was 42% based on the masses of starting OVA and polymer **1**, respectively.

Microparticles prepared from polymer **1** were characterized by transmission electron microscopy (TEM) and dynamic light scattering (DLS). According to these data (Figure 3.2 A-C), the particles were between 100-500 nm in size with an average diameter of 249 ± 5 nm. Particles of this size have been shown to be suitable for targeting DCs *in vitro* and *in vivo*,[23,24] however, there is still some debate in the literature over the optimal particle size for inducing class I peptide presentation.[8,25]

In Vitro Macrophage and Dendritic Cell MHC I Presentation of a Model Antigen

In order for a vaccine to generate an effective CTL immune response, antigen presenting cells (APCs) must efficiently present pathogen-derived peptides on MHC I molecules to $CD8^+$ T-cells. A useful *in vitro* method for quantifying T-cell presentation is the B3Z assay.[26] B3Z cells are a line of T-cells, which have been transfected with the *β*-galactosidase gene controlled by the nuclear factor of activated T-cells element of the human interleukin 2 enhancer. Due to the specificity of this assay, only upon engagement of APCs presenting SIINFEKL, the immunodominant peptide sequence of OVA on H-$2K_b$, B3Z cells produce *β*-galactosidase. The resulting *β*-galactosidase activity, which correlates directly with SIINFEKL presentation, can be colorimetrically detected. We first evaluated free OVA and OVA-loaded particles prepared from polymer **1** for their ability to stimulate T-cells by incubating them with RAW macrophages. B3Z cells were then co-cultured with the macrophages and the resulting presentation of SIINFEKL was measured (Figure 3.3A). Compared to free OVA, the use of particles made from polymer **1** led to a 28 fold increase in T-cell activation. Overall, particles prepared from polymer **1** dramatically increased the ability of macrophages to activate T-cells *in vitro*.

To further study *in vitro* T-cell activation, free OVA and OVA-loaded acid-degradable particles made from polymer **1** were tested in BMDCs in the same manner as with the

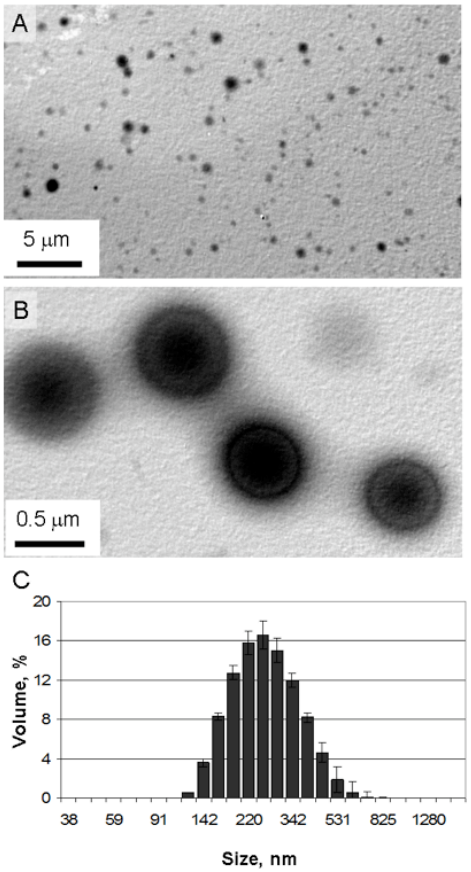

Figure 3.2. (A) TEM images of particles made from polymer **1**. (B) Magnified image of larger particles selected for their high contrast. (C) Volume distribution of polymer **1** particles with an average diameter of 249 nm, a size suitable for phagocytosis by dendritic cells.

macrophages above (Figure 3.3B). Particles made from polymer **3**, which has a similar structure to polymer **1** (Figure 3.4) but slower degradation kinetics at pH 5.0, were tested in parallel. Polymer **1** induced the best presentation of SIINFEKL, followed by polymer **3**, and finally soluble OVA. This trend correlates well with the protein release half-lives of these two polymers, which have been previously reported.[20] The importance of pH-sensitivity in vaccine carriers in the context of efficient MHC I presentation has previously been examined in DCs.[27,28] Our results further support findings that pH-sensitivity is an important factor in determining the extent of MHC I presentation in DCs.

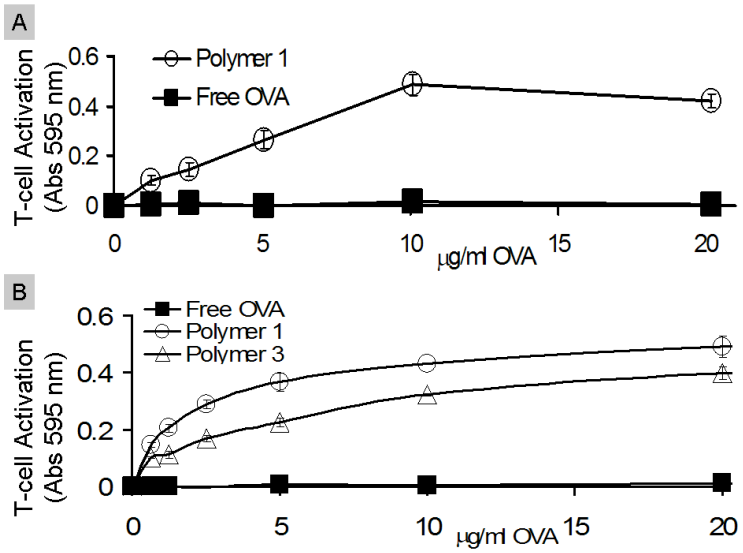

Figure 3.3. Free OVA (filled squares), polymer **1** particles (open circles), or polymer **3** particles (open triangles) were cultured with (A) RAW macrophages or (B) dendritic cells for six hours. After six hours, antigen presenting cells were cultured with B3Z cells for 16 hours and SIINFEKL presentation was measured.

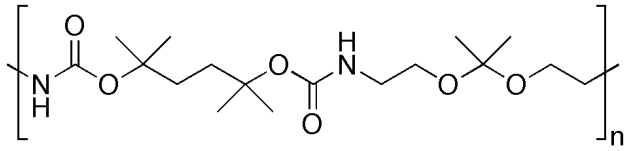

3

Figure 3.4. Structure of polymer **3**, a more hydrophobic analog of polymer **1**.

Ex Vivo CTL Cytotoxicity Assay

Encouraged by the promising *in vitro* T-cell activation results, we next tested the ability of particles made from polymer **1** to evoke a CTL response *in vivo*. To this end, mice were vaccinated twice (day -14 and day -7) with 50 μg of OVA, or an equivalent amount of OVA encapsulated in polymer **1**, or polymer **3** microparticles. On day 0, spleens were removed, stimulated *in vitro* for 5 days, and assayed for CTL activity (Figure 3.5). Similar to our findings

with the B3Z assay, polymer **1** particles induced the highest level of CTL activity. We found no statistically significant CTL response for OVA-loaded particles prepared from polymer **3**. These data further suggest that the degradation half-life and protein release half-life of pH-sensitive materials is a critical parameter governing the generation of CTL responses *in vivo*. For future studies, we anticipate being able to increase *in vivo* CTL responses by vaccinating with more particles, using adjuvants, or by increasing the degradation kinetics by fine tuning the structural features and hydrophobicity of the parent polymer.

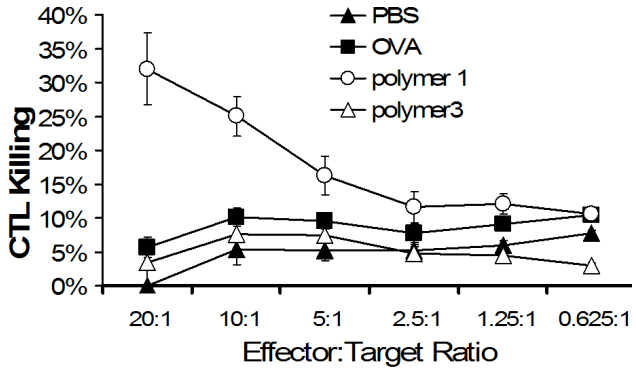

Figure 3.5. Mice were vaccinated on day -14 and day -7 with PBS (filled triangles), free OVA (filled squares), polymer **1** particles (open circles), and polymer **6** particles (open triangles). On day 0, spleen cells were removed, restimulated *in vitro* for five days then tested for CTL activity.

Scheme 3.1. Synthesis of diols **2** and **6** [a]

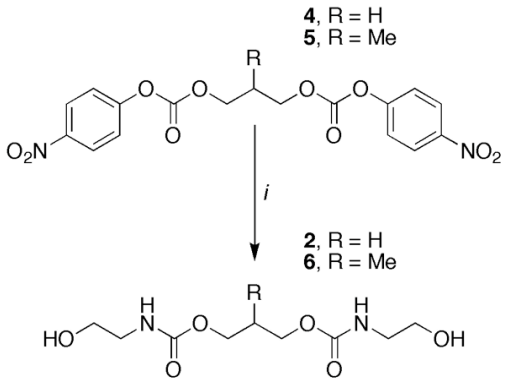

[a] (*i*) Ethanolamine, CH_2Cl_2, 0 °C → rt.

In vitro Toxicity of Compound 2

Because polymer **1** has the novel property of degrading into acetone (a non-toxic metabolic intermediate) and small molecule **2**, we synthesized (Scheme 3.1) and tested the toxicity of this compound *in vitro* (Figure 3.6). Diol **2** was synthesized in one step through the reaction of an excess of ethanolamine with bis(*para*-nitrophenyl carbonate) **4**. Diol **6**, which is identical to diol **2** except for the addition of a single methyl group, was also synthesized by a similar route to serve as an internal standard for LC-MS studies (see below).

To study the toxicity of diol **2**, serial dilutions of this compound were incubated with macrophages for 24 hours. After one day of rest, we tested the viability of the cells using an MTS assay and determined that the LC_{50} of compound **2** in RAW macrophages was approximately 12,500 μg/ml. This value is similar to that reported by Claes et al. for the degradation products of FDA approved polymers such as poly(L, DL-lactide) (PLA) and poly(L-lactide-co-glycolide) (PLGA), which were not toxic up to 15,000 μg/ml.[29] However, unlike those of PLGA, the by-products of polymer **1** should not lead to an acidic microenvironment.[30] Shenderova et al. measured the pH microenvironment of PLGA particles suspended in buffer to be 1.8. In some instances, this low pH may be unsuitable for cells, as well as the protein and drug payloads typically encapsulated in these particles. Therefore a possible advantage of polymer **1** over PLGA is that it should preserve a neutral microenvironment inside particles, which may be a beneficial feature for pH-sensitive cargoes.

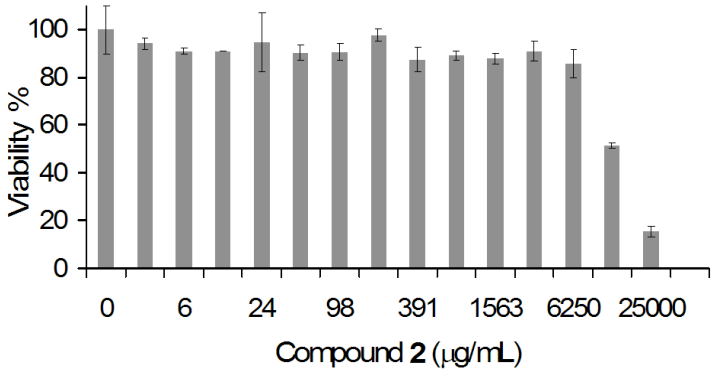

Figure 3.6. Viability of RAW macrophages incubated with compound **2** as determined by the MTS assay. Two fold dilutions of compound **2** were cultured for 24 hours with RAW macrophages. The cells were then washed, allowed to rest for an additional 24 hours and tested for cell viability.

LC-MS Detection of Compound 2 from *In Vitro* Degradation Experiments

We have previously shown that polymer **1** hydrolyzes to yield compound **2** when incubated in pH 5.0 buffer for three days at 37 ºC.[20] Because they degrade into highly water soluble small molecules, the by-products from polymer **1** should be easily eliminated from the body via renal filtration.[31] In addition, we have previously investigated the uptake and degradation of polymer **1** particles via confocal microscopy. These studies suggested that polymer **1** particles may be degraded by phagocytic cells.[20] However, to obtain direct evidence that polymer **1** particles are effectively degraded inside APCs, we needed to develop a method to detect the presence of compound **2** in cell culture. Hua et al. were able to detect the degradation products derived from PLGA *in vivo* by labeling the intact polymer with ^{125}I and measuring the distribution of the radioactive signal.[32] However, radiolabeling is a process that can significantly

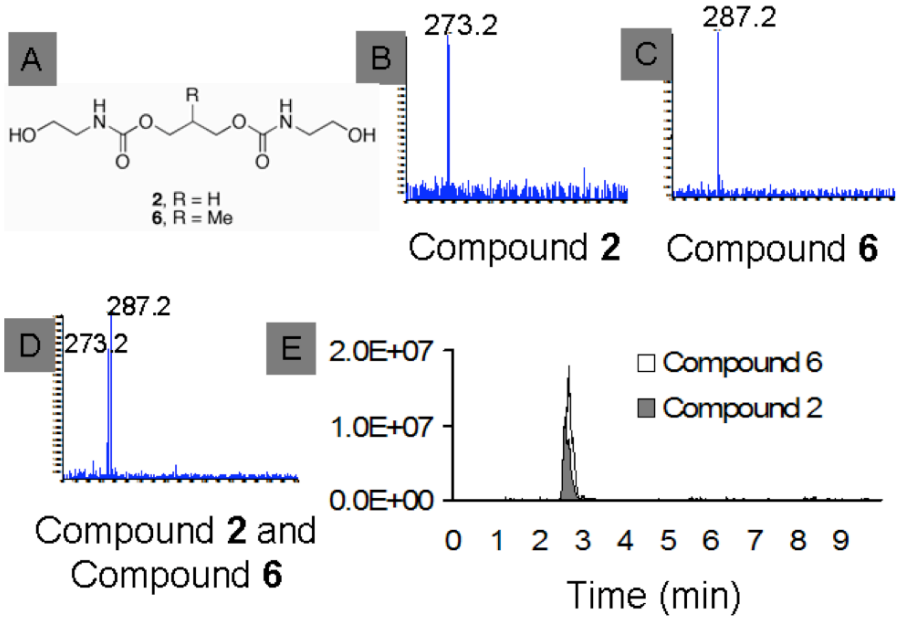

Figure 3.7. Analysis of compounds **2** and **6** by LC-MS. (A) Structure of compound **2** and compound **6.** Mass spectrum of compound **2** (B), compound **6** (C), or compound **2** and compound **6** co-injected (D). (E) Extracted chromatograms of compound **2** and compound **6** when co-injected as a 1:1 mixture.

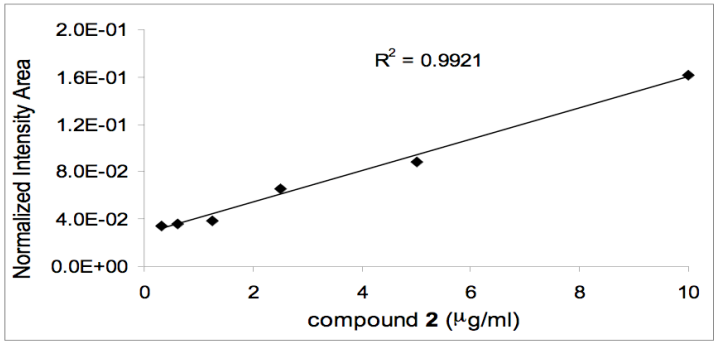

Figure 3.8. Serial two fold dilutions of compound **2** plotted vs. the normalized integration.

alter the properties of the native polymer and subsequently affect the biodistribution. In an method providing an alternative to radiolabeling, Yoo et al. were able to measure the degradation of PLGA in buffered solutions using HPLC.[33] Based on the retention times of lactic and glycolic acids, they were able to study the time dependent degradation of PLGA incubated at various pH values. However, this method is not suitable for our purposes due to the heavy signal contamination arising from proteins, nucleic acids, and a variety of small molecules (such as antibiotics and nutrients) present in cells and cell culture media.

To circumvent the issue of contamination in samples obtained from cells, we developed a liquid chromatography-electrospray mass spectrometry (LC-MS) technique to study the degradation of particles made from polymer **1** *in vitro*. To detect the degradation product of polymer **1**, we first synthesized diols **2** and **6** (see Scheme 1 and discussion above) and optimized

a method to detect them using LC-MS. When analyzed as solutions in PBS and using neutral mobile phases (to minimize background hydrolysis of acetal-containing compounds present in subsequent samples), diols **2** and **6** were both ionized primarily as their sodium adducts and found to have similar retention times (see Figure 3.7). In analogy to the work of Fent et al.,[34] we developed a semi-quantitative LC-MS technique for the detection of diol **2** wherein a fixed amount of compound **6** was spiked into each sample. After analysis, we extracted chromatograms of the intensity of masses corresponding to the sodium adducts (m/z = $[M+Na]^+$) of **2** or **6** versus time. To normalize the data, the area under the curve of diol **2** was divided by the area under the curve of diol **6** for each sample. To test our method, serial two-fold dilutions of compound **2** were spiked with 45.5 μg/mL of compound **6** and analyzed by LC-MS. The correlation coefficient for the dependence of the normalized area of diol **2** on the concentration was found to be 0.99 (Figure 3.8). Based on these data, this method was deemed suitable for analyzing the relative amounts of compound **2** in each sample.

After developing our LC-MS method, we next attempted to detect an increase in diol **2** when particles prepared from polymer **1** were cultured in the presence of RAW macrophages. In this experiment, polymer **1** particles were incubated with RAW macrophages at a concentration of 2 mg/ml. To account for background acetal hydrolysis at pH 7.4, particles were also incubated in cell culture medium under identical conditions. Macrophages cultured without particles served as a negative control. After 48 hours the cells were lysed in the cell culture medium, and analyzed using LC-MS (Figure 3.9A). To increase the sensitivity of the assay, the cell lysate and supernatant were measured together. Using the LC-MS method described above, the extracted normalized area for compound **2** was seven fold higher when particles were incubated with macrophages compared to particles incubated in medium alone (Figure 3.9B). These data suggest that the presence of phagocytic cells led to a greater degree of degradation of particles prepared from polymer **1** compared to the background hydrolysis of these acid-sensitive materials.

After confirming that we were able to detect diol **2** in a mixture of cell culture medium and cell lysate, we next wanted to explore the kinetics of removal (exocytosis) of compound **2** from macrophages pulsed with polymer **1** particles. For this experiment, RAW macrophages were cultured with particles at a concentration of 2 mg/ml. After 24 hours, the cells were washed extensively to remove residual particles and cultured for an additional zero, one, two or four days in fresh medium. After the additional culture time, the cells were separated from their medium. Samples prepared from the cell lysate or the collected medium were analyzed using LC-MS (Figure 3.10A-C) and the values from each group were normalized with respect to their respective maximum values. We found the highest concentration of diol **2** inside the cell on day 0. The amount of compound **2** on subsequent days continued to decrease, and by day four the concentration was near background levels. In contrast, the concentration of compound **2** in the cell culture medium samples followed an opposite trend. Specifically, we found the lowest concentration of diol **2** on day zero with the highest concentration on day four. Based on these findings, we conclude that once particles made from polymer **1** are internalized by macrophages, they are broken down and efficiently secreted. These findings make polymer **1** an exceptional candidate as a material for drug delivery applications due to its rapid clearance from the cell. Once exocytosed from the cell, the extremely water soluble compound **2** should be easily removed from the body via the renal system. Future experiments will explore the *in vivo* toxicity of compound **2** and whether this molecule is effectively cleared from the body. Furthermore, the

LC-MS method developed in this paper could also be applied to study the degradation of other frequently used biodegradable polymers used in *in vitro* and *in vivo* applications.

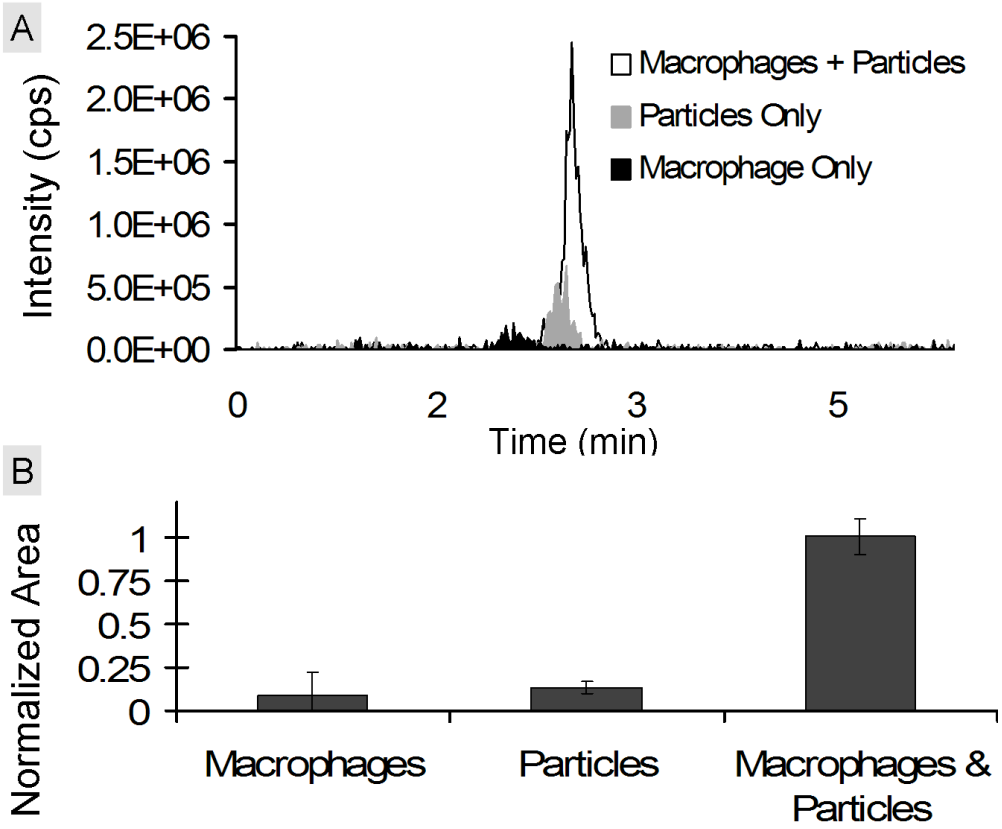

Figure 3.9. Detection of compound **2** *in vitro*. RAW macrophages were cultured with polymer **1** particles for 48 hours. Polymer **1** particles incubated in medium and macrophages alone served as controls. (A) Representative extracted chromatograms for compound **2** of RAW macrophages incubated with particles (white), macrophages alone (black), or polymer **1** particles incubated in medium alone (gray). (B) Average areas calculated from the extracted chromatograms of compound **2** in each sample. For each sample, the area for compound **2** was divided by the area of an internal standard (compound **6**) and normalized with respect to the maximum average area (macrophage & particle sample).

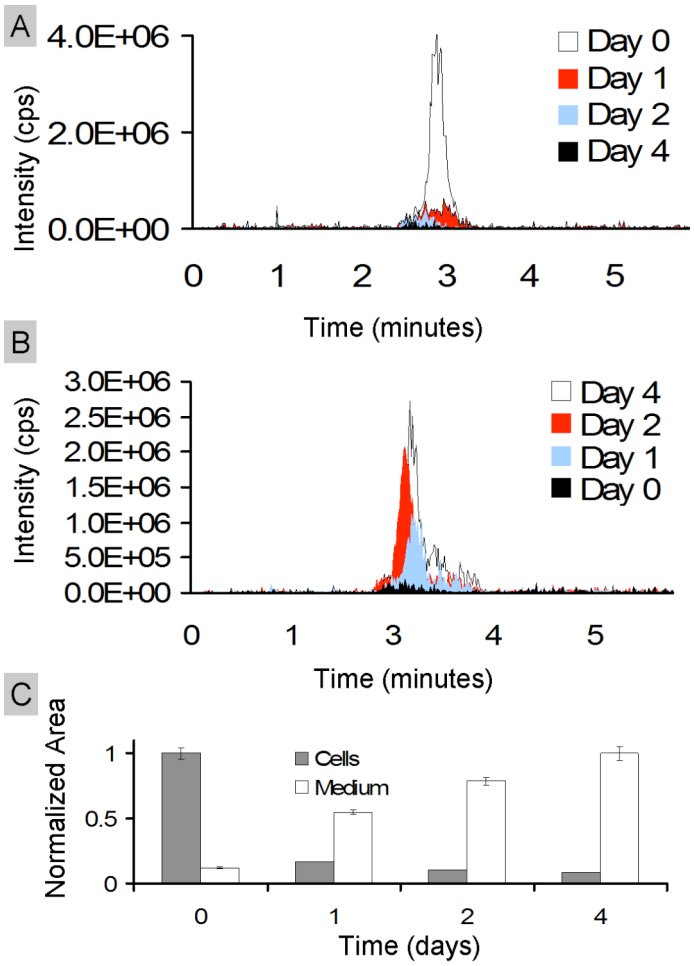

Figure 3.10. Exocytosis kinetics of compound **2** *in vitro*. RAW macrophages were cultured with polymer **1** particles for 24 hours. Cells were then washed and allowed to grow for an additional zero, one, two, or four days. (A) Representative extracted chromatograms for compound **2** inside RAW macrophages. (B) Representative extracted chromatograms for compound **2** in the cell culture medium. (C) Average areas calculated from the chromatograms of compound **2** in each sample. The area for compound **2** was divided by the area of the internal standard (compound **6**) for each sample and then normalized with respect to the maximum value for each group. For cells the maximum value was on day zero and for the medium the maximum value was on day four.

Conclusions

We have shown that protein-loaded particles made from polymer **1** increase T-cell presentation *in vitro*, generate a CTL response *in vivo* and degrade into small innocuous by-products. Together, these findings suggest that polymer **1** is a suitable material for vaccines and other *in vivo* therapeutic applications.

Experimental

General Procedures and Materials. Reagents and materials were purchased from commercial sources and were used without further purification unless otherwise noted. ^{1}H NMR spectra were recorded at 400 MHz and ^{13}C spectra were recorded at 100 MHz. Chemical shifts (ppm) are reported relative to tetramethylsilane and coupling constants are reported in Hz. High-resolution fast atom bombardment mass spectrometry (FAB-HRMS) analysis was performed at the UC Berkeley mass spectrometry facility. Elemental analyses were obtained from the UC Berkeley analytical facility. Water (dd-H_2O) for buffers and particle washing steps was purified to a resistance of 18 MΩ using a NANOpure purification system (Barnstead, USA). When used in the presence of acetal containing materials, dd-H_2O was rendered basic (pH 8) by the addition of triethylamine (TEA) (approximately 0.01%). Fluorescence measurements were obtained on a Spectra Max Gemini XS (Molecular Devices, USA), usage courtesy of Prof. Jonathan Ellman. RAW 309 cells were obtained from ATCC (Manassas, VA) and grown according to ATCC's directions. Liquid chromatography-electrospray mass spectrometry (LC-MS) analysis was performed using an API 150EX system (Applied Biosystems, USA) equipped with a Turbospray source, an 1100 series LC pump (Agilent), and Analyst software (version 1.4.2, Applied Biosystems). LC experiments were conducted using a Jupiter 5μ C18 300Å (Phenomenex, USA) reversed phase column (2.0 mm x 150 mm) at a flow rate of 0.25 ml/min with a MeCN:ddH_2O (0.1% ammonium formate, pH = 7.7) gradient. Diol **6** was added to every sample to be analyzed by LC-MS at a fixed final concentration of 45.5 μg/mL.

Polymers 1 and 3 as well as compounds 4 and 5 were prepared as described previously.[20]

Synthesis of Diol 2. Bis(*para*-nitrophenyl carbonate) **4** (0.50 g, 1.2 mmol) was dissolved in CH_2Cl_2 (20 mL) and cannulated into a solution of ethanolamine (0.45 mL, 7.4 mmol) in CH_2Cl_2 (20 mL) at 0 ºC. The resulting solution was stirred and allowed to warm to rt over 6 h. The reaction mixture was concentrated and the residue was purified by column chromatography eluting with 3% followed by 10% MeOH in CH_2Cl_2 to yield diol **2** (214 mg, 69%) as a white solid. MP: 118-119 ºC. IR (cm^{-1}): 3323 (br), 1695, 1546, 1275. ^{1}H NMR (400 MHz, MeOH-d_4): δ 1.93 (m, 2H), 3.21 (t, J = 6, 4H), 3.57 (t, J = 6, 4H), 4.12 (m, 4H). ^{13}C NMR (100 MHz, MeOH-d_4): δ 30.1, 44.3, 62.0, 62.7, 159.3. Calcd: [M+H]$^+$ ($C_9H_{19}N_2O_6$) m/z = 251.1243. Found FAB-HRMS: [M+H]$^+$ m/z = 251.1239. Anal. Calcd. for $C_9H_{18}N_2O_6$: C, 43.20; H, 7.25; N, 11.19. Found: C, 43.09; H, 7.33; N, 11.04.

Synthesis of Diol 6. This compound was prepared according to the same procedure used for diol **2** except bis(*para*-nitrophenol carbonate) **5** was used as the starting material to yield **6** (87%) as a white solid. MP: 72-73 ºC. IR (cm^{-1}): 3332 (br), 1695, 1548, 1267. ^{1}H NMR (400 MHz, MeOH-d_4): δ 0.98 (d, J = 7, 3H), 2.11 (m, 1H), 3.20 (t, J = 6, 4H), 3.57 (t, J = 6, 4H), 3.98 (d, J = 5, 4H). ^{13}C NMR (100 MHz, MeOH-d_4): δ 14.1, 34.6, 44.3, 62.0, 67.5, 159.3. Calcd: [M+H]$^+$

($C_{10}H_{21}N_2O_6$) m/z = 265.1400. Found FAB-HRMS: $[M+H]^+$ m/z = 265.1398. Anal. Calcd. for $C_{10}H_{20}N_2O_6$: C, 45.45; H, 7.63; N, 10.60. Found: C, 45.16; H, 7.71; N, 10.32.

Production of OVA-Loaded Microparticles. Acid-degradable microparticles were prepared using a double emulsion water/oil/water (w/o/w) evaporation method similar to that described by Bilati et al.[21] Briefly, ovalbumin (OVA, 10 mg) was dissolved in phosphate buffered saline (PBS, pH 7.4, 50 μL). Polymer **1** or **3** (200 mg) was dissolved in CH_2Cl_2 (1 mL) and added to the OVA solution. This mixture was then emulsified by sonicating for 30 s on ice using a probe sonicator (Branson Sonifier 450) with an output setting of 3 and a duty cycle of 10%. This primary emulsion was added to an aqueous solution of poly(vinyl alcohol) (PVA, M_W = 13,000 – 23,000 g/mol, 87-89% hydrolyzed) (2 mL, 3% w/w in PBS) and sonicated for an additional 30 s on ice using the same settings. The resulting double emulsion was immediately poured into a second PVA solution (10 ml, 0.3% w/w in PBS) and stirred for 4 h allowing the organic solvent to evaporate. The particles were then washed five times using tangential flow filters (TFF, Spectrum Laboratories, USA) with a surface area of 11 cm^2 and a pore size of 0.05 μm. To stabilize the suspensions of the particles, a solution of sucrose in water (10% w/v) was added as a cryoprotectant. The particles were then frozen and lyophilized.

Quantification of Encapsulated OVA. Particles containing OVA were suspended at a concentration of 2 mg/mL in an acetate buffer (0.3 M, pH 5.0) and incubated at 37 ˚C under gentle agitation for 3 d using a Thermomixer R heating block (Eppendorf). After the particles had been fully degraded, the resulting solution was analyzed for protein content using the fluorescamine reagent and a microplate assay as described by Lorenzen et al.[35] Empty particles were degraded in a similar fashion and used to determine a background fluorescence level. The results were compared to a standard curve and the mass of OVA encapsulated was calculated. The protein loading was found to be 2 ± 0.28 wt% and the loading efficiency was 40 ± 0.5%.

Transmission Electron Microscopy. An aqueous suspension of particles (10 μL, approximately 2 mg/mL) was deposited on a carbon coated copper grid and allowed to sit undisturbed for 3 min. The excess solution was blotted off and the grid allowed to air-dry. Specimens were observed on a FEI Technai 12 TEM equipped with a Gatan CCD camera using an accelerating voltage of 120 kV.

Particle Size Analysis by Dynamic Light Scattering. Particle size distributions and average particle diameters were determined by dynamic light scattering using a Nano ZS (Malvern Instruments, United Kingdom). Particles were suspended in dd-H_2O (pH 8) at a concentration of 1 mg/mL and three measurements were taken of the resulting dispersions. Results are presented as a volume distribution in Figure 3.2C.

Bone Marrow Derived Dendritic Cells. Bone marrow derived dendritic cells (BMDCs) were isolated in manner similar to a previously reported protocol.[36] Two to four month old female C57BL/6 mice (Jackson Laboratory) were sacrificed and the femurs and tibias were isolated. The bone marrow was flushed out with PBS using a 25-gauge needle. The cells were passed through a cell strainer and cultured with DMEM medium supplemented with FBS (10% v/v), penicillin (100 units/ml), streptomycin (100 μg/ml), L-glutamine (2 mM, GIBCO/BRL), GM-CSF and IL-4 (both 5 ng/mL, Peprotech). After six days of culture in a 24-well plate seeded at 1

million cells/ml, the BMDCs were removed from the wells, immuno-isolated using CD11c magnetic beads per the manufacturer's directions (Miltenyi Biotech) and transferred into a 96-well plate at 5 x 10^4 cells per well.

MHC Class I Presentation (B3Z) Assay. B3Z cells (a generous gift of Prof. N. Shastri, University of California, Berkeley), a $CD8^+$ T-cell hybridoma engineered to produce β-galactosidase when its T-cell receptor engages an $OVA_{257-264}$:K_b complex[26,37] were maintained in RPMI 1640 (Invitrogen, USA) supplemented with 10% fetal bovine serum, 2 mM Glutamax, 50 mM 2-mercaptoethanol, 1 mM sodium pyruvate, 100 U/ml penicillin and 100 mg/ml streptomycin. $1x10^4$ RAW macrophages or $5x10^4$ BMDCs were seeded overnight in a 96 well plate and subsequently incubated with OVA-containing particles or free OVA. After 6 h, the cells were washed and $1x10^5$ B3Z cells were added and cocultured for an additional 16 h. The medium was removed and 100 μL of CPRG buffer (91 mg of chlorophenol red β-D-galactopyranoside (Roche, USA), 1.25 mg of NP40 (EMD Sciences, USA), and 857 mg $MgCl_2$ in1 L of PBS) was added to each well. After 30 min, the absorbance at 595 nm was measured using a microplate reader. The results are presented as the mean of triplicate cultures ± 95% confidence intervals.

Immunization and CTL assay. Immunization, *in vitro* stimulation and an *in vitro* CTL assay were based on previously described procedures.[38-40] On day -14 and -7, mice were immunized subcutaneously at the base of the tail with either PBS, 50 μg OVA or particles containing an equivalent amount of protein made from polymer **1** or polymer **3**. On day 0, spleens were harvested, mechanically disassociated and RBCs were lysed with RBC lysis buffer. $5x10^6$ cells/ml from each spleen were cultured with $2.5x10^6$ syngeneic spleen cells/ml pulsed with 5 μg/ml SIINFEKL. After five days of stimulation, effector T-cells in varying concentrations were cocultured with 60,000 target cells (syngeneic spleen cells pulsed with 10 μg/ml SIINFEKL). Target cell death was determined by the release of lactate dehydrogenase using the CytoTox 96® Non-Radioactive Cytotoxicity Assay (Promega, USA) per the manufacturer's instructions. The results are presented as the mean of triplicate cultures ± 95% confidence intervals.

Toxicity of Compound 2. Compound **2** was incubated with 10,000 RAW macrophages for 24 h at various concentrations. After 24 h, compound **2** was removed, the cells were washed twice with medium and incubated overnight. Cell viability was measured the following day using CellTiter $96AQ_{ueous}$One Solution Cell Proliferation Assay MTS (Promega, USA) per the manufacturer's instructions. The results are normalized to untreated cells and presented as the mean of triplicate cultures ± 95% confidence intervals.

Analysis of Compound 2 and Compound 6 by LC-MS. Compound **2**, compound **6**, or a 1:1 mixture of these compounds were analyzed by LC-MS (all at a concentration of 75 μg/mL) using the conditions described above. Both compounds were found to ionize primarily as their respective sodium adducts (m/z = $[M+Na]^+$). The retention times for compound **2** and compound **6** were found to be nearly identical. The chromatograms of compounds **2** and **6** (Figure 3.7E) were obtained by extracting the intensity of the mass of the corresponding sodium adduct of either compound from the total ion count at each time point.

Generation of an LC-MS standard curve for Compound 2. Serial two fold dilutions in duplicate of compound **2** ranging between 0.31-10 μg/ml were analyzed by LC-MS using the conditions described above. Each sample was spiked with 45.5 μg/ml of compound **6**. The area under the curve of the extracted chromatogram for compound **2** was normalized with respect to the area for compound **6**.

Cellular Degradation of Acid-Labile Particles Analyzed by LC-MS. Particles prepared from polymer **1** were incubated at a concentration of 2 mg/ml in a 96 well plate with either RAW macrophages (40,000 cells/well) or cell culture medium. Untreated macrophages (incubated without particles) were cultured in parallel to serve as a negative control. After 2 days, the 96 well plate was removed from the incubator and immediately frozen. The cells were lysed by 5 freeze/thaw (alternating -80 ºC/rt) cycles. The lysed macrophage and medium samples were then centrifuged (12,000 x *g*) at 4 ºC for 1 h to remove cellular debris and residual particles. The supernatant was removed and EtOH (35 mL, cooled to -80 ºC, and with 1% triethylamine to avoid acid-catalyzed hydrolysis of acetal containing compounds) was added to precipitate proteins and nucleic acids. The resulting solutions were then centrifuged (15,000 x *g*) at 4 ºC for 1 h. The supernatant was removed and concentrated using a rotary evaporator. The resulting residue was dissolved in PBS (1 mL), diluted 100 fold, and analyzed for the presence of diol **2** using LC-MS. Results are presented as the mean of triplicate measurements ± 95% confidence intervals.

Intracellular Degradation and Exocytosis of Compound 2 Monitored by LC-MS. Particles prepared from polymer **1** were incubated at a concentration of 2 mg/ml in a 96 well plate with RAW macrophages (60,000 cells/well). After 24 h, the cells were trypsinized, washed 3 times with PBS to remove any residual particles and plated in T-25 flasks. The macrophages were then cultured for 1, 2 or 4 days. Untreated macrophages (incubated without particles for 4 days) were cultured in parallel to serve as a negative control. After these time points, the medium was removed from the cells, centrifuged (12,000 x *g*) at 4 ºC for 1 h to remove any residual particles and the supernatant frozen for further analysis. After removal of the medium, the cells were rinsed with PBS, dislodged from the T-25 flask using a cell scraper, washed twice with PBS and finally suspended in 1 ml of PBS. The cells were then lysed by 5 freeze/thaw (alternating -80 ºC/rt) cycles and centrifuged (12,000 x *g*) at 4 ºC for 1 h to remove cellular debris and any residual particles. This supernatant as well as the samples prepared from the medium were then directly analyzed by LC-MS. Results are presented as the mean of triplicate measurements ± 95% confidence intervals.

References

(1) Chumakov, K.; Ehrenfeld, E.; Wimmer, E.; Agol, V. I. *Nat. Rev. Microbiol.* **2007**, *5*, 952-958.
(2) Parrino, J.; Graham, B. S. *J. Allergy Clin. Immunol.* **2006**, *118*, 1320-1326.
(3) Griffin, D. E.; Pan, C. H.; Moss, W. J. *Front. Biosci.* **2008**, *13*, 1352-1370.
(4) Moron, G.; Dadaglio, G.; Leclerc, C. *Trends Immunol.* **2004**, *25*, 92-97.
(5) Kundi, M. *Expert Rev. Vaccines* **2007**, *6*, 133-140.
(6) Carbonetti, N. H.; Tuskan, R. G.; Lewis, G. K. *AIDS Res. Hum. Retroviruses* **2001**, *17*, 819-827.
(7) Susumu, S.; Nagata, Y.; Ito, S.; Matsuo, M.; Valmori, D.; Yui, K.; Udono, H.; Kanematsu, T. *Cancer Sci.* **2008**, *99*, 107-112.
(8) Kovacsovics-Bankowski, M.; Clark, K.; Benacerraf, B.; Rock, K. L. *Proc. Natl. Acad. Sci. U. S. A.* **1993**, *90*, 4942-4946.
(9) Chersi, A.; Galati, R.; Accapezzato, D.; Francavilla, V.; Barnaba, V.; Butler, R. H.; Tanigaki, N. *J. Immunol. Methods* **2004**, *291*, 79-91.
(10) Murthy, N.; Thng, Y. X.; Schuck, S.; Xu, M. C.; Frechet, J. M. *J. Am. Chem. Soc.* **2002**, *124*, 12398-12399.
(11) Murthy, N.; Xu, M.; Schuck, S.; Kunisawa, J.; Shastri, N.; Frechet, J. M. *Proc. Natl. Acad. Sci. U. S. A.* **2003**, *100*, 4995-5000.
(12) Kwon, Y. J.; James, E.; Shastri, N.; Frechet, J. M. *Proc. Natl. Acad. Sci. U. S. A.* **2005**, *102*, 18264-18268.
(13) Kwon, Y. J.; Standley, S. M.; Goodwin, A. P.; Gillies, E. R.; Frechet, J. M. *Mol. Pharmaceutics* **2005**, *2*, 83-91.
(14) Standley, S. M.; Kwon, Y. J.; Murthy, N.; Kunisawa, J.; Shastri, N.; Guillaudeu, S. J.; Lau, L.; Frechet, J. M. *Bioconjugate Chem.* **2004**, *15*, 1281-1288.
(15) Shenoy, D.; Little, S.; Langer, R.; Amiji, M. *Mol. Pharmaceutics* **2005**, *2*, 357-366.
(16) Shenoy, D.; Little, S.; Langer, R.; Amiji, M. *Pharm. Res.* **2005**, *22*, 2107-2114.
(17) Shenoy, D.; Fu, W.; Li, J.; Crasto, C.; Jones, G.; DiMarzio, C.; Sridhar, S.; Amiji, M. *Int. J. Nanomedicine* **2006**, *1*, 51-57.
(18) Heffernan, M. J.; Murthy, N. *Bioconjugate Chem.* **2005**, *16*, 1340-1342.
(19) Tomlinson, R.; Klee, M.; Garrett, S.; Heller, J.; Duncan, R.; Brocchini, S. *Macromolecules* **2002**, *35*, 473-480.
(20) Paramonov, S. E.; Bachelder, E. M.; Beaudette, T. T.; Standley, S. M.; Lee, C. C.; Dashe, J.; Frechet, J. M. *Bioconjugate Chem.* **2008**, *19*, 911-919.
(21) Bilati, U.; Allemann, E.; Doelker, E. *Pharm. Dev. Technol.* **2003**, *8*, 1-9.
(22) Dalwadi, G.; Benson, H. A.; Chen, Y. *Pharm. Res.* **2005**, *22*, 2152-2162.
(23) Hirota, K.; Hasegawa, T.; Hinata, H.; Ito, F.; Inagawa, H.; Kochi, C.; Soma, G.; Makino, K.; Terada, H. *J. Control. Release* **2007**, *119*, 69-76.
(24) Foged, C.; Brodin, B.; Frokjaer, S.; Sundblad, A. *Int. J. Pharm.* **2005**, *298*, 315-322.
(25) Fifis, T.; Gamvrellis, A.; Crimeen-Irwin, B.; Pietersz, G. A.; Li, J.; Mottram, P. L.; McKenzie, I. F.; Plebanski, M. *J. Immunol.* **2004**, *173*, 3148-3154.
(26) Karttunen, J.; Sanderson, S.; Shastri, N. *Proc. Natl. Acad. Sci. U. S. A.* **1992**, *89*, 6020-6024.

(27) Haining, W. N.; Anderson, D. G.; Little, S. R.; von Bergwelt-Baildon, M. S.; Cardoso, A. A.; Alves, P.; Kosmatopoulos, K.; Nadler, L. M.; Langer, R.; Kohane, D. S. *J. Immunol.* **2004**, *173*, 2578-2585.
(28) Hu, Y.; Litwin, T.; Nagaraja, A. R.; Kwong, B.; Katz, J.; Watson, N.; Irvine, D. J. *Nano. Lett.* **2007**, *7*, 3056-3064.
(29) Ignatius, A. A.; Claes, L. E. *Biomaterials* **1996**, *17*, 831-839.
(30) Shenderova, A.; Burke, T. G.; Schwendeman, S. P. *Pharm. Res.* **1999**, *16*, 241-248.
(31) Caliceti, P.; Veronese, F. M. *Adv. Drug Deliv. Rev.* **2003**, *55*, 1261-1277.
(32) Hua, N.; Sun, J. *J. Mater. Sci. Mater. Med.* **2008**, ASAP Article Published Online.
(33) Yoo, J. Y.; Kim, J. M.; Seo, K. S.; Jeong, Y. K.; Lee, H. B.; Khang, G. *Biomed. Mater. Eng.* **2005**, *15*, 279-288.
(34) Fent, K. W.; Jayaraj, K.; Ball, L. M.; Nylander-French, L. A. *J. Environ. Monit.* **2008**, *10*, 500-507.
(35) Lorenzen, A.; Kennedy, S. W. *Anal. Biochem.* **1993**, *214*, 346-348.
(36) Abdi, K.; Singh, N.; Matzinger, P. *Scand. J. Immunol.* **2006**, *64*, 83-92.
(37) Karttunen, J.; Shastri, N. *Proc. Natl. Acad. Sci. U. S. A.* **1991**, *88*, 3972-3976.
(38) Lee, K. Y.; Chun, E.; Seong, B. L. *Biochem. Biophys. Res. Commun.* **2002**, *292*, 682-688.
(39) Mandal, M.; Lee, K. D. *Biochim. Biophys. Acta.* **2002**, *1563*, 7-17.
(40) Wang, D.; Molavi, O.; Lutsiak, M. E.; Elamanchili, P.; Kwon, G. S.; Samuel, J. *J. Pharm. Pharm. Sci.* **2007**, *10*, 217-230.

Chapter 4 – Synthesis, pH-Dependent Degradation Behavior and Initial Biological Evaluation of Acetal-Modified Dextran Particles

Abstract

In this chapter, we describe the synthesis and characterization of a third generation acid-sensitive particle system. Given the biocompatibility issues surrounding the polyacrylamide-based system and the formulation-related difficulties with the fully-degradable polyurethane system, we sought to generate another acid-degradable material with properties superior to those of the previous two systems. Specifically, dextran, a biocompatible, water-soluble polysaccharide, was modified at its hydroxyls with acetal moieties such that it became insoluble in water but freely soluble in common organic solvents such as dichloromethane, enabling its use in the facile preparation of acid-sensitive microparticles. These particles were found to degrade in a pH-dependent manner; FITC-dextran was released with a half-life at 37 ºC of 10 hours at pH 5.0 compared to a half-life of approximately 15 days at pH 7.4. Both hydrophobic and hydrophilic cargoes were successfully loaded into these particles using single and double emulsion techniques, respectively. When used in a model vaccine application, particles loaded with the protein ovalbumin (OVA) increased the presentation of OVA-derived peptides to $CD8^+$ T-cells 16-fold relative to OVA alone. Additionally, this dextran derivative was found to be non-toxic in preliminary *in vitro* cytotoxicity assays. Due to its ease of preparation, processability, pH-sensitivity, and biocompatibility, this type of modified dextran should find use in numerous drug delivery applications.

Introduction

Polyesters,[1] polyorthoesters,[2] and polyanhydrides[3] are widely used materials for biomedical applications due to their biodegradability, biocompatibility and processability. Microparticles made from these polymers have been used as carriers for vaccine applications,[4] gene delivery[5] and chemotherapeutic agents.[6] The encapsulated cargo is typically released over the course of several months *via* surface erosion and the slow degradation of the polymer.[7]

For many drug delivery applications, it is desirable to release therapeutic agents under mildly acidic conditions, as may be found in sites of inflammation, lysosomal compartments, or in tumor tissue.[8,9] Acid-sensitive liposomes, micelles and hydrogels[10-12] have been extensively explored, but few easily-prepared polymeric materials exist that combine acid-sensitivity and biodegradability. Poly(β-amino esters), which are protonated and thus become soluble at lower pH,[13] constitute one such material. However, these polymers become polycationic under acidic conditions and must be blended with biocompatible polyesters to reduce their toxicity.[14] We sought to create a system with the flexibility and biocompatibility of polyester materials, but with the additional benefit of a change in rate of payload release sensitive to physiologically relevant acidic conditions. Therefore, a solubility switching mechanism was envisioned in which a biocompatible, water-soluble polymer could be reversibly modified to make it insoluble in water, but soluble in organic solvents. Materials made from the modified polymer could then be degraded under the specific conditions that reverse the original modification. Dextran, a bacterially derived homopolysaccharide of glucose, was chosen because of its biocompatibility,

biodegradability, wide availability, and ease of modification.[15,16] Acetals were chosen to modify dextran due to their well understood and tunable pH-dependant hydrolysis rates.[17]

Results and Discussion

Dextran was rendered insoluble in water by modification of its hydroxyl groups through reaction with 2-methoxypropene under acid catalysis (Figure 4.1). The high density of pendant acetals makes the new "acetalated-dextran" (Ac-DEX) soluble in organic solvents such as dichloromethane, ethyl acetate or acetone. Based on multi-angle light scattering data, the molecular weight of the dextran increased upon modification from 13 kDa to 29 kDa while its polydispersity remained essentially constant (1.13 to 1.20), suggesting a high degree of coverage of the hydroxyl groups and minimal polymer crosslinking. Using a standard double emulsion protocol, a model hydrophilic payload, ovalbumin (OVA), was encapsulated with a protein loading of 3.7 ± 0.4 wt % (Figure 4.1). Using a single emulsion technique, we were able to encapsulate a model hydrophobic drug, pyrene, with a loading of 3.6 ± 0.5 wt %. The particles were imaged using scanning electron microscopy (Figures 4.1 and 4.2) and particle size was analyzed using dynamic light scattering. The double emulsion particles were found to have an average diameter of 230 ± 93 nm and the single emulsion particles had similar shapes and sizes with an average diameter of 258 ± 70 nm.

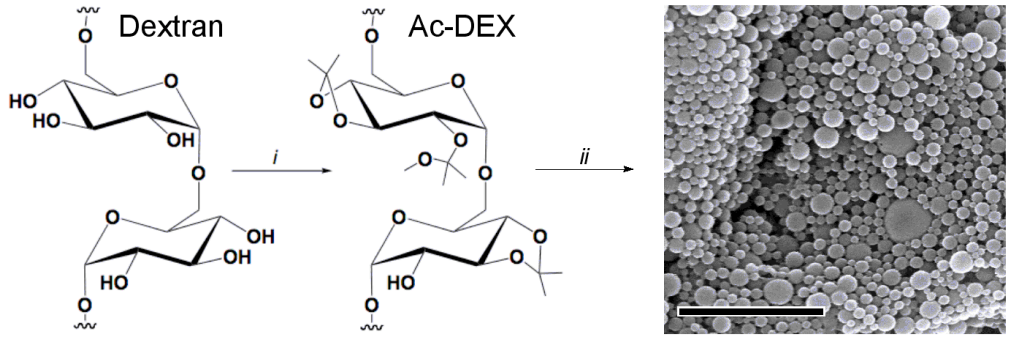

Figure 4.1. Synthesis of Ac-DEX and particle formation (i) 2-methoxypropene, pyridinium-*p*-toluenesulfonate, DMSO (ii) solvent-evaporation-based particle formation (scale bar is 2 μm).

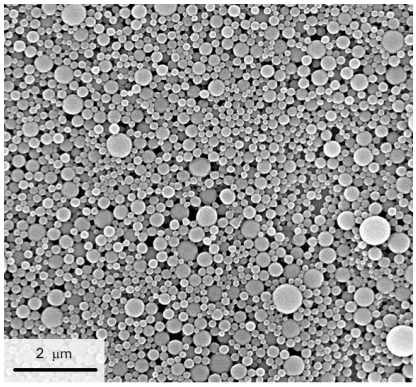

Figure 4.2. Represenative SEM image of single emulsion Ac-DEX particles.

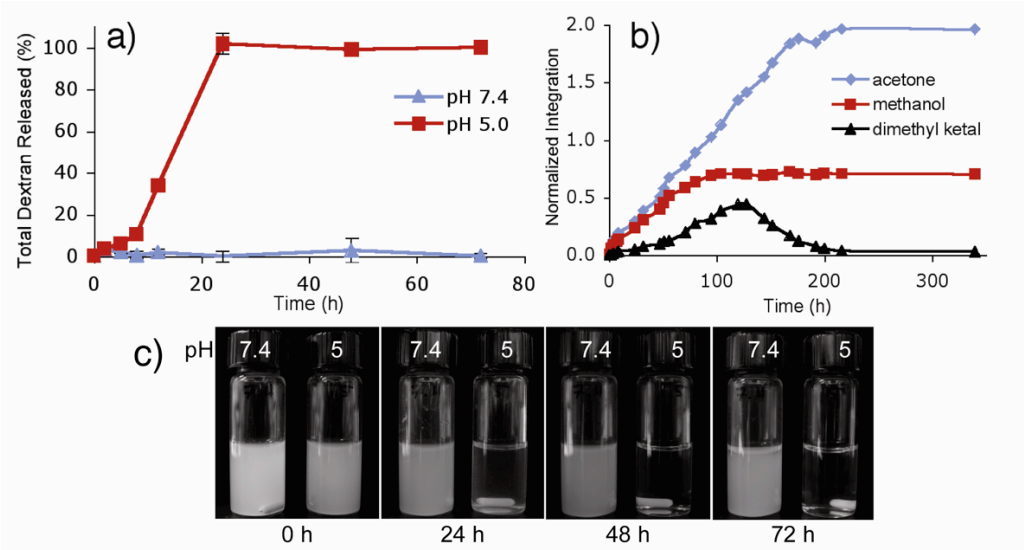

Figure 4.3. (a) Dissolution of dextran from Ac-DEX particles in either pH 5 or pH 7.4 buffer at 37 ºC. (b) Normalized ^{1}H-NMR data from the degradation of Ac-DEX particles at pH 5.5 and 37 ºC showing integrations of signals corresponding to acetone, methanol and acetal groups. (c) Time-lapse photos of Ac-DEX particles under physiological or acidic conditions.

Masking the hydroxyl groups of dextran as acetals not only provides a hydrophobic material that is easily processable using various emulsion techniques, it also provides a mechanism for introducing pH-sensitivity. Under mildly acidic aqueous conditions, the pendant acetal groups are expected to hydrolyze, thus unmasking the parent hydroxyl groups of dextran. The complete hydrolysis of Ac-DEX should result in the release of acetone, methanol and water-soluble dextran. To study the degradation of Ac-DEX, empty particles were prepared and incubated under physiological (pH 7.4) or mildly acidic conditions (pH 5.0) at 37 ºC. The supernatant was analyzed at various times for the presence of reducing polysaccharides using a bicinchoninic acid based assay.[18] Ac-DEX particles incubated in pH 7.4 buffer remained as an opaque suspension for days and essentially no soluble dextran was detected after 72 hours (Figure 4.3a,c). In contrast, suspensions of Ac-DEX particles in pH 5.0 buffer showed continuous release of soluble reducing polysaccharides, becoming transparent after 24 hours, thus suggesting full dissolution of the particles. This pH-dependent degradation of Ac-DEX particles is further reflected in the release profile of a model fluorescently labeled hydrophilic payload (Figure 4.4). In this experiment fluorescein isothiocyanate (FITC) labeled dextran was released from Ac-DEX particles much faster under acidic conditions than in pH 7.4 buffer. Specifically, the half-life of the release of FITC-dextran at 37 ˚C and pH 5.0 was about 10 hours compared to approximately 15 days at pH 7.4. These release rates may be faster than bulk particle dissolution due to potential leaching of hydrophilic cargo.

The degradation of empty Ac-DEX particles was also followed using ^{1}H-NMR. A suspension of particles was incubated at 37 ºC in deuterated PBS (pH 5.5) in a flame-sealed

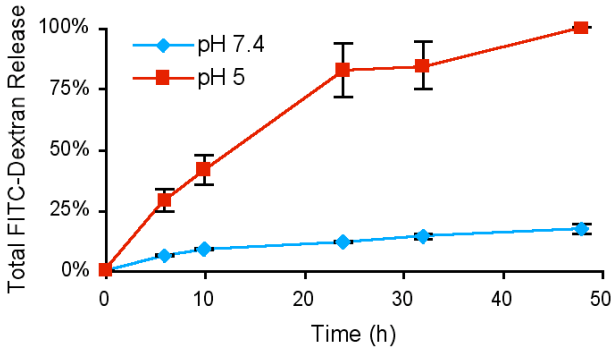

Figure 4.4. Release profile of FITC-dextran encapsulated in Ac-DEX particles at 37°C and in pH 5 or pH 7.4 buffer.

NMR tube. The release of acetone and methanol due to acetal hydrolysis was observed and the normalized integrals of these compounds were plotted as a function of time (Figure 4.3b and Figure 4.5). The particles first released a roughly equivalent amount of acetone and methanol, which is consistent with the rapid hydrolysis rate of pendant acyclic acetals.[17] Following this phase, acetone, but not methanol continued to be released from the degrading particles. This second phase is presumably due to the slower hydrolysis rate of cyclic isopropylidene acetals, signals from which appear, then subsequently disappear as the acetals are hydrolyzed.[19,20] Following complete hydrolysis, the ^{1}H-NMR spectrum of the degraded particles showed signals corresponding only to unmodified dextran, acetone and methanol (Figure 4.6). Based on this final spectrum, it was calculated that 73% of the available hydroxyl groups were modified and the ratio of cyclic to acyclic acetals was estimated at 1.8:1.[21]

We have previously shown that acid-labile polyacrylamide particles enhance protein-based vaccine efficacy in cancer treatment by enhancing MHC class I presentation and $CD8^{+}$ T cell activation.[22,23] However, because the particles are prepared from acrylamide, toxicity and biocompatibility issues might limit their future clinical applications. Ac-DEX based particles are expected to be more biocompatible than our previous system since the byproducts are dextran (a clinically used plasma expander), acetone (a non-toxic, metabolic intermediate) and methanol (non-toxic in small quantities).[24,25] To assess the biocompatibility of Ac-DEX particles, we compared them to particles prepared from an FDA approved polymer, poly (lactic-*co*-glycolic acid). We found no significant difference in toxicity between the two materials in both HeLa cells and RAW macrophages. To simulate their long-term toxicity, the degradation products of Ac-DEX particles were also tested and found to be non-toxic (Figure 4.7). In order to assess the feasibility of using Ac-DEX based materials for vaccine applications, OVA-loaded Ac-DEX particles were incubated with RAW macrophages. After six hours of incubation, Ac-DEX particles increased MHC class I presentation of the OVA-derived $CD8^{+}$ T-cell epitope, SIINFEKL, by a factor of 16 relative to free OVA (Figure 4.8) as measured by the B3Z assay.[26] This drastic increase in presentation indicates that these particles may be promising materials for vaccines against tumors and certain viruses, where MHC-I presentation is crucial for the activation and proliferation of $CD8^{+}$ T-cells.

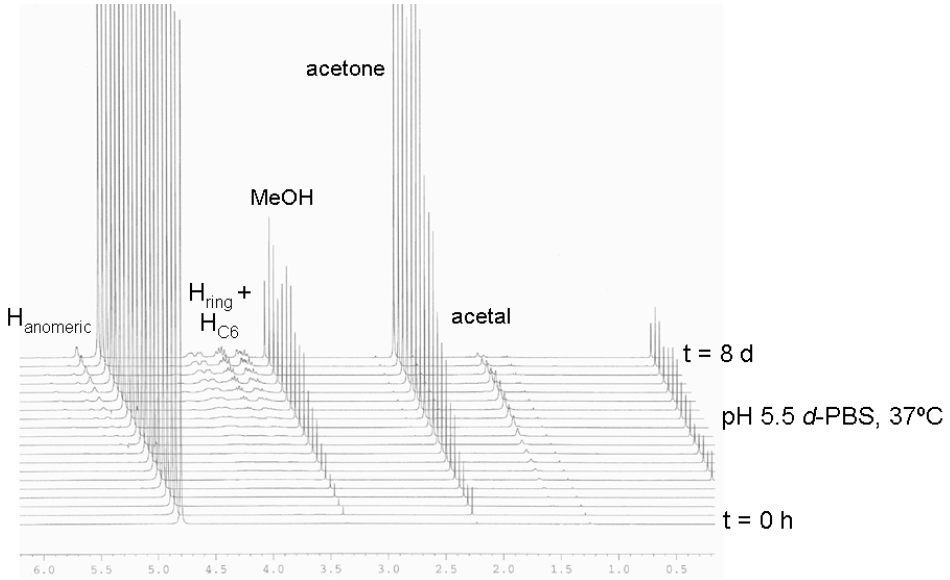

Figure 4.5. Stack plot of ^{1}H NMR spectra of empty Ac-DEX particles incubated in deuterated pH 5.5 buffer over time. Spectra are shown for the first eight days and are normalized with respect to the integration of the TMS peak.

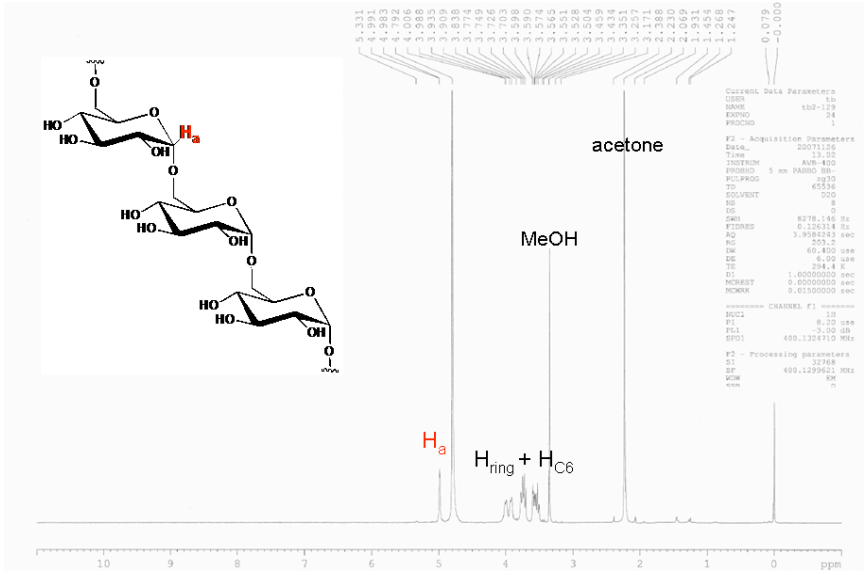

Figure 4.6. Final ^{1}H NMR spectrum of degraded Ac-DEX particles.

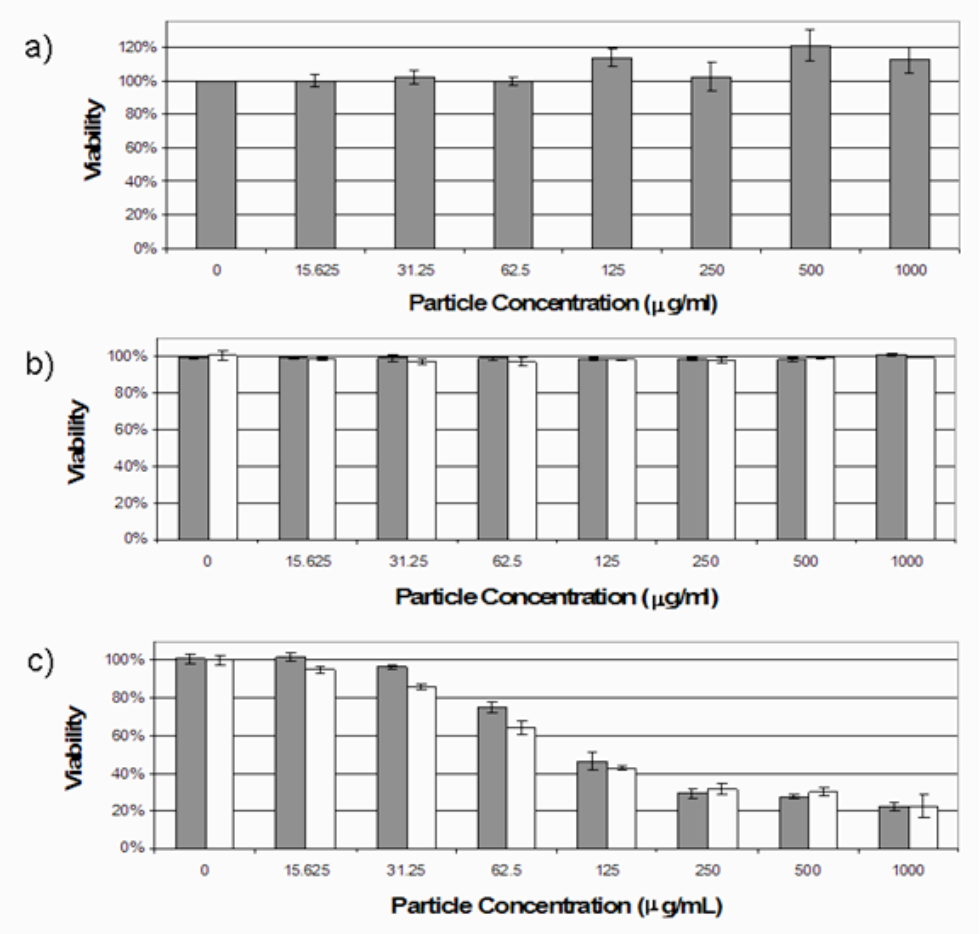

Figure 4.7. Cell viability as measured by LDH release after overnight culture with (a) Ac-DEX degradation products and RAW macrophages (b) Ac-DEX particles (shaded) or PLGA particles (white) with HeLa cells (c) Ac-DEX particles (shaded) or PLGA particles (white) with RAW macrophages. Correction for spontaneous LDH release was obtained from untreated cells. Maximum cell death was determined by freeze/thaw lysis.

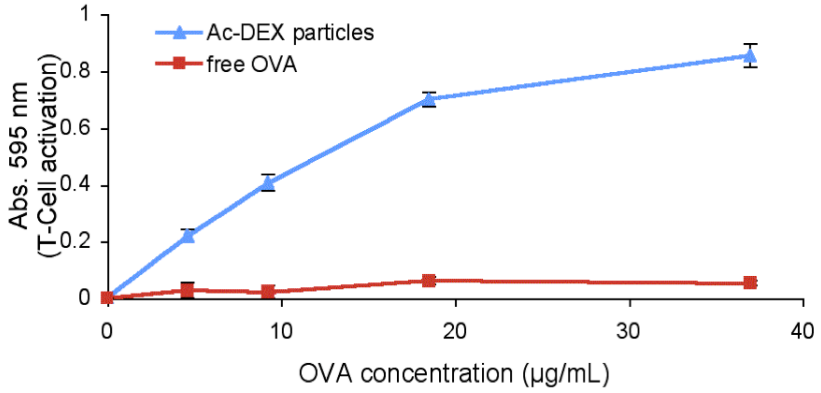

Figure 4.8. B3Z assay measuring antigen presentation of RAW macrophages pulsed with free OVA or Ac-DEX particles encapsulating OVA.

Conclusions

In conclusion, we present a new method for the preparation of acid-sensitive, biocompatible dextran-based materials. Ac-DEX is synthesized in a single step from a natural polymer, possesses a favorable toxicity profile, and can be processed into materials encapsulating either hydrophobic or hydrophilic payloads. Due to these favorable attributes, Ac-DEX based materials may have significant advantages over other pH-sensitive or biocompatible materials currently used in biomedical applications. We are currently investigating the functionalization and use of these and other modified polysaccharides in vaccine and chemotherapeutic settings. In addition, we believe Ac-DEX has the potential to be used as scaffolds, sutures, and other bulk materials *in vivo* due to its physical properties, biodegradability, and biocompatibility.

Experimental

General Procedures and Materials. All reagents were purchased from commercial sources and used without further purification unless otherwise specified. Water (dd-H_2O) for buffers and particle washing steps was purified to a resistance of 18 MΩ using a NANOpure purification system (Barnstead, USA). When used in the presence of acetal containing materials, dd-H_2O was rendered basic (pH 8) by the addition of triethylamine (TEA) (approximately 0.01%). ^1H NMR spectra were recorded at 400 MHz and ^{13}C spectra were recorded at 100 MHz. To prevent acid catalyzed hydrolysis of acetal containing compounds, $CDCl_3$ was passed through a plug of basic alumina prior to recording NMR spectra. Multiangle light scattering (MALS) experiments were performed with a Waters 510 pump, a 7125 Rheodyne injector, a Wyatt Optilab differential refractive index detector and a Wyatt DAWN-EOS MALS detector. Absolute molecular weights determined from light scattering data were calculated using Astra software from Wyatt assuming a quantitative mass recovery (online method). Columns were thermostatted at 35 °C. MALS experiments run with THF as a solvent were performed using two 7.5 x 300 mm PLgel mixed-bed C columns with a 5 micron particle size. MALS experiments run in aqueous conditions were performed using dd-H_2O with 5% acetic acid as a solvent and Viscotek C-MBMMW-3078 and C-MBHMW-3078 cationic columns (7.8 mm x 300 mm) in series. Fluorescence measurements were obtained on a Fluorolog FL3-22 spectrofluorometer (Horiba Jobin Yvon) or a Spectra Max Gemini XS (Molecular Devices, USA) for microplate-based assays, usage courtesy of Prof. Jonathan Ellman. Fourier transform infrared spectroscopy (FT-IR) was carried out on a 3100 FT-IR spectrometer (Varian, USA). UV-Vis spectroscopic measurements were obtained from samples in quartz cuvettes using a Lambda 35 spectrophotometer (Perkin Elmer, USA) or using a Spectra Max 190 (Molecular Devices, USA) for microplate-based assays, usage courtesy of Prof. Carolyn Bertozzi. RAW 309 and HeLa cells were obtained from ATCC (Manassas, VA) and grown according to ATCC's directions.

Synthesis of Acetalated Dextran (Ac-DEX). A flame-dried flask was charged with dextran (M_W = 10 500 g/mol, 1.00 g, 0.095 mmol) and purged with dry N_2. Anhydrous DMSO (10 mL) was added and the resulting mixture was stirred until complete dissolution of the dextran was observed. Pyridinium *p*-toluenesulfonate (15.6 mg, 0.062 mmol) was added followed by 2-methoxypropene (3.4 mL, 37 mmol). The flask was placed under a positive pressure of N_2, then sealed to prevent evaporation of 2-methoxypropene. After 3 h, the reaction was quenched with TEA (1 mL, 7 mmol) and the modified dextran was precipitated in dd-H_2O (100 mL). The product was isolated by centrifugation at 4 600 x *g* for 10 min and the resulting pellet was

washed thoroughly with dd-H_2O (2 x 50 mL, pH 8) by vortexing and sonication followed by centrifugation and removal of the supernatant. Residual water was removed by lyophilization, yielding "acetalated dextran" (Ac-DEX) (1.07 g) as a fine white powder. IR (KBr, cm^{-1}): 3444, 2989, 2938, 1381, 1231, 1176, 1053, 853. ^1H NMR (400 MHz, $CDCl_3$): δ 1.39 (s, br, 25H), 3.25 (br, 6H), 3.45 (br, 2H), 3.60-4.15 (br, 12H), 4.92 (br, 1H), 5.13 (br, 1H).

Preparation of Double Emulsion Particles Containing OVA. Microparticles containing ovalbumin (OVA) were made using a double emulsion water/oil/water (w/o/w) evaporation method similar to that described by Bilati *et al.*[27] Briefly, OVA (10 mg) was dissolved in phosphate buffered saline (PBS, 137 mM NaCl, 10 mM phosphate, 2.7 mM KCl, pH 7.4, 50 μl). Ac-DEX (200 mg) was dissolved in CH_2Cl_2 (1 mL) and added to the OVA solution. This mixture was then emulsified by sonicating for 30 s on ice using a probe sonicator (Branson Sonifier 450) with an output setting of 3 and a duty cycle of 10%. This primary emulsion was added to an aqueous solution of poly(vinyl alcohol) (PVA, M_W = 13 000 – 23 000 g/mol, 87-89% hydrolyzed) (2 mL, 3% w/w in PBS) and sonicated for an additional 30 s on ice using the same settings. The resulting double emulsion was immediately poured into a second PVA solution (10 ml, 0.3% w/w in PBS) and stirred for 3 h allowing the organic solvent to evaporate. The particles were isolated by centrifugation (14 800 x *g*, 15 min) and washed with PBS (50 mL) and dd-H_2O (2 x 50 mL, pH 8) by vortexing and sonication followed by centrifugation and removal of the supernatant. The washed particles were resuspended in dd-H_2O (2 mL, pH 8) and lyophilized to yield a white fluffy solid (135 mg).

Preparation of Empty Double Emulsion Particles. Particles that did not contain protein were made in the same manner as above omitting OVA.

Preparation of Empty PLGA Particles. Particles prepared from poly(DL-lactide-co-glycolide) (PLGA, 85% lactide, 15% glycolide) were made in the same manner as above substituting PLGA for Ac-DEX.

Preparation of Double Emulsion Particles Containing FITC-Dextran. Particles containing fluorescein isothiocyanate (FITC) labeled dextran were made in the same manner as above substituting FITC-dextran (M_W = 66 100 g/mol, 10 mg) for OVA.

Quantification of Encapsulated OVA. Ac-DEX particles containing OVA were suspended at a concentration of 2 mg/mL in a 0.3 M acetate buffer (pH 5.0) and incubated at 37 ˚C under gentle agitation for 3 d using a Thermomixer R heating block (Eppendorf). After the particles had been fully degraded, aliquots were taken and analyzed for protein content using the fluorescamine reagent and a microplate assay as described by Lorenzen *et al.*[28] Empty Ac-DEX particles were degraded in a similar fashion and used to determine a background fluorescence level. The results were compared to a standard curve and the mass of OVA encapsulated was calculated. The protein loading was 3.7 ± 0.4 wt % and the loading efficiency was 74%.

Single Emulsion Particle Preparation. Single emulsion particles encapsulating pyrene were prepared according to a procedure adapted from Jung *et al.*[29] Briefly, Ac-DEX (49.9 mg) and pyrene (5.5 mg) were dissolved in CH_2Cl_2 (1 mL). This solution was added to a PVA solution (3 mL, 1% w/w in PBS) and emulsified by sonicating for 30 s on ice using a probe sonicator (Branson Sonifier 450) with an output setting of 5 and a duty cycle of 70%. The resulting

emulsion was poured into a second PVA solution (50 ml, 0.3% w/w in PBS) and stirred for 4 h allowing the organic solvent to evaporate. The single emulsion particles were isolated in the same manner as described for the double emulsion particles above. The washed particles were resuspended in dd-H_2O (2 mL, pH 8) and lyophilized to yield a white fluffy solid (38 mg).

Quantification of Encapsulated Pyrene. The amount of encapsulated pyrene in single emulsion microparticles was determined by measuring pyrene's absorbance at 335 nm. Ac-DEX particles were weighed out in triplicate and dissolved in THF by sonicating the solutions for 2 min. The resulting solutions were diluted and the absorbance at 335 nm was determined. The loading of pyrene in the particles was calculated using pyrene's molar absorptivity in THF as reported by Venkataramana *et al.*[30] The pyrene loading was 3.6 ± 0.5 wt % and the loading efficiency was 36%.

Scanning Electron Microscopy. Microparticles were characterized by scanning electron microscopy using a S-5000 microscope (Hitachi, Japan). Particles were suspended in dd-H_2O (pH 8) at a concentration of 1 mg/mL and the resulting dispersions were dripped onto silicon wafers. After 15 min, the remaining water was wicked away using tissue paper and the samples were allowed to air dry. The particles were then sputter coated with a 2 nm layer of a palladium/gold alloy and imaged.

Particle Size Analysis by Dynamic Light Scattering. Particle size distributions and average particle diameters were determined by dynamic light scattering using a Nano ZS (Malvern Instruments, United Kingdom). Particles were suspended in dd-H_2O (pH 8) at a concentration of 1 mg/mL and three measurements were taken of the resulting dispersions. The results in the text are presented as average particle diameters ± half width of the distribution at half maximal height.

Particle Degradation: Detection of Soluble Polysaccharides via BCA assay. Empty Ac-DEX particles were suspended in triplicate at a concentration of 2 mg/mL in either a 0.3 M acetate buffer (pH 5.0) or PBS (pH 7.4) and incubated at 37 °C under gentle agitation using a Thermomixer R heating block (Eppendorf). At various time points, 120 μl aliquots were removed, centrifuged at 14 000 x *g* for 10 min to pellet out insoluble materials and the supernatant was stored at -20 ºC. The collected supernatant samples were analyzed for the presence of reducing polysaccharides using a microplate reductometric bicinchoninic acid based assay according to the manufacturer's protocol (Micro BCA Protein Assay Kit, Pierce, USA).[18]

pH-Dependant Release of FITC-Dextran from Ac-DEX Particles. This experiment was performed essentially in the same manner as above except FITC-dextran loaded particles were used instead of empty particles. The quantity of FITC-dextran in the supernatant samples was determined by measuring the emission at 515 nm with an excitation of 490 nm. The amount of FITC-dextran in each sample was calculated by fitting the emission to a calibration curve.

Particle Degradation: ^{1}H NMR Study. Empty Ac-DEX particles (9.5 mg) and deuterated PBS buffer (850 μL, pH 5.5) were added to an NMR tube, which was immediately flame sealed. This slightly higher pH value (compared to pH 5 used in the BCA experiment) was chosen to allow for the observation of degradation in better detail at earlier time points. An ^{1}H NMR spectrum was taken (initial time point) and the tube was placed in an oil bath heated to 37 ºC. After various time points additional ^{1}H NMR spectra were taken and the appearance of acetone,

methanol, and signals assigned to the methyl groups of cyclic isopropylidene acetals[19,20] was measured as a ratio of these peaks' integral to the integral of the internal standard peak (3-(trimethylsilyl) propionic-2,2,3,3,d_4 acid, sodium salt). The data was normalized by dividing the values for acetone and the cyclic acetals by six and the values for methanol by three. A stack plot of the NMR spectra at various time points is presented in Figure 4.5 and spectrum of the final time point, which shows signals only from dextran, methanol and acetone is presented in Figure 4.6.

Particle Degradation: Digital Photography. Empty Ac-DEX particles were suspended at a concentration of 2 mg/mL in either a 0.3 M acetate buffer (pH 5.0) or PBS (pH 7.4) and incubated at 37 ˚C under gentle stirring. Digital photographs of the samples were obtained after various time points. The white object visible in some of the vials is a magnetic stir bar.

Cytotoxicity Studies. For cell viability experiments, degradation products of empty Ac-DEX particles were tested using RAW macrophages (Figure 4.7a). Additionally, empty Ac-DEX particles and empty PLGA particles were incubated with either HeLa cells (Figure 4.7b) or RAW macrophages (Figure 4.7c). The degradation products were obtained by incubating Ac-DEX particles in a 0.3 M acetate buffer (pH 5.0) at 37 ˚C under gentle agitation for 3 d. The resulting solution was desalted using a Microcon 3 centrifugation filter (Millipore, USA) and lyophilized. During the desalting and lyophilization steps the methanol and acetone released during degradation was removed. Before use in the viability experiment, the lyophilized degradation products were dissolved in medium, and methanol and acetone were added corresponding to the maximum amount of these byproducts released, as found in the ^{1}H-NMR degradation study described above. For each viability experiment, $1x10^4$ RAW macrophages or HeLa cells were seeded in a 96 well plate and allowed to grow overnight. Serial dilutions of the degradation products, empty Ac-DEX or PLGA particles were added to the cells, which were then incubated for 20 hours per the manufacturer's instructions. The next morning, the medium was removed and an LDH assay was performed to measure toxicity according to the manufacturer's protocol (Cytotox 96 NonRadioactive Cytotoxicity Assay, Promega, USA). Correction for spontaneous LDH release was obtained from untreated cells. Maximum cell death was determined by freeze/thaw lysis. Results are presented as the mean of triplicate cultures ± 95% confidence intervals.

MHC Class I Presentation (B3Z) Assay. B3Z cells, a $CD8^+$ T-cell hybridoma engineered to secrete β-galactosidase when its T-cell receptor engages an $OVA_{257-264}$:K_b complex,[26,31] generously donated by Prof. N. Shastri (University of California, Berkeley), were maintained in RPMI 1640 (Invitrogen, USA) supplemented with 10% fetal bovine serum, 2 mM Glutamax, 50 mM 2-mercaptoethanol, 1 mM sodium pyruvate, 100 U/ml penicillin and 100 mg/ml streptomycin. $1x10^4$ RAW macrophages were seeded overnight in a 96 well plate and subsequently incubated with OVA-containing Ac-DEX particles or free OVA. After 6 h, the cells were washed and $1x10^5$ B3Z cells were added to the macrophages and cocultured for an additional 16 h. The medium was removed and 100 μL of CPRG buffer (91 mg of chlorophenol red β-D-galactopyranoside (CPRG, Roche, USA), 1.25 mg of NP40 (EMD Sciences, USA), and 900 mg $MgCl_2$ in1 L of PBS) was added to each well. After 30 min, the absorbance at 595 nm was measured using a microplate reader. Results are presented as the mean of triplicate cultures ± 95% confidence intervals.

References and Footnotes

(1) Yolles, S.; Leafe, T. D.; Meyer, F. J. *J. Pharm. Sci.* **1975**, *64*, 115-116.
(2) Heller, J. *Ann. N. Y. Acad. Sci.* **1985**, *446*, 51-66.
(3) Rosen, H. B.; Chang, J.; Wnek, G. E.; Linhardt, R. J.; Langer, R. *Biomaterials* **1983**, *4*, 131-133.
(4) Solbrig, C. M.; Saucier-Sawyer, J. K.; Cody, V.; Saltzman, W. M.; Hanlon, D. J. *Mol. Pharmaceutics* **2007**, *4*, 47-57.
(5) Gvili, K.; Benny, O.; Danino, D.; Machluf, M. *Biopolymers* **2007**, *85*, 379-391.
(6) Sengupta, S.; Eavarone, D.; Capila, I.; Zhao, G. L.; Watson, N.; Kiziltepe, T.; Sasisekharan, R. *Nature* **2005**, *436*, 568-572.
(7) Matsumoto, A.; Matsukawa, Y.; Suzuki, T.; Yoshino, H. *J. Control. Release* **2005**, *106*, 172-180.
(8) Sun-Wada, G. H.; Wada, Y.; Futai, M. *Cell Struct. Funct.* **2003**, *28*, 455-463.
(9) Helmlinger, G.; Sckell, A.; Dellian, M.; Forbes, N. S.; Jain, R. K. *Clin. Cancer Res.* **2002**, *8*, 1284-1291.
(10) Sawant, R. M.; Hurley, J. P.; Salmaso, S.; Kale, A.; Tolcheva, E.; Levchenko, T. S.; Torchilin, V. P. *Bioconjugate Chem.* **2006**, *17*, 943-949.
(11) Mandracchia, D.; Pitarresi, G.; Palumbo, F. S.; Carlisi, B.; Giammona, G. *Biomacromolecules* **2004**, *5*, 1973-1982.
(12) Murthy, N.; Thng, Y. X.; Schuck, S.; Xu, M. C.; Frechet, J. M. J. *J. Am. Chem. Soc.* **2002**, *124*, 12398-12399.
(13) Little, S. R.; Lynn, D. M.; Ge, Q.; Anderson, D. G.; Puram, S. V.; Chen, J.; Eisen, H. N.; Langer, R. *Proc. Natl. Acad. Sci. U. S. A.* **2004**, *101*, 9534-9539.
(14) Little, S. R.; Lynn, D. M.; Puram, S. V.; Langer, R. *J. Control. Release* **2005**, *107*, 449-462.
(15) Hermanson, G. T. *Bioconjugate Techniques*; Academic Press: San Diego, 1996.
(16) Naessens, M.; Cerdobbel, A.; Soetaert, W.; Vandamme, E. J. *J. Chem. Technol. Biotechnol.* **2005**, *80*, 845-860.
(17) Fife, T. H.; Jao, L. K. *J. Org. Chem.* **1965**, *30*, 1492-1495.
(18) Doner, L. W.; Irwin, P. L. *Anal. Biochem.* **1992**, *202*, 50-53.
(19) Cai, J. Q.; Davison, B. E.; Ganellin, C. R.; Thaisrivongs, S. *Tetrahedron Lett.* **1995**, *36*, 6535-6536.
(20) Debost, J. L.; Gelas, J.; Horton, D.; Mols, O. *Carbohydr. Res.* **1984**, *125*, 329-335.
(21) These values were calculated using the integration of the acetone and methanol signals compared to the integration of the anomeric proton.
(22) Murthy, N.; Xu, M.; Schuck, S.; Kunisawa, J.; Shastri, N.; Frechet, J. M. *Proc. Natl. Acad. Sci. U. S. A.* **2003**, *100*, 4995-5000.
(23) Standley, S. M.; Kwon, Y. J.; Murthy, N.; Kunisawa, J.; Shastri, N.; Guillaudeu, S. J.; Lau, L.; Frechet, J. M. J. *Bioconjugate Chem.* **2004**, *15*, 1281-1288.
(24) Paine, A.; Davan, A. D. *Hum. Exp. Toxicol.* **2001**, *20*, 563-568.
(25) Although toxic in large quantities, the level of methanol released by Ac-DEX materials (~7 wt. %) would be below the EPA recommended limit of daily exposure as long as the dosage does not exceed 7 g/kg/day. If complete elimination of methanol becomes necessary, 2-ethoxypropene instead of 2-methoxypropene could be used.
(26) Karttunen, J.; Shastri, N. *Proc. Natl. Acad. Sci. U. S. A.* **1991**, *88*, 3972-3976.

(27) Bilati, U.; Allemann, E.; Doelker, E. *Pharm. Dev. Technol.* **2003**, *8*, 1-9.
(28) Lorenzen, A.; Kennedy, S. W. *Anal. Biochem.* **1993**, *214*, 346-348.
(29) Jung, J.; Lee, I. H.; Lee, E.; Park, J.; Jon, S. *Biomacromolecules* **2007**, *8*, 3401-3407.
(30) Venkataramana, G.; Sankararaman, S. *Eur. J. Org. Chem.* **2005**, *2005*, 4162-4166.
(31) Karttunen, J.; Sanderson, S.; Shastri, N. *Proc. Natl. Acad. Sci. U. S. A.* **1992**, *89*, 6020-6024.

Chapter 5 – Functionalization of Acid-Sensitive Dextran-Based Particles using Alkoxyamine Reagents

Abstract

In this chapter, we discuss the development of a simple, mild, and chemoselective strategy for the conjugation of biologically active molecules to the surface of the dextran-based microparticles described in the previous chapter. Alkoxyamine-bearing reagents were used to form stable oxime conjugates, presumably with latent aldehyde functionality present in reducing carbohydrate chain ends. We demonstrate the functionalization of dextran-based microparticles with a fluorophore as well as a cell-penetrating peptide sequence, which facilitated the delivery of cargo to non-phagocytic cells leading to a 60-fold increase in the expression of a reporter gene when plasmid DNA-loaded particles were used.

Scheme 5.1. General method for the functionalization of Ac-DEX particles with alkoxyamine reagents[a]

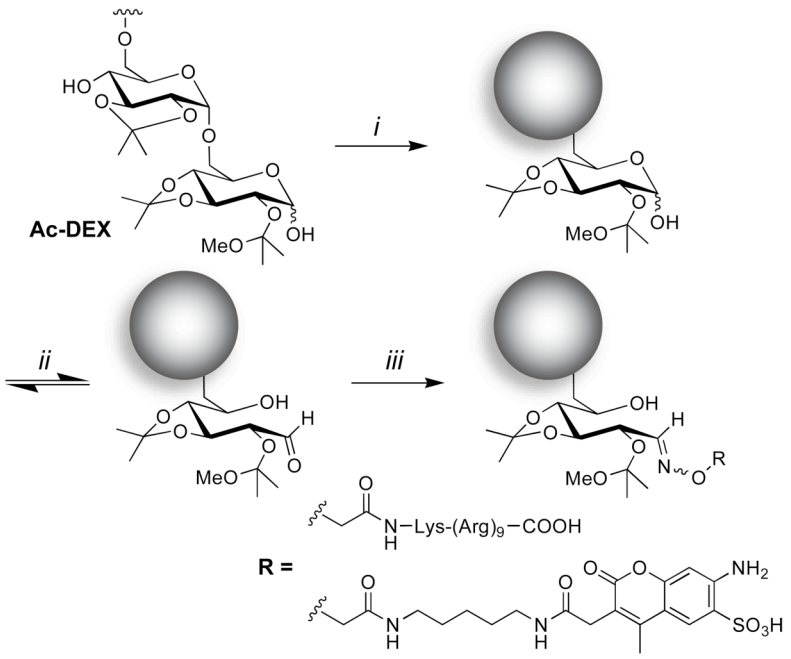

[a] (*i*) Preparation of micro- or nanoparticles via an emulsion/solvent-evaporation procedure. (*ii*) Reducing end equilibrium between hemiacetal and straight-chain forms. (*iii*) Reaction of reducing end aldehyde with alkoxyamine reagents (R-ONH$_2$) to form stable oxime conjugates.

Introduction

The ability to readily functionalize the surface of colloidal inorganic materials has been essential in the advancement of bionanotechnology.[1] Similar to their inorganic counterparts, polymeric nano- and microparticles have been extensively investigated as vehicles for biomedical applications including gene delivery,[2] vaccines,[3] and chemotherapy.[4] However, there exist few, if any, simple, versatile and chemoselective strategies for the functionalization of

synthetic polymer-based particulate drug delivery vehicles. The *in vivo* behavior, and ultimately, the efficacy of these carriers would almost certainly be enhanced through the functionalization of their surfaces with biologically relevant moieties. Particles made from the polyester poly(lactic-*co*-glycolic acid) (PLGA), a widely-studied biodegradable polymer, have been functionalized with agents such as antibodies[5] and aptamers.[6] However, these typical examples utilize functionalization routes based on the synthesis of complicated copolymer conjugates or non-specific bioconjugation reactions, which may inadvertently modify the encapsulated cargo or functionalizing ligand and consequently alter their activity. Herein we demonstrate a one-step, chemoselective method for the surface modification of polysaccharide-based particles.

We recently developed a biocompatible and pH-sensitive polymer based on acetal-modified dextran (Ac-DEX, Scheme 5.1), which may offer advantages over polyester-based materials such as PLGA.[7] Due to their pH-sensitivity, Ac-DEX particles can selectively and rapidly release their encapsulated payload under mildly acidic conditions including those found in sites of inflammation, tumor tissue, or endocytic vesicles. In contrast to particles made from PLGA, Ac-DEX particles degrade to yield neutral (as opposed to acidic) byproducts, and their rate of degradation can be easily tuned within the time scale of relevant cellular processes. The latter feature has been found to significantly affect the biological activity of the particles, for example, in the case of vaccine formulations.[8]

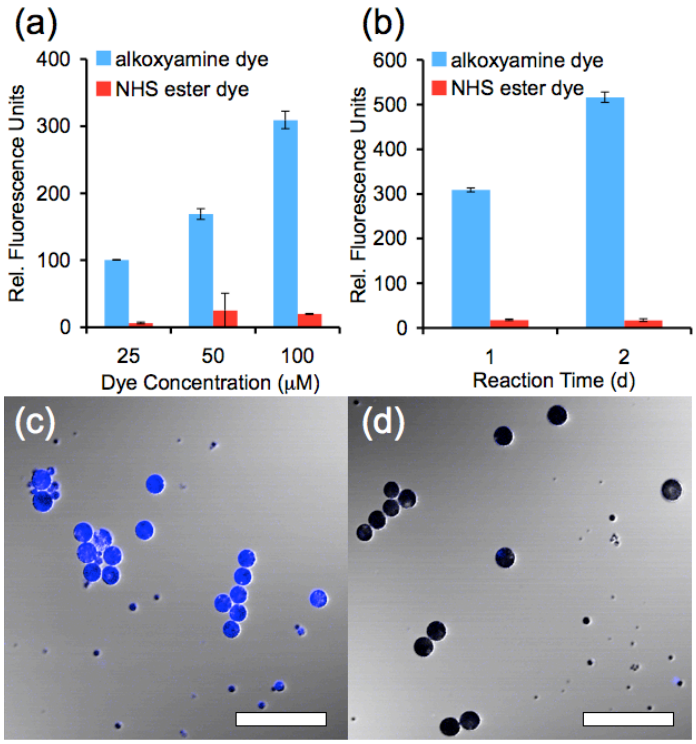

Figure 5.1. Surface functionalization of Ac-DEX particles using a fluorophore. Particles were treated with an alkoxyamine or control dye at (a) various concentrations for one day or for (b) various times keeping the dye concentration constant (100 μM). Confocal microscopy was used to visualize particles treated with an alkoxyamine (c) or NHS ester control dye (d). Scale bars = 50 μm.

Results and Discussion

Given the potential for precisely targeted or otherwise functionalized polymeric nanoparticles, we sought to develop a simple, mild and selective ligation strategy for the surface modification of Ac-DEX-based delivery vehicles (Scheme 5.1). Based on prior examples of oxime formation with complex polysaccharides[9-11] and other small molecule examples,[12-14] we hypothesized that carbohydrate reducing chain ends present at the surface of the particles could be exploited to form stable oxime conjugates with alkoxyamine-bearing molecules.[15] To test this hypothesis, sub-micron-sized Ac-DEX particles were prepared and treated with aqueous solutions of either an alkoxyamine-functionalized fluorophore or an NHS-ester-functionalized version of the fluorophore to control for the possibility of non-specific dye adsorption. Due to the acid-sensitivity of Ac-DEX particles, all conjugation reactions were performed at neutral pH. Oxime formation typically proceeds faster under slightly acidic conditions,[16] however the rate may be accelerated at neutral pH using a nucleophilic catalyst if desired.[17] As shown in Figure 5.1, use of the alkoxyamine-functionalized dye led to both concentration and time dependent labeling of the particles, with essentially no fluorescence observed from particles treated with the NHS ester dye, suggesting minimal non-specific dye adsorption. The bulk measurements were visually confirmed by preparing larger particles which were labeled and examined using confocal microscopy (Figure 5.1c-d). Importantly, we did not observe any particle degradation or aggregation as a result of these or any subsequent particle functionalization attempts (See Table 5.1 and Figures 5.6 and 5.7 for an analysis of particle stability as determined by scanning electron microscopy and light scattering measurements).

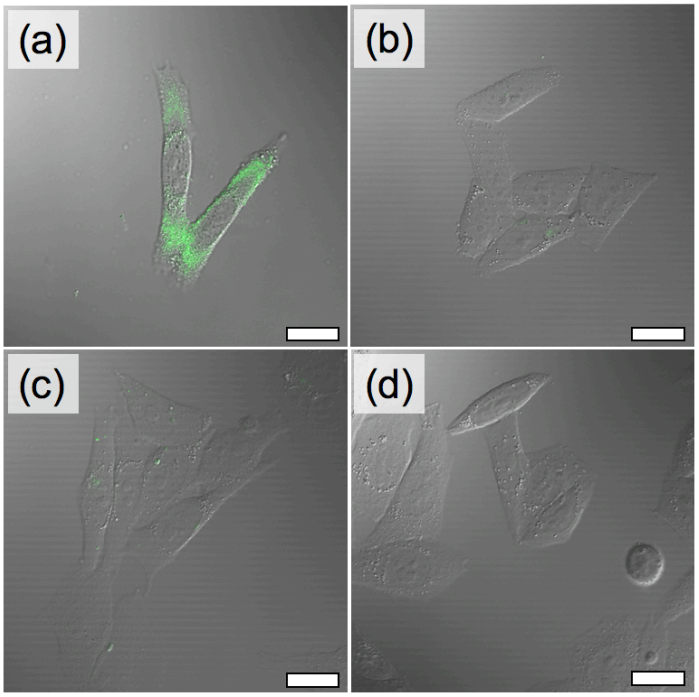

Figure 5.2. Representative confocal microscopy images of HeLa cells incubated with fluorescent particles treated with (a) an alkoxyamine-functionalized CPP, (b) PBS only, or (c) an unfunctionalized CPP. Cells incubated in medium alone are shown in (d). Scale bars = 20 μm.

We next investigated the possibility of adding therapeutically relevant functionality to the surface of our particles. Although polymeric particles are readily taken up by phagocytic cells of the immune system, uptake and delivery of therapeutic agents to non-phagocytic cells remains challenging. We therefore attempted to functionalize particles with cell-penetrating peptides (CPPs), a class of cationic peptides known to facilitate delivery of cargo across cell membranes.[18,19] Ac-DEX particles were incubated with solutions of an alkoxyamine-terminated poly(arginine) CPP sequence ($K\text{-}R_9$), an unmodified amine-terminated version of the CPP, or buffer only. Particles treated with the alkoxyamine CPP were found to have a higher zeta potential (see Table 5.1) compared to control samples.[20,21,22] Additionally, the CPP loading was measured using fluorescamine, an amine reactive probe capable of reacting with a lysine residue present in the CPP sequence,[23] which led us to estimate that there were several thousand CPPs per particle. Based on these data, CPP-modified particles were evaluated *in vitro* for their ability to be taken up by non-phagocytic cells. Ac-DEX particles encapsulating fluorescently labeled protein were treated with solutions of the alkoxyamine-functionalized CPP or control solutions, washed, and then incubated with HeLa cells for 12 hours. As shown in Figure 5.2, fluorescence was only observed for cells incubated with the alkoxyamine-CPP treated particles. Using this same functionalization technique, particles might also be modified with a number of cancer cell-specific peptide sequences[24] for chemotherapy applications.

To assess the feasibility of using functionalized particles for the delivery of biologically relevant payloads, we performed proof-of-concept *in vitro* transfection experiments with plasmid-loaded Ac-DEX particles. Blending PLGA with poly(β-amino ester) polymers has been shown to enhance transfection efficiency in phagocytic cell lines, presumably due to a proton-sponge effect.[25] We hypothesized that functionalizing similarly prepared Ac-DEX particles with CPPs would enhance the uptake of these particles by non-phagocytic cells and lead to efficient transfection. Ac-DEX particles blended with 20% (w/w) poly(β-amino ester) polymer (Polymer **1**, Figure 5.3), and encapsulating plasmid DNA encoding firefly luciferase as a reporter, were prepared and functionalized with CPPs as described above.[26] The loading was found to be 10.2 μg of plasmid per mg of particles, which represents a 99.8% loading efficiency. Additionally, the plasmid was found to be approximately 52% supercoiled with the remainder observed in the relaxed/open circular conformation (Figure 5.4). After a two day incubation, HeLa cells treated with CPP-modified Ac-DEX particles demonstrated up to a 60-fold increase in expression of the luciferase reporter compared to cells incubated with unmodified particles (Figure 5.5), which strongly suggests efficient particle uptake and delivery of the encapsulated DNA.

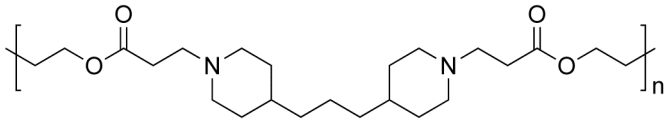

Polymer **1**

Figure 5.3. Structure of Polymer 1.

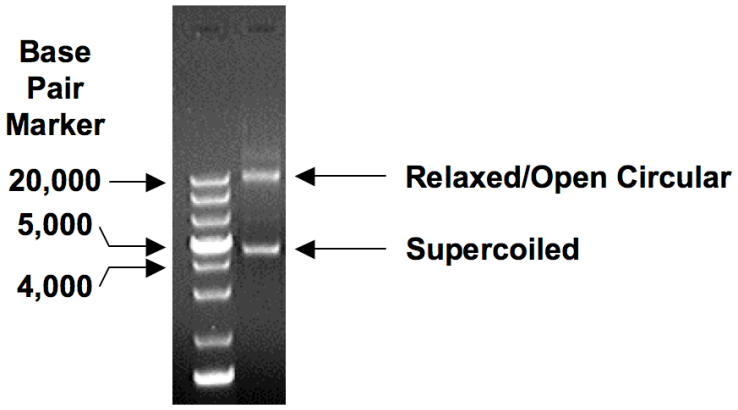

Figure 5.4. Agarose gel electrophoresis of plasmid DNA extracted from microparticles used to determine supercoil content.

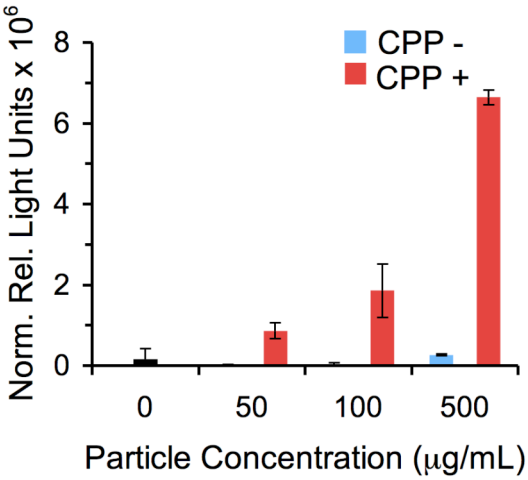

Figure 5.5. Ac-DEX particles modified with CPPs transfect non-phagocytic cells in vitro. Ac-DEX particles blended with 20% poly(β-amino ester) polymer, encapsulating luciferase-encoding plasmid DNA, and functionalized with CPPs were incubated with HeLa cells for two days. Cells were then lysed and assayed for expression of luciferase. Relative light unit output was normalized to total protein content in each sample.

Summarized Particle Characterization Data

Entry	Particle Description	Average Diameter (nm)	Distribution Standard Deviation (nm)	Zeta Potential (mV)
1	empty/single emulsion particles	244	66	—
2	entry 1 particles treated with AF-350 NHS ester (100 μM, 2 d)	285	100	—
3	entry 1 particles treated with AF-350 alkoxyamine (100 μM, 2 d)	310	120	—
4	entry 1 particles treated with PBS (2 d)	265	69	-5.0 ± 0.2
5	entry 1 particles treated with unmodified CPP sequence (2 d)	283	84	-1.3 ± 0.3
6	entry 1 particles treated with alkoxyamine functionalized CPP (2 d)	279	82	+1.3 ± 0.2
7	double emulsion particles encapsulating FITC-BSA	261	98	—
8	Ac-DEX/PBAE particles encapsulating plasmid DNA	4500	1900	+1.2 ± 0.1
9	entry 8 particles treated with alkoxyamine functionalized CPP (1 d)	5000	2400	+12.0 ± 0.1
10	empty microparticles used for confocal imaging	7300	2700	—

Table 5.1. Particle summary statistics. Particle size and zeta potential data were determined by light scattering measurements.

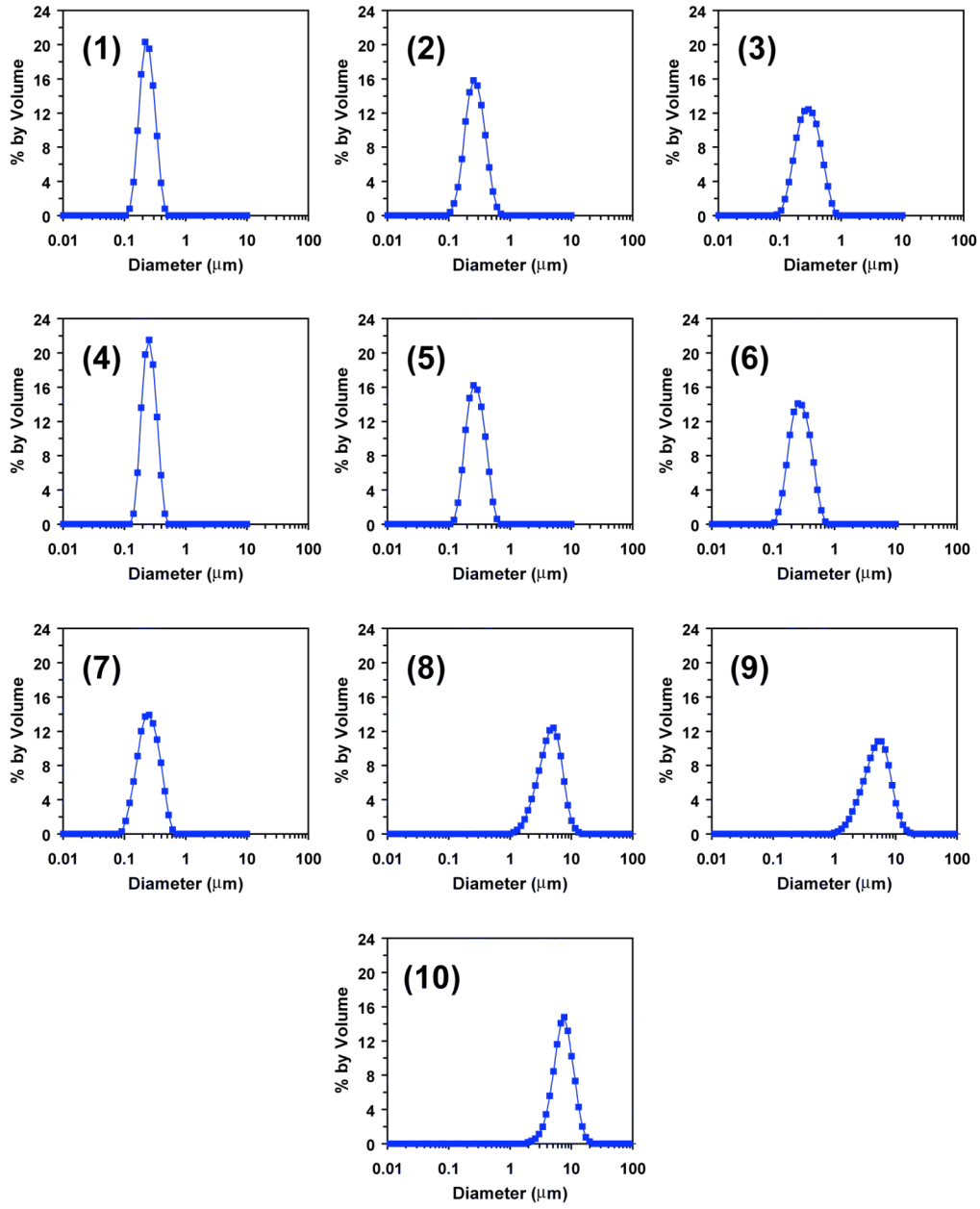

Figure 5.6. Particle size distributions obtained by light scattering measurements for Ac-DEX particle samples. The numbering scheme corresponds to the entries in Table 5.1.

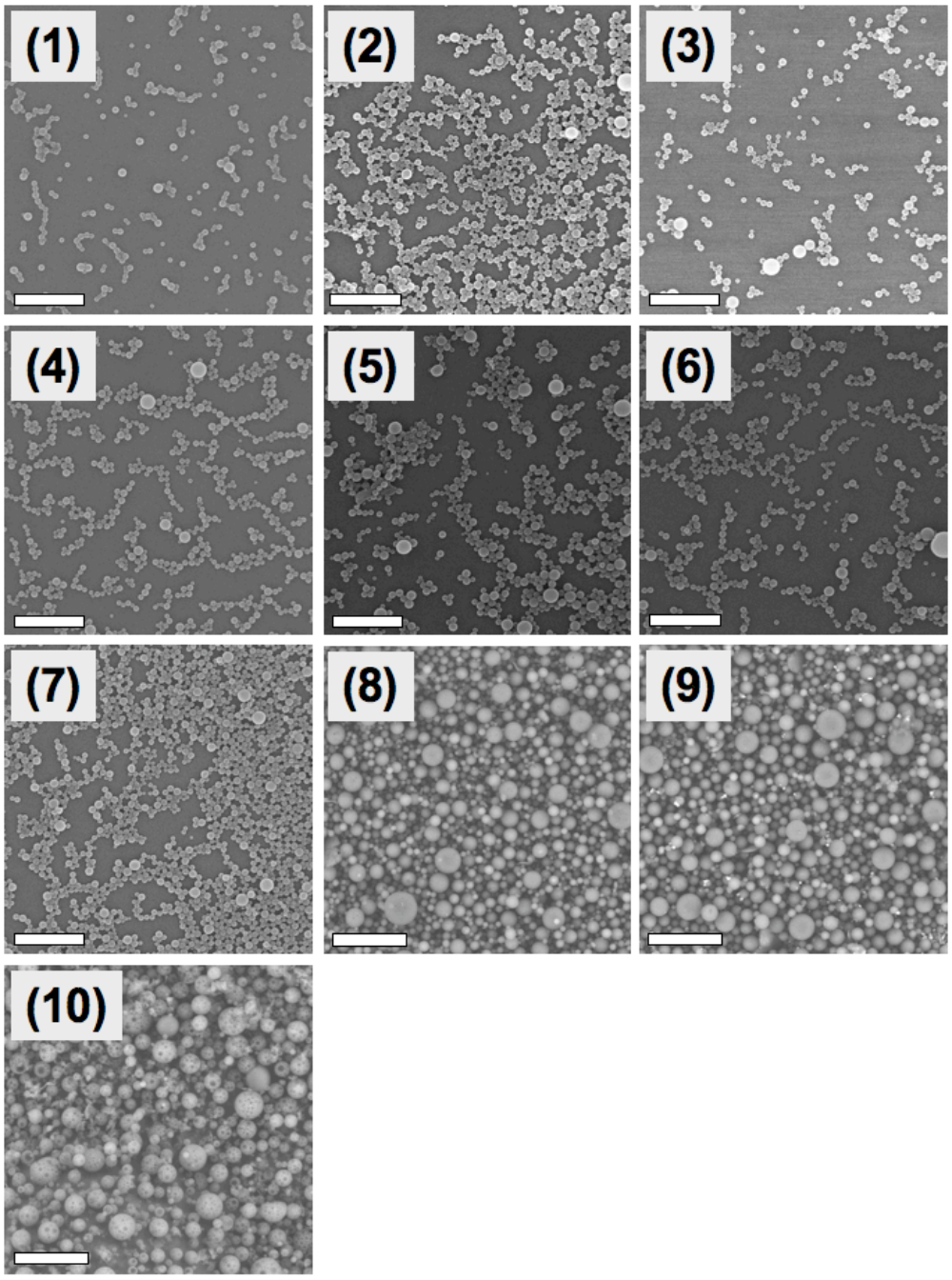

Figure 5.7. Scanning electron micrographs of Ac-DEX particle samples. The numbering scheme corresponds to the entries in Table 5.1. Scale bars correspond to 2 μm (images 1-7) and 25 μm (images 8-10).

Conclusions

In conclusion, we have demonstrated a one-step, chemoselective method for the functionalization of polysaccharide-based particles using alkoxyamine reagents. We anticipate that the mild reaction conditions and functional group tolerance of this ligation strategy will enable a variety of materials to be similarly modified with any number of complex bioactive molecules. In addition, this concept could readily be generalized to other biocompatible polymeric particles used commonly in delivery systems through the introduction of functional groups that enable oxime ligation.

Experimental

General Procedures and Materials

All reagents were purchased from commercial sources and used without further purification unless otherwise specified. Water (dd-H_2O) for buffers and particle washing steps was purified to a resistance of 18 MΩ using a NANOpure purification system (Barnstead, USA). When used in the presence of acetal containing materials, dd-H_2O was rendered basic (pH ~8) by the addition of triethylamine (TEA) (approximately 0.01%). Dulbecco's phosphate buffered saline (PBS, 138 mM NaCl, 9.5 mM phosphate, 2.7 mM KCl, pH 7.4), Alexa Fluor 350 C_5-aminooxyacetamide trifluoroacetate salt (AF-350 alkoxyamine), and Alexa Fluor 350 carboxylic acid succinimidyl ester (AF-350 NHS ester) were purchased from Invitrogen (USA). Dyes were stored as 5 mg/mL solutions in anhydrous DMSO at -20 ºC. ^{1}H NMR spectra were recorded at 400 MHz. Fluorescence measurements were obtained using a Spectra Max Gemini XS plate-reading fluorimeter (Molecular Devices, USA). The cell penetrating peptides (CPPs) NH_2-K-$(R)_9$-COOH and aminooxyacetyl-K-$(R)_9$-COOH were purchased from Applied Peptech Suzhou (China). The lysine residue was incorporated to facilitate subsequent quantification.

Polymer Synthesis

Synthesis of Acetalated Dextran (Ac-DEX) was performed as previously described.[7] Briefly, a flame-dried flask was charged with dextran (M_W = 10,500 g/mol, 2.00 g, 0.19 mmol) and purged with dry N_2. Anhydrous DMSO (20 mL) was added and the resulting mixture was stirred until complete dissolution of the dextran was observed. Pyridinium *p*-toluenesulfonate (31.0 mg, 0.12 mmol) was added followed by 2-methoxypropene (7.1 mL, 74 mmol). The flask was placed under a positive pressure of N_2, then sealed to prevent evaporation of 2-methoxypropene. After 5 h, the reaction was quenched with TEA (1 mL, 7 mmol) and the modified dextran was precipitated in dd-H_2O (300 mL, pH 8). The product was isolated by vacuum filtration, washed thoroughly with dd-H_2O (2 x 50 mL, pH 8) and lyophilized to remove residual water. The polymer was dissolved in acetone (5.5 mL) and further purified by precipitation into dd-H_2O (300 mL, pH 8). Following isolation and lyophilization as described above, the "acetalated dextran" (Ac-DEX) was obtained as a fine white powder (1.40 g). Using the ^{1}H-NMR method described by Broaders et al., the ratio of cyclic to acyclic acetals was found to be 1.8:1.[8]

Synthesis of Poly(β-amino ester) Polymer 1 (Figure 5.3) was generated from the Michael-type addition of 4,4'-trimethylenedipiperidine to 1,4-butanediol diacrylate as previously reported.[27]

Particle Preparation

Sub-micron Single Emulsion Particles (Table 5.1, entry 1) were prepared according to a procedure adapted from Jung et al.[28] Briefly, Ac-DEX (250 mg) was dissolved in CH_2Cl_2 (5 mL). This solution was added to an aqueous solution of poly(vinyl alcohol) (PVA, M_W = 13,000 -23,000 g/mol, 87-89% hydrolyzed) (15 mL, 1% w/w in PBS) and emulsified by sonicating for 30 s on ice using a probe sonicator (Branson Sonifier 450) with an output setting of 5 and a duty cycle of 70% with a 1/2-inch flat tip. The resulting emulsion was poured into a second PVA solution (250 ml, 0.3% w/w in PBS) and stirred for 5.5 h allowing the organic solvent to evaporate. The particles were isolated by centrifugation (14,800 x *g*, 15 min) and washed with dd-H_2O (2 x 50 mL, pH 8) by vortexing and sonication followed by centrifugation and removal of the supernatant. The washed particles were resuspended in dd-H_2O (5 mL, pH 8) and lyophilized to yield a white fluffy solid (139 mg).

Sub-micron Double Emulsion Particles Containing FITC-BSA (Table 5.1, entry 7) were made using a double emulsion water/oil/water evaporation method similar to that described by Bilati et al.[29] Briefly, FITC-BSA (fluorescein isothiocyanate conjugated to bovine serum albumin, 10 mg) was dissolved in PBS (50 μL). Ac-DEX (200 mg) was dissolved in CH_2Cl_2 (1 mL) and added to the protein solution. This mixture was then emulsified by sonicating for 30 s on ice using a probe sonicator (Branson Sonifier 450) with an output setting of 5 and a duty cycle of 70%. This primary emulsion was added to an aqueous solution of PVA (2 mL, 3% w/w in PBS) and sonicated for an additional 30 s on ice using the same settings. The resulting double emulsion was immediately poured into a second PVA solution (10 ml, 0.3% w/w in PBS) and stirred for 4 h allowing the organic solvent to evaporate. The double emulsion particles were isolated in the same manner as described for the single emulsion nanoparticles above. The washed particles were resuspended in dd-H_2O (1 mL, pH 8) and lyophilized to yield a fluffy solid (149 mg).

Plasmid-loaded Microparticles (Table 5.1, entry 8) were made using a modified double emulsion water/oil/water evaporation method. Ac-DEX (40 mg) and polymer **1** (10 mg) were dissolved in ice-cold CH_2Cl_2 (1 mL). Plasmid DNA encoding firefly luciferase reporter protein, gWIZ Luciferase, was purchased from Aldevron/Genlantis (USA) and was dissolved in TE buffer (10 mM Tris, 1 mM EDTA, pH 8.5) at a concentration of 5 mg/mL. The plasmid solution (100 μL) was added to the polymer solution and the mixture was emulsified by sonicating for 5 s using a Branson Sonifier 450 sonicator with a microtip probe, an output setting of 1, and a continuous duty cycle. This primary emulsion was added to an ice-cold aqueous solution of PVA (20 mL, 3% w/w in PBS) and homogenized for 30 s at 10,000 rpm using an IKA T-25 Ultra-Turrax digital homogenizer with an S25N-10G generator. The resulting double emulsion was immediately poured into a second PVA solution (40 mL, 0.3% w/w in PBS) and stirred for 2 h allowing the organic solvent to evaporate. The particles were isolated by centrifugation (3,000 x *g*, 5 min) and washed with PBS (1 x 20 mL) and dd-H_2O (2 x 20 mL, pH 8). The washed particles were resuspended in dd-H_2O (2 mL, pH 8) and lyophilized to yield a white fluffy solid (34 mg).

Empty Microparticles (Table 5.1, entry 10) used to confirm dye attachment using confocal microscopy (Figure 5.1c-d) were prepared in the same manner as described above, except that the aqueous buffer in the primary emulsion consisted of PBS (50 μL) and no plasmid. In addition, the primary emulsion was homogenized at 9400 rpm in 12.5 mL of 3% w/w PVA solution, and the resulting double emulsion was added to 25 mL of 0.3% w/w PVA solution.

Particle Characterization

Particle Size Analysis by Light Scattering. Particle size distributions of sub-micron diameter particles were determined by dynamic light scattering using a Nano ZS ZetaSizer (Malvern Instruments, United Kingdom). Particles were suspended in dd-H_2O (pH 8) at a concentration of 1 mg/mL and three measurements were taken of the resulting dispersions at 25 ºC.

Particle size distributions of micron diameter particles were determined using a Horiba Partica LA-950 laser scattering particle size distribution analyzer after suspending the particles at 2 mg/mL in PBS. The refractive indices of PBS and Ac-DEX used in the size distribution calculations were 1.33 and 1.46 respectively, and the viscosity of PBS was 0.888 cP.

Particle size distributions for both measurement techniques were volume-weighted and are presented in Table 5.1 and Figure 5.6. The results are presented as average particle diameters ± standard deviation of the distribution. As seen in Table 5.1 and Figure 5.6, the particles appear to be stable under the various modification conditions.

Zeta-potential Measurements of CPP-modified Particles. The CPP modified and control particles (prepared as described below) were suspended in HEPES (5 mM, pH 7.4) at a concentration of 1 mg/mL and three zeta-potential measurements were taken of the resulting dispersions using a Nano ZS ZetaSizer (Malvern Instruments, United Kingdom) at 25 ºC. The results are presented as averages ± standard deviations in Table 5.1.

Scanning Electron Microscopy. Sub-micron diameter particles were characterized by scanning electron microscopy using a S-5000 microscope (Hitachi, Japan). Particles were suspended in dd-H_2O (pH 8) at a concentration of 1 mg/mL and the resulting dispersions were dripped onto silicon wafers. After 15 min, the water was wicked away using tissue paper and the samples were further dried under a stream of N_2 gas. The particles were then sputter coated with a 2 nm layer of a palladium/gold alloy and imaged.

Micron diameter particles were characterized using a Hitachi (USA) TM-1000 scanning electron microscope. Dry particles were mounted directly on double-sided carbon tape and were not coated prior to imaging.

Quantification of Plasmid Loading was determined by suspending 3 mg of particles in 0.3 mL of TAE buffer (40 mM Tris-acetate, 1 mM EDTA, pH 8.3), adding 1 mL of CH_2Cl_2 (1 mL), and mixing rapidly end-over-end for 1.5 h at 4 ºC. The mixture was centrifuged (10,000 x *g*, 5 min), and the aqueous layer containing the extracted DNA was removed and stored at 4 ºC. The concentration of DNA in the extract was quantified using the Quant-iT PicoGreen dsDNA assay (Invitrogen, USA) according to the manufacturer's instructions using the original plasmid solution as a standard.

The supercoil content of the encapsulated plasmid was determined by 1% agarose gel electrophoresis in TAE buffer at 100 V for 80 min using 150 ng of plasmid extracted as above. O'GeneRuler 1kb Plus DNA Ladder (Fermentas, USA) was used as a base pair marker. The gel was stained with ethidium bromide and visualized under UV illumination. Captured digital images were analyzed using ImageJ software (version 1.37) to determine the relative peak area of bands.

Preparation of and Studies Performed with Functionalized Particles

Functionalization of Ac-DEX particles using Fluorescent Dyes.

General Procedure: Empty Ac-DEX particles (Table 5.1, entry 1) were suspended in PBS at a concentration of 2 mg/mL. Aliquots (0.5 mL) were then transferred to microcentrifuge tubes containing solutions of dyes in PBS (0.5 mL, dye concentrations listed below). The samples were vortexed then gently agitated in the dark at rt using a Thermomixer R heating block (Eppendorf). After a given time (see below) the particles were centrifuged (10,000 x *g*, 15 min) and the supernatant removed. The resulting pellet was washed with PBS (2 x 1 mL) and the particles were then resuspended in PBS (1 mL) using a bath sonicator. The particles were centrifuged again (10,000 x *g*, 15 min), the supernatant was removed and the particles were suspended in PBS (1 mL). The dispersions were diluted two fold in PBS and the fluorescence of the resulting solutions was measured using a plate-reading fluorimeter (excitation = 350 nm, emission = 440 nm). Particles treated with PBS only were used to determine background fluorescence levels.

Concentration Dependent Labeling Experiment: For this experiment, the particles were added in triplicate to solutions of dye (either AF-350 alkoxyamine or AF-350 NHS ester) at 200, 100 or 50 μM concentrations. The particles were allowed to react for 24 h before washing and fluorescence measurements.

Time Dependent Labeling Experiment: For this experiment, the particles were added in triplicate to dye solutions (either AF-350 alkoxyamine or AF-350 NHS ester) at 200 μM concentrations. The particles were allowed to react for 24 or 48 h before washing and fluorescence measurements.

Confocal Microscopy of Dye-labeled Microparticles. Empty microparticles (Table 5.1, entry 10) were suspended in PBS at a concentration of 2 mg/mL. Aliquots (0.5 mL) were transferred to microcentrifuge tubes containing AF-350 alkoxyamine (200 μM in 0.5 mL PBS), AF-350 NHS ester (200 μM in 0.5 mL PBS) or PBS only (0.5 mL). After 4 d at rt under gentle agitation, the particles were washed as described above. Following the washing procedure, the particles were suspended at 1 mg/mL in dd-H_2O (pH 8) and dripped onto glass microscope slides. The majority of the water was wicked away with tissue paper and the remaining moisture evaporated under a stream of dry N_2 gas. A drop of immersion oil was added to the particles, and the slide was then coverslipped (#1.5 glass). Fluorescence imaging was performed using a Zeiss LSM 510 Meta confocal microscope with a 40x objective (Carl Zeiss, Germany) using an excitation wavelength of 361 nm. DIC images were simultaneously obtained using a 543 nm laser line. The images presented in the text (Figure 5.1c-d) are an overlay of the DIC and fluorescence channels.

Functionalization of Ac-DEX particles with CPPs. Ac-DEX particles (Table 5.1, entry 1) were suspended in PBS at a concentration of 1 mg/mL and aliquots (1.5 mL) were transferred to three microcentrifuge tubes. The samples were centrifuged (10,000 x *g*, 15 min) and the supernatant was removed. Using a bath sonicator, the particles were resuspended in solutions (1.5 mL) of NH_2-K-$(R)_9$-COOH (10 mg/mL in PBS, pH 7.4), aminooxyacetyl-K-$(R)_9$-COOH (10

mg/mL in PBS, pH 7.4), or PBS only. After 2 d at rt under gentle agitation, these particles were washed as described above.

Particles encapsulating plasmid and functionalized with CPP (Table 5.1, entry 9, prepared from entry 8 particles) were prepared in the same manner, except the reaction was only allowed to proceed for 1 d.

Quantification of Peptide Content on CPP-modified Particles. The CPP and control particles (prepared above) were suspended in PBS at a concentration of 3 mg/mL. These suspensions were analyzed for peptide content using the fluorescamine reagent and a microplate assay adapted from Lorenzen et al.[23] Briefly, the particle suspensions (50 μL) were added to the wells of a microplate in triplicate. A solution of fluorescamine (150 μL, 1 mg/mL in acetone) was added to each well and the fluorescence was quantified using a plate-reading fluorimeter (excitation = 400 nm, emission = 460 nm). PBS treated Ac-DEX particles were used to determine a background fluorescence level. The results were compared to a standard curve and the CPP content was calculated. The peptide loading was found to be 0.12 ± 0.01 wt %.

Cell Lines and Culture. HeLa cells (CCL-2) used in uptake experiments were purchased from ATCC (USA) and cultured in Dulbecco's Modified Eagle Medium (DMEM) containing 4.5 g/L D-glucose, and supplemented with 10% fetal bovine serum, 100 units/mL of penicillin, 100 μg/mL streptomycin, and 2 mM GlutaMAX. All culture media components were from Invitrogen (USA) with the exception of the serum, which was from Hyclone (USA). Cell incubations were performed in a water-jacketed 37 ºC/5% CO_2 incubator.

HeLa cells used in transfection experiments were cultured as above, except that antibiotics were omitted from the culture medium.

Uptake of CPP-modified Particles by HeLa Cells. Ac-DEX particles containing a fluorescently-labeled protein (FITC-BSA, Table 5.1 entry 7) were treated with NH_2-K-$(R)_9$-COOH (10 mg/mL in PBS, pH 7.4), aminooxyacetyl-K-$(R)_9$-COOH (10 mg/mL in PBS, pH 7.4), or PBS only as described above. After 2 d at rt in the dark, the particles were washed as described above and suspended in DMEM. The CPP-modified and control particles (125 μg particles/mL DMEM) were incubated with $3x10^5$ HeLa cells seeded the night before in a poly-D-lysine coated 35 mm culture dish with a #1.5 glass coverslip bottom (MatTek, USA). After 15 h, the medium was removed and the cells were washed with PBS (3 x 1 mL). The cells were then imaged by confocal microscopy using a 63x objective and an excitation wavelength of 488 nm. DIC images were simultaneously obtained using a 543 nm laser line. The images presented in the text (Figure 5.2) are an overlay of the DIC and fluorescence channels.

Transfection of HeLa Cells. HeLa cells were plated at 3 x 10^4 cells/well (100 μl/well) in white and clear 96-well tissue culture plates (Corning, USA), and cultured overnight. Particle samples were prepared at 500 μg/mL in medium (without antibiotics) by alternately vortexing and sonicating in a Branson 2510 water bath for 20 s to generate homogeneous suspensions. The samples were then serially diluted in medium to give the indicated particle concentrations. Existing medium was replaced with 100 μl of each particle dilution (or medium only) in triplicate wells of each 96-well plate. After 2 d, the cells of the white plate were washed with PBS (containing Mg^{2+} and Ca^{2+}, 3 x 100 μl), Glo Lysis Buffer (100 μl, Promega, USA) was

added to each well and the plate was incubated at rt for 10 min. Bright-Glo luciferase assay reagent (Promega) was reconstituted according to the manufacturer's instructions and added to each well (100 μl). After 2 min, the plate was read using a GloMax 96 microplate luminometer (Promega) with a 1 s integration time.

To determine the total protein content in each well, the cells of the clear plate were washed as above and lysed with M-PER mammalian protein extraction reagent (50 μl, Pierce-Thermo Fisher, USA) for 10 min at rt. PBS (50 μl) was added to each well, and the plate was briefly vortexed to mix. Samples from each well (25 μl) were added to the wells of a black 96-well tissue culture plate (Corning) already containing PBS (125 μl per well). A solution of 0.3 mg/mL fluorescamine in acetone (50 μl) was added to each well, and the plate was briefly vortexed to mix. After 5 min, the fluorescence in each well was measured using a plate-reading fluorimeter (excitation = 400 nm, emission = 460 nm). Protein concentrations were determined using BSA as a standard.

The reported transfection values represent the mean ± standard deviation of the relative light units obtained from the luminometer divided by the total protein content (in mg) per well.

References and Footnotes

(1) Giljohann, D. A.; Seferos, D. S.; Prigodich, A. E.; Patel, P. C.; Mirkin, C. A. *J. Am. Chem. Soc.* **2009**, *131*, 2072-2073.
(2) Park, T. G.; Jeong, J. H.; Kim, S. W. *Adv. Drug Delivery Rev.* **2006**, *58*, 467-486.
(3) Reddy, S. T.; Swartz, M. A.; Hubbell, J. A. *Trends Immunol.* **2006**, *27*, 573-579.
(4) Peer, D.; Karp, J. M.; Hong, S.; Farokhzad, O. C.; Margalit, R.; Langer, R. *Nat. Nanotechnol.* **2007**, *2*, 751-760.
(5) McCarron, P. A.; Marouf, W. M.; Quinn, D. J.; Fay, F.; Burden, R. E.; Olwill, S. A.; Scott, C. J. *Bioconjugate Chem.* **2008**, *19*, 1561-1569.
(6) Gu, F.; Zhang, L.; Teply, B. A.; Mann, N.; Wang, A.; Radovic-Moreno, A. F.; Langer, R.; Farokhzad, O. C. *Proc. Natl. Acad. Sci. U. S. A.* **2008**, *105*, 2586-2591.
(7) Bachelder, E. M.; Beaudette, T. T.; Broaders, K. E.; Dashe, J.; Frechet, J. M. J. *J. Am. Chem. Soc.* **2008**, *130*, 10494-10495.
(8) Broaders, K. E.; Cohen, J. A.; Beaudette, T. T.; Bachelder, E. M.; Frechet, J. M. J. *Proc. Natl. Acad. Sci. U. S. A.* **2009**, *106*, 5497-5502.
(9) Nishimura, S. I.; Niikura, K.; Kurogochi, M.; Matsushita, T.; Fumoto, M.; Hinou, H.; Kamitani, R.; Nakagawa, H.; Deguchi, K.; Miura, N.; Monde, K.; Kondo, H. *Angew. Chem., Int. Ed.* **2005**, *44*, 91-96.
(10) Thygesen, M. B.; Sauer, J.; Jensen, K. J. *Chem. Eur. J.* **2009**, *15*, 1649-1660.
(11) Zhao, Y. M.; Kent, S. B. H.; Chait, B. T. *Proc. Natl. Acad. Sci. U. S. A.* **1997**, *94*, 1629-1633.
(12) Cervigni, S. E.; Dumy, P.; Mutter, M. *Angew. Chem., Int. Ed.* **1996**, *35*, 1230-1232.
(13) Hatanaka, Y.; Kempin, U.; Jong-Jip, P. *J. Org. Chem.* **2000**, *65*, 5639-5643.
(14) Richard, A.; Barras, A.; Ben Younes, A.; Monfilliette-Dupont, N.; Melnyk, P. *Bioconjugate Chem.* **2008**, *19*, 1491-1495.
(15) Kalia, J.; Raines, R. T. *Angew. Chem., Int. Ed.* **2008**, *47*, 7523-7526.
(16) Jencks, W. P. *J. Am. Chem. Soc.* **1959**, *81*, 475-481.
(17) Dirksen, A.; Hackeng, T. M.; Dawson, P. E. *Angew. Chem., Int. Ed.* **2006**, *45*, 7581-7584.
(18) Deshayes, S.; Morris, M. C.; Divita, G.; Heitz, F. *Cell. Mol. Life Sci.* **2005**, *62*, 1839.
(19) Goun, E. a.; Shinde, R.; Dehnert, K. W.; Adams-Bond, A.; Wender, P. A.; Contag, C. H.; Franc, B. L. *Bioconjugate Chem.* **2006**, *17*, 787-796.
(20) As seen in Table 5.1, the changes in zeta-potential between CPP-modified and unmodified particles are statistically significant, but subtle (~ 6 mV for samples 4 and 6, and ~ 11 mV for samples 8 and 9). It should be noted that it is difficult to directly compare zeta-potential measurements between different materials, but the following examples may provide some points of reference for the observations found in this report. After incorporating an acrylamide modified CPP sequence into polyacrylamide hydrogel particles, we found that the zeta-potential of these particles increased by approximately 12 mV compared to particles containing no CPP (see reference 21). These particles contained approximately 20-fold more CPP (2 wt%) than the particles described in this manuscript, however, due to the method in which the acrylamide particles were prepared, it is likely that a majority of the peptide content was encapsulated inside the particles and not necessarily located on the surface. In an example reported by Zahr et al., heparin sulfate-coated nanoparticles were treated with poly-L-lysine in a layer-by-layer assembly process (see reference 22). The addition of a multilayer of the

polycationic polymer increased the zeta-potential by approximately 40 mV. However, in contrast to the particles prepared in this study, the heparin sulfate-coated particles began with a highly negative (as opposed to nearly neutral) surface charge, and a large amount of polycation was adsorbed onto the particle surface.
(21) Cohen, J. L.; Almutairi, A.; Cohen, J. A.; Bernstein, M.; Brody, S. L.; Schuster, D. P.; Frechet, J. M. J. *Bioconjugate Chem.* **2008**, *19*, 876-881.
(22) Zahr, A. S.; Davis, C. A.; Pishko, M. V. *Langmuir* **2006**, *22*, 8178-8185.
(23) Lorenzen, A.; Kennedy, S. W. *Anal. Biochem.* **1993**, *214*, 346-348.
(24) Aina, O. H.; Liu, R. W.; Sutcliffe, J. L.; Marik, J.; Pan, C. X.; Lam, K. S. *Mol. Pharmaceutics* **2007**, *4*, 631-651.
(25) Little, S. R.; Lynn, D. M.; Ge, Q.; Anderson, D. G.; Puram, S. V.; Chen, J. Z.; Eisen, H. N.; Langer, R. *Proc. Natl. Acad. Sci. U. S. A.* **2004**, *101*, 9534-9539.
(26) The plasmid-loaded particles (corresponding to entries 8 and 9 in Table 5.1) would be too large for intravenous use. These particles could however be administered by other routes, used for delivering cargo to mucosal membranes (i.e., pulmonary delivery), or made smaller. As the main focus of this chapter was the demonstration of a functionalization method, we did not investigate the effect of particle size or specific administration methods.
(27) Lynn, D. M.; Langer, R. *J. Am. Chem. Soc.* **2000**, *122*, 10761-10768.
(28) Jung, J.; Lee, I. H.; Lee, E.; Park, J.; Jon, S. *Biomacromolecules* **2007**, *8*, 3401-3407.
(29) Bilati, U.; Allemann, E.; Doelker, E. *Pharm. Dev. Technol.* **2003**, *8*, 1-9.